

Graduate School for Cellular and Biomedical Sciences

University of Bern

# **Nanoparticle transport across the human placenta**

PhD Thesis submitted by

**Stefanie Grafmüller**

from **Germany**

for the degree of

PhD in Biomedical Sciences

Supervisor

Prof. Dr. Harald Krug  
International Research  
Cooperation Manager  
Empa St. Gallen

Co-advisor

Prof. Dr. Barbara Rothen-Rutishauser  
BioNanomaterials  
Adolphe Merkle Institute  
Université de Fribourg

Co-supervisor

Prof. Dr. Ursula von Mandach  
Department of Obstetrics  
University Hospital Zurich

Co-supervisor

Dr. Peter Wick  
Laboratory for Materials-Biology Interactions  
Empa St. Gallen





Accepted by the Faculty of Medicine, the Faculty of Science and the Vetsuisse  
Faculty of the University of Bern at the request of the Graduate School for  
Cellular and Biomedical Sciences

Bern, Dean of the Faculty of Medicine

Bern, Dean of the Faculty of Science

Bern, Dean of the Vetsuisse Faculty Bern



*To my grandfather*



## TABLE OF CONTENTS

|   |               |
|---|---------------|
| <b>Abbreviations.....</b>   | <b>1</b>      |
| <b>1. SUMMARY .....</b>   | <b>3</b>      |
| <b>2. INTRODUCTION.....</b>   | <b>5</b>      |
| <b>2.1 Nanoparticles.....</b>   | <b>5</b>      |
| 2.1.1 Definition .....  | 5             |
| 2.1.2 Opportunities of nanoparticles .....  | 5             |
| 2.1.3 Uptake of nanoparticles.....  | 7             |
| 2.1.4 Safety of nanoparticles .....   | 9             |
| <b>2.2 The human placenta.....</b>  | <b>12</b>     |
| 2.2.1 Biological barriers .....   | 12            |
| 2.2.2 Structure and functions of the placenta .....   | 12            |
| 2.2.3 Models to study placental transfer .....  | 20            |
| 2.2.4 Current knowledge about nanoparticle-placenta interactions .....  | 23            |
| <b>2.3 Aims of the thesis.....</b>  | <b>25</b>     |
| <b>2.4 References .....</b>   | <b>26</b>     |
| <b>3. RESULTS .....</b>   | <b>37</b>     |
| <br><b>PART I: Determination of the transport rate of xenobiotics and nanomaterials<br/>    across the placenta using the <i>ex vivo</i> human placental perfusion model.....</b> | <br><b>39</b> |
| <br><b>PART II: Bidirectional transfer study of polystyrene nanoparticles across the<br/>    placental barrier reveals different transport kinetics .....</b>                     | <br><b>51</b> |
| <br><b>PART III: Challenges and common pitfalls in nanoparticle characterization for<br/>    transport studies across the human placenta.....</b>                                 | <br><b>81</b> |

|   |            |
|---|------------|
| <b>PART IV: Evaluation of nanoparticle-placenta interactions <i>in vitro</i>.....</b> | <b>105</b> |
| <b>4. FINAL DISCUSSION AND OUTLOOK.....</b>   | <b>133</b> |
| 4.1 Final discussion.....   | 133        |
| 4.2 Outlook.....  | 138        |
| 4.3 References .....  | 141        |
| <b>5. ACKNOWLEDGEMENTS .....</b>  | <b>145</b> |
| <b>6. CURRICULUM VITAE .....</b>  | <b>147</b> |
| <b>Declaration of Originality .....</b>   | <b>151</b> |

**Abbreviations**

|        |  |
|--------|--|
| ATP    | Adenosine triphosphate                       |
| BSA    | Bovine serum albumin                         |
| cAMP   | Cyclic adenosine monophosphate               |
| CK-7   | Cytokeratin 7                                |
| CLSM   | Confocal laser scanning microscopy           |
| CNT    | Carbon nanotubes                             |
| DAPI   | 4',6-diamidino-2-phenylindole                |
| DCF    | 2',7'-dichlorofluorescein                    |
| DD     | Double distilled                             |
| DLS    | Dynamic light scattering                     |
| DMSO   | Dimethylsulfoxide                            |
| DNA    | Deoxyribonucleic acid                        |
| EDTA   | Ethylenediaminetetraacetic acid              |
| EGF    | Epithelial growth factor                     |
| ELISA  | Enzyme-linked immunosorbent assay            |
| ENM    | Engineered nanomaterial                      |
| EPR    | Enhanced permeability and retention          |
| F      | Fetal  |
| FACS   | Fluorescence-activated cell sorting          |
| FC     | Fetal capillary                              |
| FCS    | Fetal calf serum                             |
| hCG    | Human chorionic gonadotropin                 |
| HE     | Hematoxylin and eosin                        |
| HLA    | Human leukocyte antigen                      |
| hPL    | Human placental lactogen                     |
| hr     | Hour   |
| ICP-MS | Inductively coupled plasma mass spectrometry |
| Ig     | Immunoglobulin                               |
| IL     | Interleukin                                  |
| LPS    | Lipopolysaccharide                           |
| M      | Maternal                                     |

|               |  |
|---------------|--|
| MB            | Maternal blood space   |
| MHC           | Major histocompatibility complex   |
| MRI           | Magnetic resonance imaging   |
| MTS           | 3-[4,5-dimethylthiazol-2-yl]-5-[3-carboxymethoxyphenyl]-2-[4-sulfophenyl]-2H-tetrazolium |
| MV            | Microvilli   |
| MWCNT         | Multi-walled carbon nanotubes  |
| NP            | Nanoparticle   |
| PBS           | Phosphate buffered saline  |
| PEG           | Polyethylene glycol  |
| PFA           | Paraformaldehyde   |
| PLGA          | Poly(lactic- <i>co</i> -glycolic acid)   |
| PM            | Perfusion medium   |
| PMA           | Phorbol-12-myristat-13-acetat  |
| ppm           | Parts per million  |
| PS            | Polystyrene beads  |
| RES           | Reticuloendothelial system   |
| ROS           | Reactive oxygen species  |
| SD            | Standard deviation   |
| SDS           | Sodium dodecyl sulfate   |
| Sin-1         | 3-Morpholinosydnonimine  |
| SPION         | Superparamagnetic iron oxide nanoparticle  |
| ST            | Syncytiotrophoblast  |
| TEM           | Transmission electron microscopy   |
| TGF- $\beta$  | Transforming growth factor beta  |
| TNF- $\alpha$ | Tumor necrosis factor alpha  |
| QSAR          | Quantitative structure-activity relationship   |



## 1. SUMMARY

Today, nanotechnology is part of our everyday life. Engineered nanomaterials (ENM) have several novel specific properties compared to the respective bulk material. These characteristics make them highly attractive for many industries. Although there are already numerous consumer products containing a broad variety of ENMs, the field of nanotechnology is still growing. Particularly, applications of ENMs in medicine have been established or are currently under development. However, many studies showed that nanomaterials can have negative effects on human health. Besides the commonly investigated primary biological barriers such as skin, lung and intestine, exposure to ENMs at internal barriers gets increasingly important. Especially medical ENMs are intravenously injected and can directly enter the blood stream. One transient, but highly important internal barrier is the human placenta, which regulates the fetal nutrient supply and protects the fetus from harmful endogenous and exogenous substances. It has been shown that different ENMs can cross the placental barrier in humans and rodents and even cause pregnancy complications in mice. However, the placenta is the most species-specific mammalian organ and results from placental transport studies in rodents cannot simply be translated to humans. ENMs also offer the opportunity to develop new therapeutic strategies to treat specifically the pregnant mother, placental abnormalities or the fetus. Though, for the development of such nanomedical applications, an extensive knowledge about the physicochemical properties of ENMs, which are responsible for their placental transfer, and the transport mechanisms of ENMs is a prerequisite.

In the first part of this thesis, we established and improved the *ex vivo* human placental perfusion model. The placentas were obtained after informed consent of the pregnant women and only from uncomplicated term pregnancies after caesarean delivery. The fetal and maternal vessels of an intact cotyledon were cannulated and perfused for six hours. This perfusion model was chosen, because it delivers reliable, comparable and physiological relevant results about placental transfer of chemical compounds as well as ENMs.

In the second part of this thesis, we examined the mechanisms underlying ENM transport across the human placenta using the *ex vivo* human placental perfusion model and fluorescently labeled polystyrene particles with different sizes and surface modifications (plain and carboxylate-modified) as model particles. The placental transfer of carboxylate-modified polystyrene beads was significantly lower compared to plain polystyrene beads. These results

indicate that not only size, but also the surface modifications and charge are determinants of ENM transport across the human placenta. However, to corroborate this finding further studies with a broader variety of surface functionalized nanoparticles are required. Bidirectional transfer studies revealed an increased translocation of polystyrene beads from the fetal to maternal direction compared to the transport from the maternal to the fetal circulation. Based on these results, a passive placental transport mechanism of polystyrene particles could be excluded. We suggest that energy-dependent mechanisms in the syncytiotrophoblast layer of the human placenta contribute predominantly to the transfer of polystyrene particles.

In the third part of this thesis, we presented some common challenges, which emerged during evaluation and selection of polystyrene nanoparticles with different physicochemical properties. We showed that a thorough particle characterization comprising size distribution analysis, detection of the chemical groups on functionalized polystyrene beads and assessment of dye elution in the appropriate biological environment are indispensable in order to obtain meaningful results from placental transfer studies.

In the fourth part of this thesis, we elucidated if the cellular responses after ENM exposure differ between BeWo cells, a cell line derived from a malignant gestational choriocarcinoma, and primary human cytotrophoblasts. BeWo cells are frequently used in placental *in vitro* models, but primary cytotrophoblasts isolated from the human term placenta are physiologically more relevant. This comparison is required in order to evaluate the suitability of these cell types for the development of advanced *in vitro* models for the human placenta. Due to the limitations of the *ex vivo* human placental perfusion model e.g. constrained feasibility of high throughput screenings of many different ENMs as well as of long-term exposure studies, *in vitro* models are necessary. This study is still ongoing, but preliminary results demonstrated that the isolation of primary human cytotrophoblasts is technically challenging and the yield quite low. Though, these cells might be only suitable for *in vitro* models such as three-dimensional microtissues or microfluidic chips, where a low number of cells is required.

Overall, the results presented in this thesis are essential for the understanding of the translocation mechanisms of ENMs across the placenta barrier. Furthermore, these findings will be important for organ toxicology, reproductive toxicology (teratogenicity) as well as for pharmaceutical engineering of new drug carriers.

## 2. INTRODUCTION

### 2.1 Nanoparticles

#### 2.1.1 Definition

According to the recommendation of the European Union commission from the 18th October 2011, nanomaterials are defined as materials containing 50 % or more particles in the number size distribution with at least one external dimension in a size range between 1 and 100 nm. Nanoparticles (NPs) are nanomaterials with all three external dimensions in the nanoscale (see also ISO/TS 27687:2008, International Organization for Standardization). This classification is based on observations that materials in the ‘nano’ size range show special properties, which are substantially different from the bulk material. The high surface-to-volume ratio of NPs leads to a massively higher chemical reactivity and NPs also show size-dependent quantum effects e.g. color and luminescence of quantum dots (Goesmann and Feldmann, 2010). There is controversial discussion about the strict definition of NPs (Auffan et al., 2009, Goesmann and Feldmann, 2010). However, in the field of biology and toxicology it is widely known that also larger particles can induce similar responses in biological systems as NPs. Therefore, the definition of NPs should be considered with caution (Krug and Wick, 2011). In general NPs can be further discriminated by their origin. Naturally occurring NPs e.g. ultrafine dust particles are released during volcano eruptions or forest fires, unintentionally produced NPs are mainly liberated through distinct combustion processes and intentionally produced NPs are specifically engineered for plenty industrial applications. The latter nanomaterials including nanoparticles, nanofibers and nanoplates, are often summarized under the term engineered nanomaterials (ENMs).

#### 2.1.2 Opportunities of nanoparticles

A great number of industrial products containing ENMs are already on the market and it is anticipated that this number will even increase in the future (Maynard, 2007, Service, 2004). Due to the novel and exciting properties of ENMs they are used in many various areas such as energy production and storage, construction, computer, car, packaging, textile and cosmetics industries (Figure 1). For example titanium dioxide nanoparticles are used in wood preservatives, textile fibers and sunscreens due to their high resistance to ultraviolet light

## 2. Introduction

(Figure 1A). The small size of ENMs allows them to enter cells more easily than the bulk material. This characteristic makes ENMs especially interesting for medical purposes.

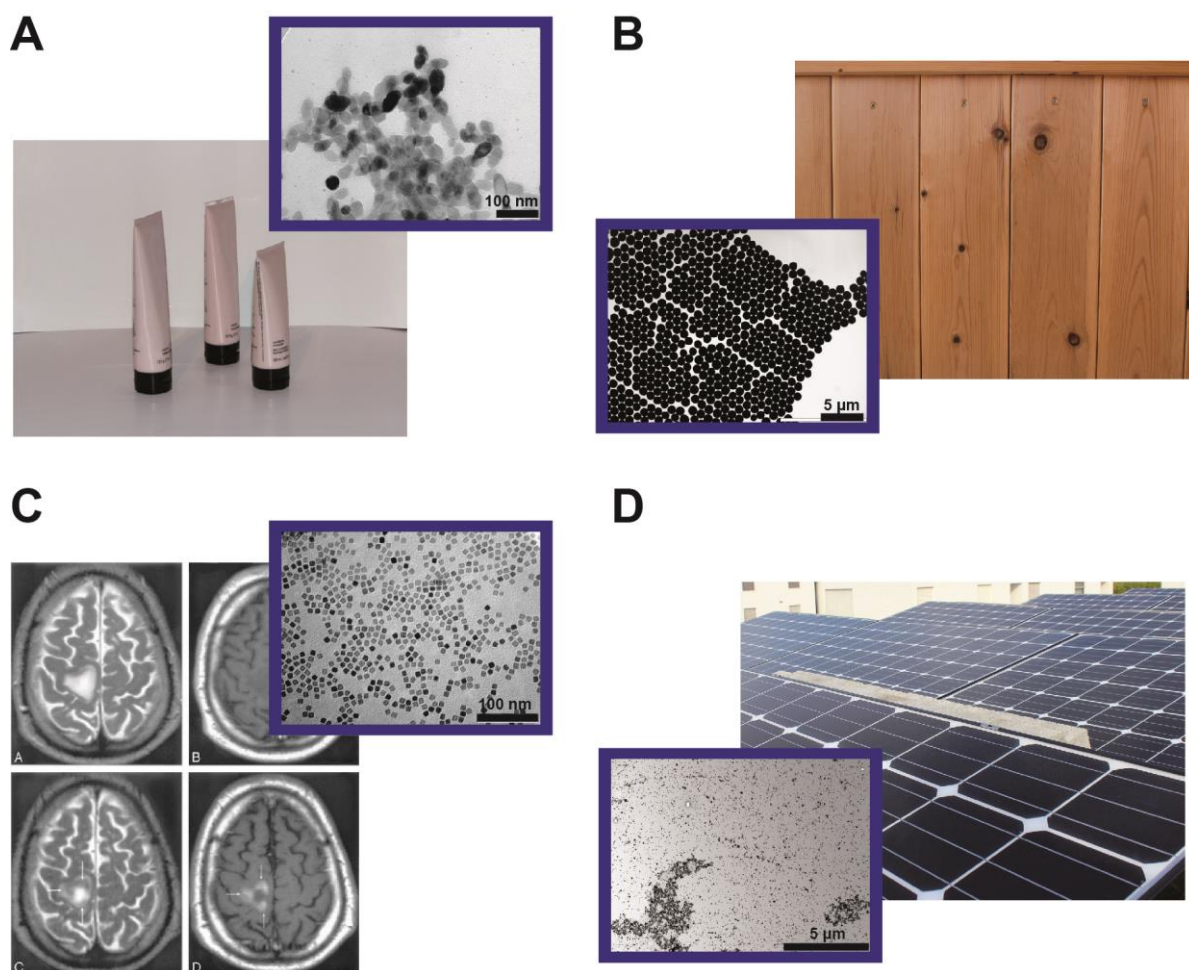


**Figure 1:** TEM micrographs and potential applications of metal oxide nanoparticles: titanium dioxide in cosmetics (A), silicon dioxide in wood preservatives or paints (B), iron oxide nanoparticles as contrast agents in MRI (C) and zinc oxide in solar cells (D). Reprinted with permission from (Wick et al., 2014). MRI image in (C) was adapted with permission from (Mahmoudi et al., 2011), Copyright © 2011, American Chemical Society.

Nanomedicine is a fast growing area and essentially means the application of nanotechnology concepts in medicine. Nanomedical ENMs are developed for diagnostics, imaging as well as for therapeutic use especially in cancer treatment (Riehemann et al., 2009). For example superparamagnetic iron oxide nanoparticles (SPIONs) and silica nanovectors can be used in diverse biomedical applications such as contrast agents in magnetic resonance imaging (MRI), cancer therapy, cell tracking and as drug delivery vehicles (nanocarriers) (Gupta and Gupta, 2005, Tang et al., 2012) (Figure 1C). Most of these ENMs belong to the first generation of nanocarriers and utilize the EPR (enhanced permeability and retention) effect in order to reach their targets, which are mainly tumor cells. In contrast, nanocarriers of the second generation

contain a certain receptor ligand or antibody on their surface, which directs them specifically to the target cells. Often they also comprise a mechanism for drug release after reaching the target cell, e.g. pH-sensitive polymers or SPIONs activated by an external magnetic field. In addition, a third generation of nanocarriers are currently under development and are designed with specific abilities to efficiently overcome biological barriers in order to further enhance the drug concentration in the diseased tissue. Furthermore, nanotechnology contributes significantly to the progression in the field of personalized medicine by providing new tools for the development of biosensors as well as micro- and nanoarrays for diagnostic applications (Riehemann et al., 2009).

ENMs also offer various possibilities in the field of obstetrics. Target-oriented therapy could be used to either specifically treat fetal diseases or placental dysfunctions. Moreover, the number of women needing medication during pregnancy is strongly growing (Andrade et al., 2004, Gendron et al., 2009, Mitchell et al., 2011). In many cases drugs have to be prescribed despite of their known off-target effects and the subsequent potentially harmful influence on the developing fetus. Therefore, nanocarriers without the ability to be transferred to the fetus would be of great interest and solve the problem of teratogenicity (capability of many drugs to cause birth defects).

### **2.1.3 Uptake of nanoparticles**

The small size of ENMs enables them to utilize a broad variety of uptake mechanisms into cells (Treuel et al., 2013, Kettiger et al., 2013, Zhu et al., 2013) (Figure 2). However, the main uptake routes involve vesicular transport. Specialized immune cells (macrophages, monocytes, neutrophils, dendritic cells) engulf larger particles ( $> 500$  nm) via phagocytosis. This process is triggered by different receptors specific for distinct ligands, which are predominantly expressed on pathogens or stressed cells (Aderem and Underhill, 1999). It has been shown that different ENMs are taken up via phagocytosis, even if they have a diameter below 500 nm (Franca et al., 2011, Krpetic et al., 2010, Lunov et al., 2011). Pinocytosis is another mechanism reported to play a role in ENM uptake in non-phagocytic cells (Jin et al., 2009, Xia et al., 2008). Pinocytosis comprises macropinocytosis, clathrin- and caveolin-mediated endocytosis as well as clathrin/caveolin-independent endocytosis. Particles  $> 1$   $\mu$ m and some viruses are commonly ingested unspecifically via macropinocytosis, whereas smaller particles usually utilize other endocytosis pathways (Conner and Schmid, 2003, Mercer and Helenius, 2009, Kettiger et al., 2013). Clathrin-mediated endocytosis is either triggered by receptor binding or by nonspecific

adsorption of cationic ENMs to the negatively charged plasma membrane. ENMs with an average size between 120 – 150 nm and a maximum of 200 nm are internalized via clathrin-dependent endocytosis (Chithrani et al., 2006, McMahon and Boucrot, 2011, Rejman et al., 2004). Caveolin-coated vesicles are usually in a size range between 60 – 80 nm (Parton and Simons, 2007). However, it has been observed that smaller ENMs (20 – 40 nm) are also able to use caveolin-mediated endocytosis and that their uptake is even more efficient compared to larger ENMs (Gratton et al., 2008, Wang et al., 2009). Of note, many caveolin- and clathrin-independent endocytosis mechanisms exist and it is discussed that particles with a diameter of about 90 nm or larger get access into cells via such pathways (Mayor and Pagano, 2007). Most vesicles enter the endosomal/lysosomal trafficking route, but transcytosis is also possible especially in polarized barrier cells (Conner and Schmid, 2003). Additionally, some few studies reported a passive uptake pathway of ENMs in erythrocytes, which lack conventional endocytosis mechanisms (Rothen-Rutishauser et al., 2006, Wang et al., 2012). These findings demonstrate that different cell types can interact differently with the same ENMs.

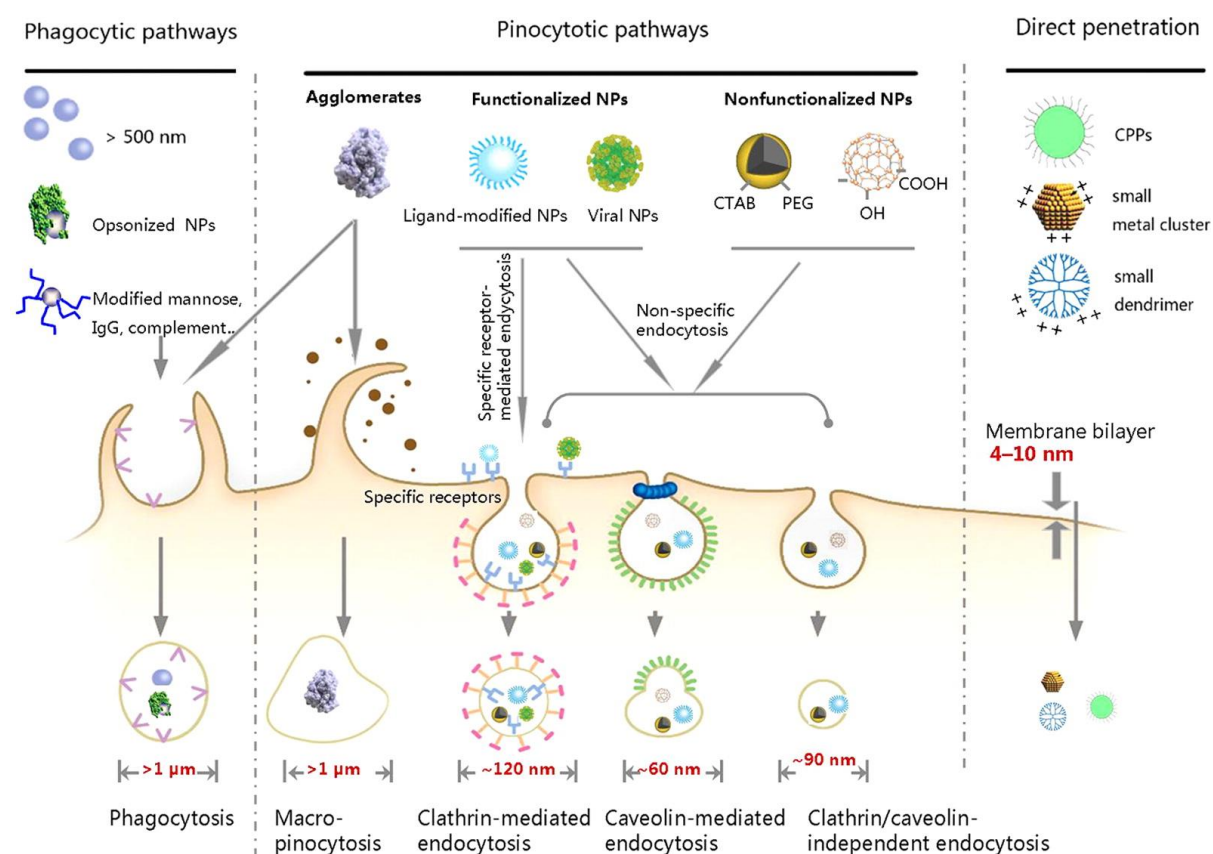


**Figure 2:** Schematic illustration of potential cellular uptake mechanisms for ENMs. Adapted with permission from (Zhu et al., 2013), Copyright © 2013, American Chemical Society.

Besides cellular mechanisms, the characteristics of ENMs are also major determinants of cellular uptake. ENMs with a diameter of about 50 nm are internalized faster and more efficiently than smaller (15 – 30 nm) or larger (70 – 240 nm) particles (Chithrani et al., 2006, Lu et al., 2009). In addition, ENMs with a size of 30 – 50 nm have a greater potential to interact with diverse cellular receptors and induce receptor-mediated endocytosis (Kettiger et al., 2013, Lu et al., 2009). The shape of ENMs also influences cellular uptake. Spherical ENMs enter cells more easily compared to elongated ENMs such as carbon nanotubes (Champion et al., 2007, Ferrari, 2008). Surface properties (surface charge and surface modifications) of ENMs are also important factors. In most cells cationic ENMs are more efficiently taken up due to their strong interaction with the anionic plasma membrane and subsequent induction of adsorption-triggered endocytosis (Qiu et al., 2010, Xia et al., 2008).

After contact with a biological environment ENMs acquire a protein corona dependent on their size, shape, chemistry and surface characteristics. Proteins and other biomolecules contained in plasma or other biological fluids are adsorbed to the surface of ENMs. This protein corona leads to an altered hydrodynamic diameter and net charge of ENMs. Consequently, these adsorbed proteins can considerably change the mechanisms of cellular uptake (Hirsch et al., 2013, Lundqvist et al., 2008, Monopoli et al., 2011).

#### **2.1.4 Safety of nanoparticles**

Besides the great opportunities for various new applications of nanotechnology, the potential risks of ENMs on human health should not be neglected. Risk assessment of ENMs comprises the evaluation of exposure as well as the identification and characterization of the hazard. Exposure relates to the probability to be exposed to a critical dose of ENMs in the environment, while hazard refers to the biological effect of ENMs (Krug and Wick, 2011). To cause adverse effects ENMs have to cross certain primary biological barriers (Ferin et al., 1992), except if they are administered directly by intravenous injection. The role of biological barriers is discussed in the following section 2.2.1. This section is focused on the exposure scenario of nanomedical ENMs. When ENMs enter the blood stream, they will adsorb proteins or they can also be opsonized by other biomolecules, which results in a rather fast clearance by the phagocytes of the reticuloendothelial system (RES) (Garnett and Kallinteri, 2006). ENMs with a diameter between 5 – 10 nm are eliminated by glomerular filtration in the kidney (Choi et al., 2007). All particles, which escape these protecting mechanisms, predominantly accumulate in the liver, lung and spleen (Semmler-Behnke et al., 2008, Xie et al., 2010). Like

ENM uptake, biodistribution of ENMs is dependent on the physicochemical characteristics (Kunzmann et al., 2011, Nel et al., 2009). For example hydrophobic ENMs are faster removed from the blood circulation by cells of the RES than hydrophilic ENMs (Duan and Li, 2013, Gessner et al., 2000, Shah et al., 2012). To prolong the circulation time, many medical ENMs are coated with polyethylene glycol (PEG), which reduces the opsonization with biomolecules and thus diminishes or even prevents the recognition and clearance by the RES (Shah et al., 2012, Owens and Peppas, 2006).

Many epidemiological, *in vitro* and *in vivo* (in animal models) studies have been performed during the last years to analyze the toxicity and hazard of ENMs and revealed that ENMs can have several adverse effects on health (Oberdorster et al., 2005). The skin, respiratory, cardiovascular, nervous and reproductive system could be negatively affected by ENMs (Pietrojusti, 2012). On a cellular level it has been observed that ENMs may cause cytotoxicity, inflammation, genotoxicity and oxidative stress dependent on their physicochemical properties (Nel et al., 2006, Nel et al., 2009). For example carbon nanotubes longer than 20  $\mu\text{m}$  and with a diameter less than 3  $\mu\text{m}$  cannot be internalized by phagocytes and induce inflammation, fibrosis or even cancer in the lung (Oberdorster, 2002, Donaldson et al., 2013).

Few years ago, three principles about nanotoxicology were published in order to elucidate if ENMs possess unique features leading to different interactions at the nano-bio interface compared to their bulk material (Krug and Wick, 2011, Nel et al., 2006). The transport principle was already discussed on the previous section and is based on the small size of ENMs, which enables them to use different uptake pathways. Many metal oxide nanoparticles are slowly dissolving and therefore the ionic forms of the metal can be found. An imbalance in cellular ion balance has fatal consequences. Therefore, cellular ion transport is strongly regulated. However, ENMs can infiltrate cells via diverse pathways and release ions once they are inside the cells inducing severe cytotoxic effects. This effect is termed ‘Trojan Horse Mechanism’ and is very specific for ENMs (Deng et al., 2009, George et al., 2010, Limbach et al., 2007, Park et al., 2010). The surface principle describes the consequences of the high surface-to-volume ratio of ENMs. If the same mass of differently sized ENMs is taken, the specific surface and the particle number are significantly higher for smaller ENMs. This makes more chemical reactive groups available on the surface and offers more possibilities for nano-bio interactions (Nel et al., 2006). The material principle refers to the many different materials from which ENMs can be composed of. Different chemistry can induce distinct effects in cells (Brunner et al., 2006, Gojova et al., 2007). It becomes evident that nanomaterials have unique



properties and a different behavior than the bulk material, which requires that the toxicological effects of ENMs in biological systems have to be studied in a systematic manner. This study domain is known as Nanotoxicology.

## 2.2 The human placenta

### 2.2.1 Biological barriers

Biological barriers build the border between different compartments inside the body as well as between an organism and its environment. They strongly regulate the exchange of diverse substances such as nutrients, gases or water between these interfaces. Depending on their specific function biological barriers consist of several layers and different cell types. In humans the skin, the lung, the intestine and the olfactory epithelium are barriers, which either directly face the environment e.g. the air or are in contact with fluids containing exogenous substances in case of the intestine. If a substance is able to cross one of these primary barriers and enter the blood stream, the endothelium of the capillaries constitutes the next hurdle before it can reach other internal organs. The endothelium in most tissues is continuous with strong tight junctions and a close connection to the basement membrane (Mehta and Malik, 2006). Though, in some specialized organs such as the liver and the spleen the endothelium is fenestrated and allows also transfer of larger molecules, proteins or particles. In contrast, special internal barriers like the placenta, the blood-brain and blood-retinal barrier are required to protect organs or tissues, which are particularly susceptible to potentially toxic exogenous substances and to disturbance of the homeostasis. They are composed of highly specialized cells, which regulate the transport of nutrients, gases and xenobiotics. The placenta is a barrier with a unique physiology and structural complexity (Huppertz and Gauster, 2011). The placenta is probably the most important barrier at all due to its function to feed and protect the sensitive developing fetus. The consequences of placental dysfunctions are absolutely detrimental for the fetus.

### 2.2.2 Structure and functions of the placenta

#### *Human placental development and structure*

The placenta is mainly derived from fetal tissue. Four days after fertilization the morula (developmental embryonic stage with 16 cells) develops into the blastocyst, which consists of an outer cell layer and a fluid filled cavity with an inner cell mass. The embryo arises from the inner cell mass whereas the placenta originates from the outer trophoblast cells. Six days after gestation, the blastocyst begins to attach to the endometrium (the inner layer of the maternal uterus) and placenta development is initiated (Verma and Verma, 2013). The trophoblast cells in the outer blastocyst layer give rise to two different trophoblast populations, the

mononucleated cytotrophoblast and the multinucleated syncytiotrophoblast (Benirschke, 2012). These cell types are the basis of the first primary placental villi, which start to invade the uterus wall. The syncytiotrophoblast is formed by fusion of several trophoblasts and builds the outer layer of the villous placental structure facing the maternal side, while the mononucleated cytotrophoblasts line the inner surface of the villi. It has been shown that the development and differentiation of the syncytiotrophoblast is mainly driven by cyclic adenosine monophosphate (cAMP), epidermal growth factor (EGF) and human chorionic gonadotropin (hCG) (Maruo et al., 1987, Ringler et al., 1989, Shi et al., 1993). At the tip of the invading villi some cytotrophoblasts differentiate further into the invasive extravillous trophoblasts. These cells infiltrate all layers of the uterus as well as the uterine arteries leading to the formation of lacunas filled with maternal blood. Later these blood filled sinuses develop into the huge intervillous space, where the maternal blood enters via the spiral arteries and leaves through endometrial veins. The human placenta has a hemochorial structure, which means that the fetal villi extend into the intervillous space and the maternal blood has direct contact with the fetal syncytiotrophoblast (Figure 3). Subsequently, the primary villi mature into secondary villi by acquiring an inner core filled with extraembryonic mesoderm. After three weeks of gestation these mesenchymal cells give rise to the fetal capillaries and the connective tissue containing fibroblasts and macrophages (Hofbauer cells) (Figure 3). The fetal capillaries of these tertiary villi are successively connected to the vessels of the umbilical cord.

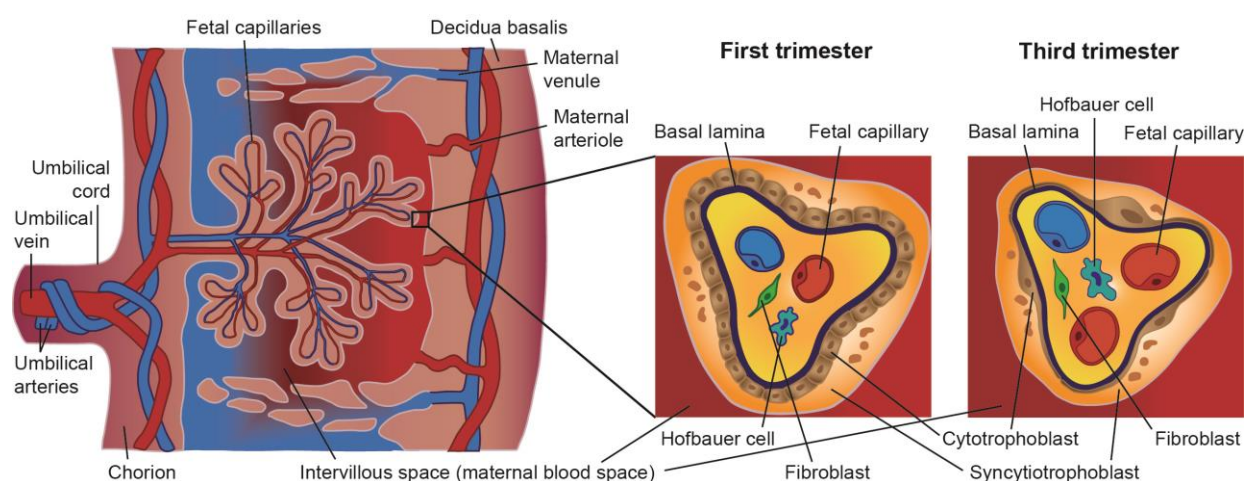


**Figure 3:** Illustration of the placental structure in humans. Left panel depicts an overview of one cotyledon, the middle and right panels demonstrate the structure of the cellular barrier during early (first trimester) and late (third trimester) pregnancy. Graph on the left was modified from (BIOG, 2013). Magnified illustrations on the right were adapted by permission from Macmillan Publishers Ltd: Nature Reviews Genetics (Rossant and Cross, 2001), Copyright © 2001.

During the first trimester (week 1 to 12 of gestation) the fetal-maternal barrier comprises the endothelial cells of the fetal capillaries embedded in the connective tissue and two continuous layers of trophoblast cells, the inner layer of cytotrophoblasts and the multinucleated syncytiotrophoblast (Figure 3). During progression of pregnancy the inner cytotrophoblast layer gets thinner, the number of fetal capillaries rises and the capillaries move closer to the syncytiotrophoblast. In the third trimester (week 28 of gestation until birth) only few single mononucleated cytotrophoblasts are left (Figure 3, Figure 4) (Juch et al., 2013, Syme et al., 2004, Verma and Verma, 2013). Moreover, maternal blood flow is marginal until week 10 – 11 post conception in order to maintain hypoxic conditions in the placenta. During early development, the embryo is highly vulnerable for oxidative stress and increase in placental oxygen pressure is associated with severe pregnancy complications such as spontaneous abortion, intrauterine growth restriction or preeclampsia (Burton and Jauniaux, 2011, Burton et al., 2009). To prevent substantial maternal blood flow in this early phase, the spiral arteries are plugged by extravillous cytotrophoblast cells (Duc-Goiran et al., 1999). Hence, maternal blood cells have to pass this cellular filter via intercellular channels to access the intervillous space. Successively, these cellular plugs vanish, the spiral arteries gain a direct connection to the intervillous space and perfusion with maternal blood is completely established at the end of the first trimester (Burton et al., 1999). Overall, these structural changes of the placenta during development, lead to an improved exchange of nutrients between the mother and the fetus (Verma and Verma, 2013). The fetal side of the term placenta with all fetal vessels emanating from the umbilical cord is named the chorionic plate or chorion. The part of the maternal endometrium contributing to placentation is called the decidua basalis. From the decidua several septa divide the placenta in different functional units, the cotyledons, of which each includes one fetal villous tree. At term the placenta consist of 20 - 40 cotyledons with a total exchange area of about  $13\text{ m}^2$  (Larsen et al., 1995, Syme et al., 2004) (Figure 5). This large surface is generated through the extensive division of the fetal villi in a tree-like structure and through the microvillous structure of the syncytiotrophoblast at the brush border membrane, which faces the maternal blood sinus (Figure 4D). The membrane of syncytiotrophoblast touching the villous stroma is the basal membrane.

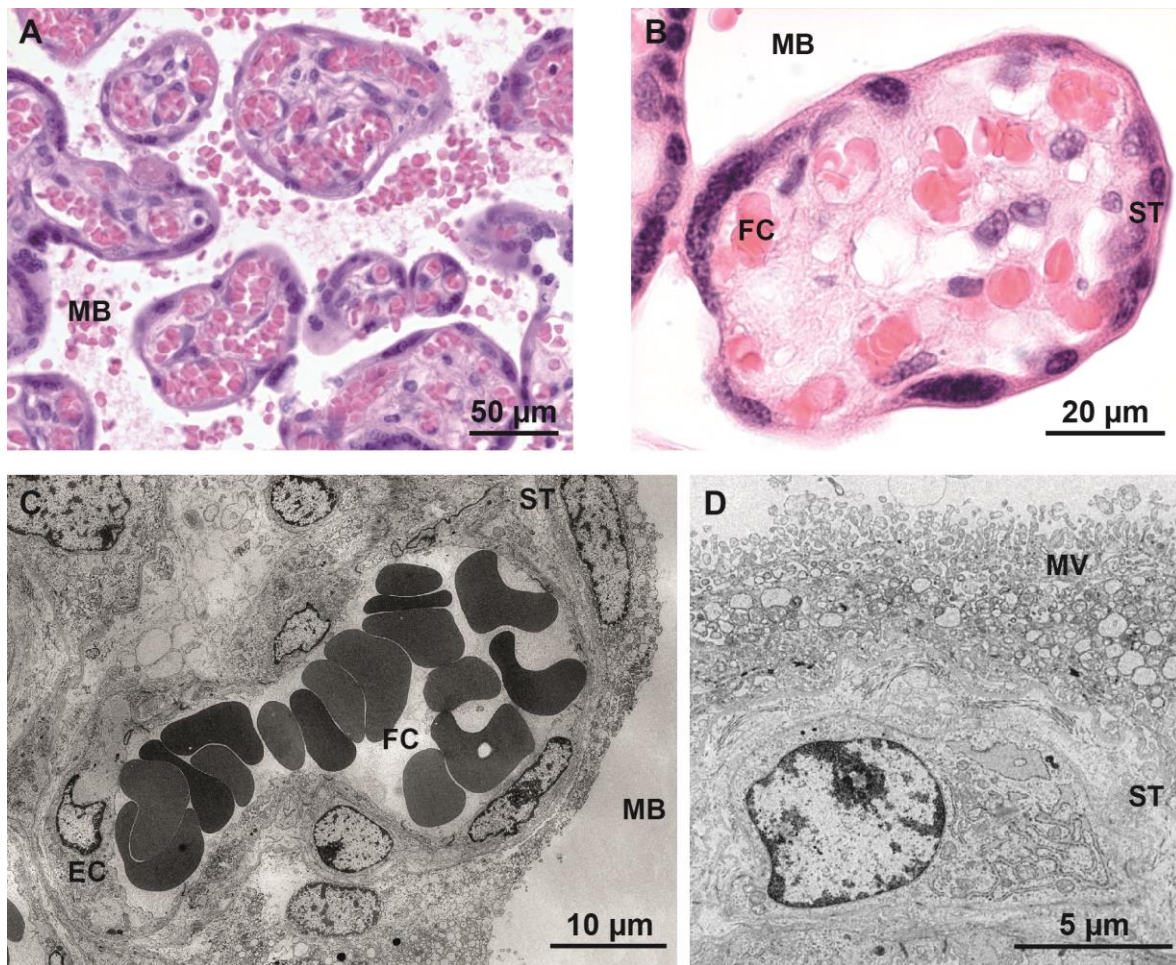


**Figure 4:** (A + B) Images from light microscopic analyses of human placental tissue at term after hematoxylin/eosin (HE) staining. The samples were prepared and analyzed in collaboration with the Department of Pathology at the Cantonal Hospital in St. Gallen. (C + D) TEM micrographs demonstrate the cellular structure of human placental tissue at term. The samples were prepared and analyzed by Liliane Diener at Empa St. Gallen. MB: maternal blood space; FC: fetal capillary; ST: syncytiotrophoblast; MV: microvilli of the brush border membrane of the syncytiotrophoblast

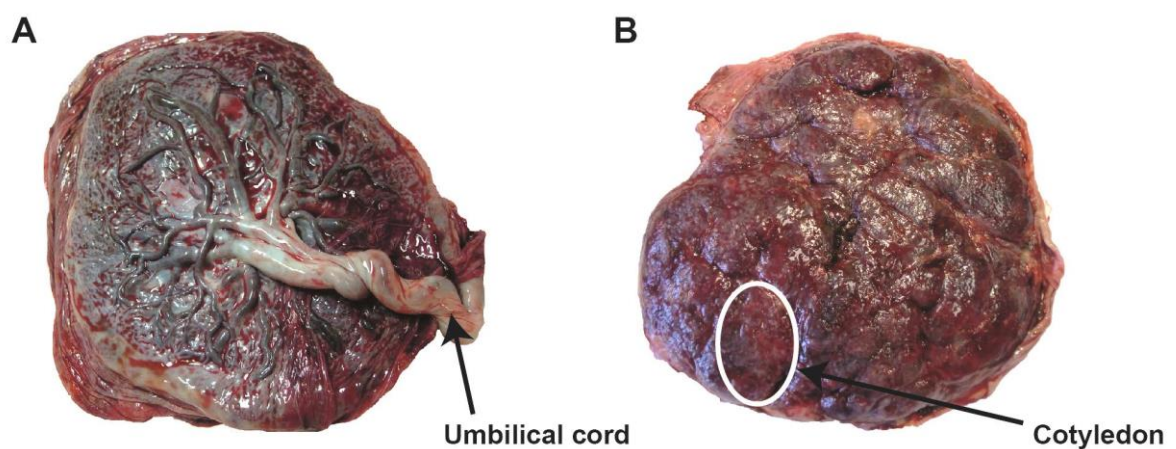


**Figure 5:** Macroscopic images of the human placenta after delivery. The picture shows the (A) fetal side with the chorionic plate and the umbilical cord and (B) the maternal side with several cotyledons.



### *Interspecies differences in placental structure*

The structure of the placenta differs massively between mammals. Three major types of placentas can be distinguished: the hemochorial (e.g. in humans, rodents, primates), the endotheliochorial (e.g. in dogs, cats) and the epitheliochorial (e.g. in pigs, horses, sheep) type. They mainly differ in the organization of the maternal side. As mentioned above, in the hemochorial placenta the fetal trophoblast is directly exposed to the maternal blood, whereas in the endotheliochorial placenta the trophoblast and the maternal blood are separated by an additional layer of maternal endothelial cells or in case of the epitheliochorial placenta by a layer of uterine epithelial cells (Enders and Blankenship, 1999).

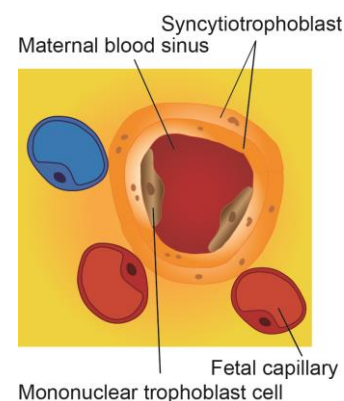


**Figure 6:** Hemotrichorial structure of the mouse placenta with three trophoblast layers.

Each placental type can even be further divided in several subclasses. A hemochorial placenta can have a single trophoblast layer at term such as the human placenta (hemomonochorial), or up to three trophoblast layers such as the mouse placenta (hemotrichorial) (Figure 6). Furthermore, the placenta can be organized in different zones with distinct functions. For example the mouse placenta consists of a junctional zone associated with the endocrine function and a labyrinthine zone for the feto-maternal exchange (Dilworth and Sibley, 2013). In humans the syncytiotrophoblast layer throughout the whole placenta conducts both placental functions. In addition, the human placenta has a unique multivillous blood perfusion system with a pulsatile flow, while the labyrinth of the mouse placenta embraces a normal capillary bed (Benirschke, 2012). All these anatomical differences can lead to differences between different species concerning placental functions e.g. transport of xenobiotics (Dilworth and Sibley, 2013, Syme et al., 2004).

### *Functions*

The placenta has various important functions to assure the proper development of the fetus. It regulates the exchange of nutrients, gases and waste products between mother and fetus, mediates maternal tolerance to fetal tissues and secretes hormones to maintain the pregnancy.

**Endocrine functions:** The syncytiotrophoblast produces a broad variety of hormones such as peptide and steroid hormones. Human chorionic gonadotropin (hCG) is the earliest secreted product of the fetal trophoblastic tissue. It guarantees continuation of pregnancy, promotes

normal placental development, is involved in implantation and regulates trophoblast differentiation in an autocrine as well as paracrine manner (Verma and Verma, 2013). Human chorionic gonadotropin is widely used as marker for the endocrine function of healthy trophoblasts in several *in vitro* and *in vivo* placenta models (Malek et al., 2001, Prouillac and Lecoeur, 2010). Human placental lactogen (hPL) belongs also to the peptide hormones produced by the syncytiotrophoblast and controls the lipid and carbohydrate metabolism of the mother throughout pregnancy to ensure an optimal nutrient supply for the fetus (Verma and Verma, 2013). Leptin is another pleiotropic peptide hormone and is produced by many different organs such as adipose tissue, skeletal muscle, pituitary gland cells as well as placental trophoblast cells. Leptin modulates predominantly satiety and energy homeostasis in all mentioned tissues and not only during pregnancy. In the placenta leptin acts in an autocrine way and prevents apoptosis of trophoblast cells by promoting cell survival and proliferation, especially during implantation (Pérez-Pérez et al., 2013). Of note, there are many more peptide hormones produced by the placenta, like corticotropin releasing hormone (CRH), insulin-like growth factors (IGF), vascular endothelial growth factor (VEGF) or placental growth factor (PGH), which are involved in maintenance of pregnancy and adequate nutrient supply. Trophoblast cells also secrete large amounts of steroid hormones such as estrogen and progesterone. Progesterone plays an important role in preventing immunological rejection due to its anti-inflammatory and immunosuppressive functions. In addition, it decreases the contractility of uterine smooth muscle cells to ensure a relaxed uterus during pregnancy (Verma and Verma, 2013).

***Transport functions:*** The key function of the placenta is the supply of the fetus with nutrients, exchange of gases and the removal of waste products from the fetal circulation. Transport across barriers can occur via passive or active (energy-dependent) mechanisms. Passive mechanisms are energy-independent, whereas active mechanisms rely on the consumption of energy. The highly polarized syncytiotrophoblast with its two membranes carrying distinct transport proteins is the key exchange surface in the human term placenta (Menezes et al., 2011). Therefore the transport mechanisms discussed below refer mainly to the syncytiotrophoblast. However, most of the pathways can also occur at the continuous endothelial layer of the fetal vessels, which mainly acts as restrictive molecular sieve (Firth and Leach, 1996).

Small non-polar, lipophilic molecules and gases cross the placental barrier by simple diffusion. Simple diffusion is the passive transfer of a substance driven by a concentration gradient. In biological systems such as the placenta diffusion is also dependent on the permeability of the barrier, the exchange surface area, the blood flow, the physicochemical properties of the substance and its capability to bind to plasma proteins or to placental tissue (Menezes et al., 2011, Syme et al., 2004, Malek and Bersinger, 2013). Furthermore, the placenta pH plays also a role during placenta transfer. Due to the more acidic pH in the fetal blood compared to the maternal circulation, weak bases are often more ionized in the fetal compartment, which can lead to a higher concentration of the free unionized substance in the maternal blood and consequently creates gradient towards the fetus (Syme et al., 2004). Hydrophilic substances with low molecular weight like glucose can be still passively transferred across the placenta via facilitated diffusion through specialized carrier proteins or transporters, which are highly expressed at the brush border and basal membrane of the syncytiotrophoblast. This mechanism does not require energy, but is dependent on a concentration gradient and can be saturated at high concentrations (Syme et al., 2004). Water can enter the placenta through aquaporins or water channels in the syncytiotrophoblast membrane mainly driven by a pressure gradient (bulk flow) (Verma and Verma, 2013).

Most ionized substances and large lipophilic molecules (molecular weight > 500 Da) have to be actively transported across the placenta (Syme et al., 2004). One possible mechanism is vesicular transport (Malek and Bersinger, 2013). Endocytotic vesicles are transported from the apical brush border membrane to the basal membrane of the syncytiotrophoblast (transcytosis) where they fuse again with the plasma membrane and release their content on the other side of the barrier. Transport of maternal IgG (immunoglobulin G) antibodies occurs via transcytosis, which is in this particular case receptor-mediated. Binding to a receptor on the brush border membrane specific for IgG initiates the endocytosis (Malek and Bersinger, 2013). Another active transport mechanism is passage through a specific transporter, which either requires hydrolysis of adenosine triphosphate (ATP) or an electrochemical gradient. The brush border and the basal membrane express a broad repertoire of different influx and efflux transport proteins (Ganapathy et al., 2000, Prouillac and Lecoecur, 2010). For example amino acids, folic acid and nucleosides are transported via such specific transport proteins. An important group of transport proteins highly expressed at the placental barrier is the ATP-binding cassette (ABC) transporter family. P-glycoprotein is one pharmacological relevant member of this family, located at the brush border membrane and responsible for the efflux transport of many different



cationic xenobiotics including morphine derivatives, antibiotics, anti-cancer as well as antiretroviral drugs (Ganapathy et al., 2000).

Some studies proposed the existence of transtrophoblastic channels with a diameter around 20 nm as another placental transfer route. Electron micrographs of the placenta from several species showed a narrow branched channel system through the syncytiotrophoblast, which may be responsible for the regulation of fetal water balance (Kertschanska et al., 1997, Kertschanska et al., 2000). However, these findings are controversially discussed and reliable evidence is still missing (Menezes et al., 2011).

***Metabolic functions:*** The extensive metabolic activity of the placenta is strongly associated with the endocrine and transport functions of the placenta and should also guarantee an appropriate supply with nutrients. This metabolic activity involves modifications, conversions, storage and synthesis of lipids, proteins, amino acids, vitamins and carbohydrates as well as detoxification of potential harmful exogenous or endogenous substances via different metabolizing enzymes such as the cytochrome P450 enzymes (Mathiesen and Knudsen, 2013, Verma and Verma, 2013).

***Immunologic functions:*** HLA tissue antigens (HLA-A,-B,-C) or major histocompatibility complexes (MHC) vary extremely between individuals and present small peptides derived from self or foreign proteins to T lymphocytes. Since the developing embryo inherits only one allele from the mother, the parental HLA antigens would be recognized as non-self by the maternal T cells which leads to rejection of the embryo. However, the absence of HLA tissue antigens on the syncytiotrophoblast as sole cell layer with direct contact to immune cells in the maternal blood, prevents fetal rejection by the maternal immune system (Verma and Verma, 2013). Additionally, maternal immunological tolerance against the fetus is also sustained by placental secretion of immunosuppressive factor such as progesterone from the syncytiotrophoblast and cytokines (e.g. IL-10 and TGF- $\beta$ ) from decidua macrophages (Szekeres-Bartho et al., 1997, Cupurdija et al., 2004).

### **2.2.3 Models to study placental transfer**

Decades ago the placenta was considered as an impenetrable barrier. However, not only the discovery of the thalidomide induced birth defects in the 1960's, but also the growing perception that environmental pollutants and many drugs are able to cross the placenta, led to a huge change in this mind-set (Martin and Holloway, 2014). Today, developmental toxicology of xenobiotics is an active field of research. Numerous studies show that the number of women who need medication during pregnancy is continuously increasing (Andrade et al., 2004, Gendron et al., 2009, Mitchell et al., 2011). Hence, a careful assessment of placental translocation of these drugs is necessary. Obviously, placental functions cannot be studied directly in pregnant women due to ethical concerns. Therefore, many placental models have been developed and used to study placental transfer and metabolism as well as embryo implantation. Cells and tissue isolated from the human placenta can be only obtained after informed consent of the pregnant woman and with approval of the local ethics committee.

#### ***Placental membrane vesicles***

Membrane vesicles can be isolated from the human term syncytiotrophoblast and prepared from the brush border or basal membrane in order to study the expression and activity of specific transport proteins on each membrane separately (Boyd, 1991). Certainly, this model is least reflecting the *in vivo* situation, because of the lacking regulatory factors (Prouillac and Lecoecur, 2010).

#### ***Placental tissue explants***

Villous explants are obtained from the human placenta, can be cultured *in vitro* and include trophoblastic, stromal, endothelial, blood as well as immune cells. They are used to study uptake of different substances, metabolism, endocrine functions, cell proliferation and differentiation. Although real kinetic transfer studies from the maternal to the fetal circulation are not feasible and blood flow is missing in this model, it offers the great possibility to investigate also pathological placental tissue and placental tissue from early gestation from terminated pregnancies (Miller et al., 2005).

### ***Placental cell models***

Many immortal cell lines with placental origin are available to model the placental barrier. The most frequently used cell type is the BeWo cell line derived from a human malignant gestational choriocarcinoma. BeWo cells resemble undifferentiated cytotrophoblasts and are used to examine placental metabolism, trophoblast differentiation and syncytium formation (Prouillac and Lecoeur, 2010, Wice et al., 1990). Moreover, BeWo cells are cultured on a permeable membrane insert in a transwell system (Figure 7). This model is widely used to study the transport of various endogenous and exogenous substances (Li et al., 2013, Mathiesen et al., 2014, Bode et al., 2006). Additionally, there are also the less frequently used JEG-3 and JAR cell lines, which are derived from BeWo cells. However, it is controversially discussed if JEG-3 and JAR cells are also able to form a polarized monolayer such as BeWo cells, which is required for transplacental transfer studies (Bode et al., 2006). In general, the transwell model is suitable for long-term exposure studies and cell lines are easy to handle, but the model still lacks flow and tissue integrity including the endothelial cells which also contribute to the placental barrier. An alternative for BeWo cells is the isolation of primary cytotrophoblasts from the human placenta (Petroff et al., 2006). These cells form spontaneously a syncytium *in vitro*, but they do not build a tight confluent monolayer and are not viable for many passages (Liu et al., 1997, Yui et al., 1994). The advantages and disadvantages of BeWo and human primary trophoblast cells are discussed in more detail in chapter 3, part IV.

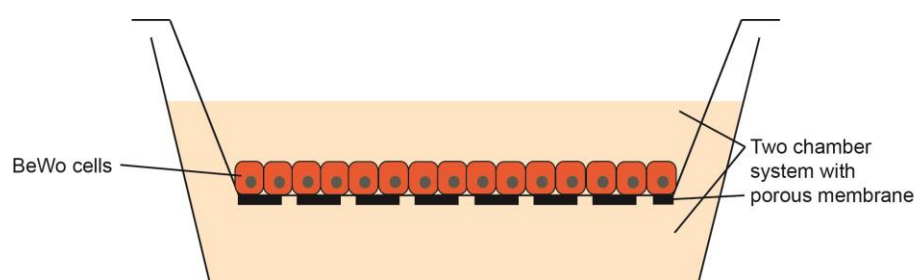


**Figure 7:** Transwell model with BeWo cells to investigate placental transfer of xenobiotics. BeWo cells were cultured on a porous membrane. The xenobiotic of interest is added to the apical chamber and the transport into the basal chamber can be monitored over time. Adapted with permission from (Wick et al., 2014).

### ***Ex vivo human placental perfusion***

The *ex vivo* human placental perfusion model is the ‘gold standard’ for transplacental transfer studies providing reliable data with a high predictability for the *in vivo* transfer (Grafmüller et al., 2013, Hutson et al., 2011). Human placentas are obtained immediately after delivery and are reperfused *ex vivo*. This method was extensively used and further optimized during my PhD project. The detailed perfusion procedure as well as the benefits and limitations of this model are described thoroughly in chapter 3, part I.

### ***Fetal/maternal blood concentration ratio***

The transfer of substances, which are administered during pregnancy anyway to treat severe diseases of the mother such as epilepsy, is often evaluated by analyzing the concentration in the maternal blood and the umbilical cord blood representing the fetal circulation. The ratio of both concentrations illustrates transport rate of the drug. Though, in this method the influence of placental drug metabolism and drug distribution in the fetal tissue are not considered (Prouillac and Lecoœur, 2010).

### ***Animal models***

Many placental transfer studies have been performed in mice and rats (Campagnolo et al., 2013, Challier et al., 1973, Yamashita et al., 2011). Rodent models are perfectly suitable to investigate biodistribution and developmental toxicity of a specific xenobiotic. Nevertheless, the translation of data concerning placental transfer of xenobiotics obtained in a rodent model to humans is difficult or even impossible due to the huge differences in placental structure, physiology and implantation between the mammalian species (see section 2.2.2). Of course, the usage of nonhuman primates like chimpanzees with a similar placental structure (compared to humans) for placental transfer studies would lead to more predictable and transferrable results, but intensive costs, complex handling as well as ethical concerns will constrain the application of such models.

### 2.2.4 Current knowledge about nanoparticle-placenta interactions

We are exposed to engineered nanomaterials (ENM) in our daily life. Their increasing application in several products also raised major concerns about reproductive toxicology of these ENMs. Recently, Buerki-Thurnherr et al. reviewed current studies on nanoparticle-placenta interactions (Buerki-Thurnherr et al., 2012). Several epidemiological studies demonstrated that exposure to particulate matter (PM10 includes particles with an aerodynamic diameter  $< 10 \mu\text{m}$  and PM2.5 comprises particles with an aerodynamic diameter  $< 2.5 \mu\text{m}$ ) in ambient air during pregnancy is linked with lower birth weight, preterm birth and a higher incidence of respiratory diseases (Bobak, 2000, Lacasana et al., 2005, Huynh et al., 2006, Latzin et al., 2009, Shah et al., 2011). However, none of these studies provides evidence if these birth outcomes were caused direct by adverse effects of the particles transported across the placenta or indirect by induction of inflammation in the mother and transmission of mediators to the placenta and the fetus. To clarify the ability of nanoparticles to overcome the placental barrier and induce acute toxicity in the placenta and the fetus, many different studies were performed using rodent and *in vitro* cell culture models as well as the *ex vivo* perfusion model.

Exposure to combustion derived diesel exhaust particles in pregnant mice lead to inflammatory responses and DNA damage in the litter (Fujimoto et al., 2005, Reliene et al., 2005, Auten et al., 2012). First proof that low amounts 1.4 nm and 18 nm gold particles cross the placental barrier in a size-dependent manner have been shown in rats after intratracheal instillation and intravenous injection (Semmler-Behnke et al., 2008), while previous studies with gold colloid and particle exposure during pregnancy in mice did not illustrate any significant placental transfer (Challier et al., 1973, Sadauskas et al., 2007). Later investigations on gold nanoparticles also demonstrated uptake of gold particles in the murine placenta as well as transplacental transfer, but no toxic effects on the offspring were found (Rattanapinyopituk et al., 2014, Tian et al., 2013, Yang et al., 2012).

In contrast, other ENMs such as titanium dioxide nanoparticles, amine-modified polystyrene beads, quantum dots, cadmium oxide nanoparticles, fullerenes, silver nanoparticles, silica particles and different carbon nanotubes have been reported to negatively influence the fetus in mice or rats (Blum et al., 2012, Campagnolo et al., 2013, Chu et al., 2010, Hougaard et al., 2010, Huang et al., 2014, Melnik et al., 2013, Onoda et al., 2014, Pietroiusti et al., 2011, Qi et al., 2014, Refuerzo et al., 2011, Shimizu et al., 2009, Stapleton et al., 2013, Sumner et al., 2010, Takeda et al., 2009, Tian et al., 2009, Yamashita et al., 2011, Yoshida et al., 2010).

Adverse effects such as low birth weight, higher abortion rate and impaired fetal growth, reproductive functions and neurobehavioral alterations of the litter were observed. The findings concerning placental transfer of these ENMs were quite controversial probably because of the different routes of particle administration, the model animal, particle coating and size.

Transfer of polystyrene, PLGA (poly D,L-lactide-co-glycolide), iron oxide and silica particles also occurs *in vitro* in the BeWo transwell model (Ali et al., 2013, Cartwright et al., 2012, Correia Carreira et al., 2013, Sonnegard Poulsen et al., 2013). Iron oxide nanoparticles even induce cytotoxicity in BeWo cells (Correia Carreira et al., 2013, Faust et al., 2014). Of note, cobalt-chromium nanoparticles indirectly cause DNA damage in fibroblast across a BeWo cell barrier *in vitro* by stimulation of cytokine production. Interestingly, the effect is more prominent with increasing thickness of the BeWo cell layer (Bhabra et al., 2009, Sood et al., 2011).

In contrast to the results of the animal experiments, gold particles show no significant transfer in the *ex vivo* human placental perfusion model, while low transfer is observed for silica particles, polystyrene beads and dendrimers (Menjoge et al., 2011, Myllynen et al., 2008, Sonnegard Poulsen et al., 2013, Wick et al., 2010).

Although many research studies about placental transfer of ENMs exist, only few investigated the determinants of transfer in a relevant experimental set-up allowing data translation to the human system. For example polystyrene beads are transported dependent on their size across a BeWo cell layer and across the placental barrier during *ex vivo* perfusion with a higher transfer of smaller beads (Cartwright et al., 2012, Wick et al., 2010). However, systematic approaches investigating a broader variety of particles physicochemical properties (e.g. surface charge or particle chemistry) responsible for placental transfer are still missing.

## 2.3 Aim of the thesis

It becomes increasingly evident that a better understanding of nanoparticle-placenta interactions is urgently required. Since many women take medication during pregnancy, this is particularly important for reproductive toxicology to ensure the safety of existing ENMs and to prevent another case of deleterious impacts on fetal development as it happened with thalidomide (Martin and Holloway, 2014, Mitchell et al., 2011). Furthermore, nanotechnology also offers the opportunity to develop new target-orientated treatments using ENMs as drug carriers to either specifically treat fetal disorders (e.g. intrauterine growth restriction), placental complications (e.g. preeclampsia) or maternal diseases (e.g. diabetes, epilepsy). To specifically design nanoparticles for these purposes a greater knowledge about the physicochemical properties of nanoparticles, which determine the placental transfer in humans, and a better understanding of placental transport mechanisms of ENMs are indispensable. Only few studies dealt with these questions and most of them were performed in animal models, which should be interpreted with caution due to the huge interspecies differences in placental anatomy (see section 2.2.2 and 2.2.4).

The aim of this study was to determine the influence of particle properties such as chemistry and surface modifications on placental transfer as well as the main transport mechanisms responsible for placental nanoparticle transfer in humans. As a model for investigation, the *ex vivo* human placental perfusion model was chosen based on its reliable prediction of the *in vivo* placental transfer (Hutson et al., 2011). However, since the *ex vivo* human placental perfusion model also has its limitations and is not applicable to screen a broad variety of ENMs with different properties, physiologically relevant advanced placental *in vitro* models have to be developed. Most placental *in vitro* models include BeWo cells, however it is not known yet if these tumor-derived cells are appropriate to reflect the placental barrier. Therefore, acute and subacute toxic effects of ENMs on primary human cytotrophoblast cells and BeWo cells have to be assessed in order to reveal if BeWo cells show similar responses as primary cells, which are considered as the physiological more relevant cell type.

The combination of both models, the *ex vivo* human placental perfusion and the *in vitro* cell culture system should help us to better understand the transport mechanisms of ENMs across the placental barrier. Thus, evaluation, improvement and application of these models to specifically investigate interactions at the nano-placenta interface have been integral parts of this thesis.

### 2.4 References

- ADEREM, A. & UNDERHILL, D. M. 1999. Mechanisms of phagocytosis in macrophages. *Annu Rev Immunol*, 17, 593-623.
- ALI, H., KALASHNIKOVA, I., WHITE, M. A., SHERMAN, M. & RYTTING, E. 2013. Preparation, characterization, and transport of dexamethasone-loaded polymeric nanoparticles across a human placental in vitro model. *Int J Pharm*, 454, 149-57.
- ANDRADE, S. E., GURWITZ, J. H., DAVIS, R. L., CHAN, K. A., FINKELSTEIN, J. A., FORTMAN, K., MCPHILLIPS, H., RAEBEL, M. A., ROBLIN, D., SMITH, D. H., YOOD, M. U., MORSE, A. N. & PLATT, R. 2004. Prescription drug use in pregnancy. *Am J Obstet Gynecol*, 191, 398-407.
- AUFFAN, M., ROSE, J., BOTTERO, J. Y., LOWRY, G. V., JOLIVET, J. P. & WIESNER, M. R. 2009. Towards a definition of inorganic nanoparticles from an environmental, health and safety perspective. *Nat Nanotechnol*, 4, 634-41.
- AUTEN, R. L., GILMOUR, M. I., KRANTZ, Q. T., POTTS, E. N., MASON, S. N. & FOSTER, W. M. 2012. Maternal diesel inhalation increases airway hyperreactivity in ozone-exposed offspring. *Am J Respir Cell Mol Biol*, 46, 454-60.
- BENIRSCHKE, K. 2012. *Pathology of the human placenta*, New York, Springer.
- BHABRA, G., SOOD, A., FISHER, B., CARTWRIGHT, L., SAUNDERS, M., EVANS, W. H., SURPRENANT, A., LOPEZ-CASTEJON, G., MANN, S., DAVIS, S. A., HAILS, L. A., INGHAM, E., VERKADE, P., LANE, J., HEESOM, K., NEWSON, R. & CASE, C. P. 2009. Nanoparticles can cause DNA damage across a cellular barrier. *Nat Nanotechnol*, 4, 876-83.
- BIOG 2013. The Placenta. <http://www.biog1445.org/demo/07/ovaryplacenta.html>: Cornell University BIOG 1445.
- BLUM, J. L., XIONG, J. Q., HOFFMAN, C. & ZELIKOFF, J. T. 2012. Cadmium associated with inhaled cadmium oxide nanoparticles impacts fetal and neonatal development and growth. *Toxicol Sci*, 126, 478-86.
- BOBAK, M. 2000. Outdoor air pollution, low birth weight, and prematurity. *Environ Health Perspect*, 108, 173-6.
- BODE, C. J., JIN, H., RYTTING, E., SILVERSTEIN, P. S., YOUNG, A. M. & AUDUS, K. L. 2006. In vitro models for studying trophoblast transcellular transport. *Methods Mol Med*, 122, 225-39.
- BOYD, C. A. 1991. Placental transport studied by means of isolated plasma membrane vesicles. *Proc Nutr Soc*, 50, 337-43.
- BRUNNER, T. J., WICK, P., MANSER, P., SPOHN, P., GRASS, R. N., LIMBACH, L. K., BRUININK, A. & STARK, W. J. 2006. In vitro cytotoxicity of oxide nanoparticles: comparison to asbestos, silica, and the effect of particle solubility. *Environ Sci Technol*, 40, 4374-81.
- BUERKI-THURNHERR, T., VON MANDACH, U. & WICK, P. 2012. Knocking at the door of the unborn child: engineered nanoparticles at the human placental barrier. *Swiss Med Wkly*, 142, w13559.
- BURTON, G. J. & JAUNIAUX, E. 2011. Oxidative stress. *Best Pract Res Clin Obstet Gynaecol*, 25, 287-99.



- BURTON, G. J., JAUNIAUX, E. & WATSON, A. L. 1999. Maternal arterial connections to the placental intervillous space during the first trimester of human pregnancy: the Boyd collection revisited. *Am J Obstet Gynecol*, 181, 718-24.
- BURTON, G. J., WOODS, A. W., JAUNIAUX, E. & KINGDOM, J. C. 2009. Rheological and physiological consequences of conversion of the maternal spiral arteries for uteroplacental blood flow during human pregnancy. *Placenta*, 30, 473-82.
- CAMPAGNOLO, L., MASSIMIANI, M., PALMIERI, G., BERNARDINI, R., SACCHETTI, C., BERGAMASCHI, A., VECCHIONE, L., MAGRINI, A., BOTTINI, M. & PIETROIUSTI, A. 2013. Biodistribution and toxicity of pegylated single wall carbon nanotubes in pregnant mice. *Part Fibre Toxicol*, 10, 21.
- CARTWRIGHT, L., POULSEN, M. S., NIELSEN, H. M., POJANA, G., KNUDSEN, L. E., SAUNDERS, M. & RYTTING, E. 2012. In vitro placental model optimization for nanoparticle transport studies. *Int J Nanomedicine*, 7, 497-510.
- CHALLIER, J. C., PANIGEL, M. & MEYER, E. 1973. Uptake of colloidal  $^{198}\text{Au}$  by fetal liver in rat, after direct intrafetal administration. *Int J Nucl Med Biol*, 1, 103-6.
- CHAMPION, J. A., KATARE, Y. K. & MITRAGOTRI, S. 2007. Particle shape: a new design parameter for micro- and nanoscale drug delivery carriers. *J Control Release*, 121, 3-9.
- CHITHRANI, B. D., GHAZANI, A. A. & CHAN, W. C. 2006. Determining the size and shape dependence of gold nanoparticle uptake into mammalian cells. *Nano Lett*, 6, 662-8.
- CHOI, H. S., LIU, W., MISRA, P., TANAKA, E., ZIMMER, J. P., ITTY IPE, B., BAWENDI, M. G. & FRANGIONI, J. V. 2007. Renal clearance of quantum dots. *Nat Biotechnol*, 25, 1165-70.
- CHU, M., WU, Q., YANG, H., YUAN, R., HOU, S., YANG, Y., ZOU, Y., XU, S., XU, K., JI, A. & SHENG, L. 2010. Transfer of quantum dots from pregnant mice to pups across the placental barrier. *Small*, 6, 670-8.
- CONNER, S. D. & SCHMID, S. L. 2003. Regulated portals of entry into the cell. *Nature*, 422, 37-44.
- CORREIA CARREIRA, S., WALKER, L., PAUL, K. & SAUNDERS, M. 2013. The toxicity, transport and uptake of nanoparticles in the in vitro BeWo b30 placental cell barrier model used within NanoTEST. *Nanotoxicology*.
- CUPURDIJA, K., AZZOLA, D., HAINZ, U., GRATCHEV, A., HEITGER, A., TAKIKAWA, O., GOERDT, S., WINTERSTEIGER, R., DOHR, G. & SEDLMAYR, P. 2004. Macrophages of human first trimester decidua express markers associated to alternative activation. *Am J Reprod Immunol*, 51, 117-22.
- DENG, X., LUAN, Q., CHEN, W., WANG, Y., WU, M., ZHANG, H. & JIAO, Z. 2009. Nanosized zinc oxide particles induce neural stem cell apoptosis. *Nanotechnology*, 20, 115101.
- DILWORTH, M. R. & SIBLEY, C. P. 2013. Review: Transport across the placenta of mice and women. *Placenta*, 34 Suppl, S34-9.
- DONALDSON, K., SCHINWALD, A., MURPHY, F., CHO, W. S., DUFFIN, R., TRAN, L. & POLAND, C. 2013. The biologically effective dose in inhalation nanotoxicology. *Acc Chem Res*, 46, 723-32.
- DUAN, X. & LI, Y. 2013. Physicochemical characteristics of nanoparticles affect circulation, biodistribution, cellular internalization, and trafficking. *Small*, 9, 1521-32.
- DUC-GOIRAN, P., MIGNOT, T. M., BOURGEOIS, C. & FERRE, F. 1999. Embryo-maternal interactions at the implantation site: a delicate equilibrium. *Eur J Obstet Gynecol Reprod Biol*, 83, 85-100.

- ENDERS, A. C. & BLANKENSHIP, T. N. 1999. Comparative placental structure. *Adv Drug Deliv Rev*, 38, 3-15.
- FAUST, J. J., ZHANG, W., CHEN, Y. & CAPCO, D. G. 2014. Alpha-Fe(2)O(3) elicits diameter-dependent effects during exposure to an in vitro model of the human placenta. *Cell Biol Toxicol*, 30, 31-53.
- FERIN, J., OBERDORSTER, G. & PENNEY, D. P. 1992. Pulmonary retention of ultrafine and fine particles in rats. *Am J Respir Cell Mol Biol*, 6, 535-42.
- FERRARI, M. 2008. Nanogeometry: beyond drug delivery. *Nat Nanotechnol*, 3, 131-2.
- FIRTH, J. A. & LEACH, L. 1996. Not trophoblast alone: a review of the contribution of the fetal microvasculature to transplacental exchange. *Placenta*, 17, 89-96.
- FRANCA, A., AGGARWAL, P., BARSOV, E. V., KOZLOV, S. V., DOBROVOLSKAIA, M. A. & GONZALEZ-FERNANDEZ, A. 2011. Macrophage scavenger receptor A mediates the uptake of gold colloids by macrophages in vitro. *Nanomedicine (Lond)*, 6, 1175-88.
- FUJIMOTO, A., TSUKUE, N., WATANABE, M., SUGAWARA, I., YANAGISAWA, R., TAKANO, H., YOSHIDA, S. & TAKEDA, K. 2005. Diesel exhaust affects immunological action in the placentas of mice. *Environ Toxicol*, 20, 431-40.
- GANAPATHY, V., PRASAD, P. D., GANAPATHY, M. E. & LEIBACH, F. H. 2000. Placental transporters relevant to drug distribution across the maternal-fetal interface. *J Pharmacol Exp Ther*, 294, 413-20.
- GARNETT, M. C. & KALLINTERI, P. 2006. Nanomedicines and nanotoxicology: some physiological principles. *Occup Med (Lond)*, 56, 307-11.
- GENDRON, M. P., MARTIN, B., ORAICHI, D. & BERARD, A. 2009. Health care providers' requests to Teratogen Information Services on medication use during pregnancy and lactation. *Eur J Clin Pharmacol*, 65, 523-31.
- GEORGE, S., POKHREL, S., XIA, T., GILBERT, B., JI, Z., SCHOWALTER, M., ROSENAUER, A., DAMOISEAUX, R., BRADLEY, K. A., MADLER, L. & NEL, A. E. 2010. Use of a rapid cytotoxicity screening approach to engineer a safer zinc oxide nanoparticle through iron doping. *ACS Nano*, 4, 15-29.
- GESSNER, A., WAICZ, R., LIESKE, A., PAULKE, B., MADER, K. & MULLER, R. H. 2000. Nanoparticles with decreasing surface hydrophobicities: influence on plasma protein adsorption. *Int J Pharm*, 196, 245-9.
- GOESMANN, H. & FELDMANN, C. 2010. Nanoparticulate functional materials. *Angew Chem Int Ed Engl*, 49, 1362-95.
- GOJOVA, A., GUO, B., KOTA, R. S., RUTLEDGE, J. C., KENNEDY, I. M. & BARAKAT, A. I. 2007. Induction of inflammation in vascular endothelial cells by metal oxide nanoparticles: effect of particle composition. *Environ Health Perspect*, 115, 403-9.
- GRAFMULLER, S., MANSER, P., KRUG, H. F., WICK, P. & VON MANDACH, U. 2013. Determination of the transport rate of xenobiotics and nanomaterials across the placenta using the ex vivo human placental perfusion model. *J Vis Exp*.
- GRATTON, S. E., ROPP, P. A., POHLHAUS, P. D., LUFT, J. C., MADDEN, V. J., NAPIER, M. E. & DESIMONE, J. M. 2008. The effect of particle design on cellular internalization pathways. *Proc Natl Acad Sci U S A*, 105, 11613-8.
- GUPTA, A. K. & GUPTA, M. 2005. Synthesis and surface engineering of iron oxide nanoparticles for biomedical applications. *Biomaterials*, 26, 3995-4021.
- HIRSCH, V., KINNEAR, C., MONIATTE, M., ROTHEN-RUTISHAUSER, B., CLIFT, M. J. & FINK, A. 2013. Surface charge of polymer coated SPIONs influences the serum

- protein adsorption, colloidal stability and subsequent cell interaction in vitro. *Nanoscale*, 5, 3723-32.
- HOUGAARD, K. S., JACKSON, P., JENSEN, K. A., SLOTH, J. J., LOSCHNER, K., LARSEN, E. H., BIRKEDAL, R. K., VIBENHOLT, A., BOISEN, A. M., WALLIN, H. & VOGEL, U. 2010. Effects of prenatal exposure to surface-coated nanosized titanium dioxide (UV-Titan). A study in mice. *Part Fibre Toxicol*, 7, 16.
- HUANG, X., ZHANG, F., SUN, X., CHOI, K. Y., NIU, G., ZHANG, G., GUO, J., LEE, S. & CHEN, X. 2014. The genotype-dependent influence of functionalized multiwalled carbon nanotubes on fetal development. *Biomaterials*, 35, 856-65.
- HUPPERTZ, B. & GAUSTER, M. 2011. Trophoblast fusion. *Adv Exp Med Biol*, 713, 81-95.
- HUTSON, J. R., GARCIA-BOURNISSEN, F., DAVIS, A. & KOREN, G. 2011. The human placental perfusion model: a systematic review and development of a model to predict in vivo transfer of therapeutic drugs. *Clin Pharmacol Ther*, 90, 67-76.
- HUYNH, M., WOODRUFF, T. J., PARKER, J. D. & SCHOENDORF, K. C. 2006. Relationships between air pollution and preterm birth in California. *Paediatr Perinat Epidemiol*, 20, 454-61.
- JIN, H., HELLER, D. A., SHARMA, R. & STRANO, M. S. 2009. Size-dependent cellular uptake and expulsion of single-walled carbon nanotubes: single particle tracking and a generic uptake model for nanoparticles. *ACS Nano*, 3, 149-58.
- JUCH, H., NIKITINA, L., DEBBAGE, P., DOHR, G. & GAUSTER, M. 2013. Nanomaterial interference with early human placenta: Sophisticated matter meets sophisticated tissues. *Reprod Toxicol*, 41, 73-9.
- KERTSCHANSKA, S., KOSANKE, G. & KAUFMANN, P. 1997. Pressure dependence of so-called transtrophoblastic channels during fetal perfusion of human placental villi. *Microsc Res Tech*, 38, 52-62.
- KERTSCHANSKA, S., STULCOVA, B., KAUFMANN, P. & STULC, J. 2000. Distensible transtrophoblastic channels in the rat placenta. *Placenta*, 21, 670-7.
- KETTIGER, H., SCHIPANSKI, A., WICK, P. & HUWYLER, J. 2013. Engineered nanomaterial uptake and tissue distribution: from cell to organism. *Int J Nanomedicine*, 8, 3255-69.
- KRPETIC, Z., PORTA, F., CANEVA, E., DAL SANTO, V. & SCARI, G. 2010. Phagocytosis of biocompatible gold nanoparticles. *Langmuir*, 26, 14799-805.
- KRUG, H. F. & WICK, P. 2011. Nanotoxicology: an interdisciplinary challenge. *Angew Chem Int Ed Engl*, 50, 1260-78.
- KUNZMANN, A., ANDERSSON, B., THURNHERR, T., KRUG, H., SCHEYNIUS, A. & FADEEL, B. 2011. Toxicology of engineered nanomaterials: focus on biocompatibility, biodistribution and biodegradation. *Biochim Biophys Acta*, 1810, 361-73.
- LACASANA, M., ESPLUGUES, A. & BALLESTER, F. 2005. Exposure to ambient air pollution and prenatal and early childhood health effects. *Eur J Epidemiol*, 20, 183-99.
- LARSEN, L. G., CLAUSEN, H. V., ANDERSEN, B. & GRAEM, N. 1995. A stereologic study of postmature placentas fixed by dual perfusion. *Am J Obstet Gynecol*, 172, 500-7.
- LATZIN, P., ROOSLI, M., HUSS, A., KUEHNI, C. E. & FREY, U. 2009. Air pollution during pregnancy and lung function in newborns: a birth cohort study. *Eur Respir J*, 33, 594-603.

- LI, H., VAN RAVENZWAAY, B., RIETJENS, I. M. & LOUISSE, J. 2013. Assessment of an in vitro transport model using BeWo b30 cells to predict placental transfer of compounds. *Arch Toxicol*, 87, 1661-9.
- LIMBACH, L. K., WICK, P., MANSER, P., GRASS, R. N., BRUININK, A. & STARK, W. J. 2007. Exposure of engineered nanoparticles to human lung epithelial cells: influence of chemical composition and catalytic activity on oxidative stress. *Environ Sci Technol*, 41, 4158-63.
- LIU, F., SOARES, M. J. & AUDUS, K. L. 1997. Permeability properties of monolayers of the human trophoblast cell line BeWo. *Am J Physiol*, 273, C1596-604.
- LU, F., WU, S. H., HUNG, Y. & MOU, C. Y. 2009. Size effect on cell uptake in well-suspended, uniform mesoporous silica nanoparticles. *Small*, 5, 1408-13.
- LUNDQVIST, M., STIGLER, J., ELIA, G., LYNCH, I., CEDERVALL, T. & DAWSON, K. A. 2008. Nanoparticle size and surface properties determine the protein corona with possible implications for biological impacts. *Proc Natl Acad Sci U S A*, 105, 14265-70.
- LUNOV, O., SYROVETS, T., LOOS, C., BEIL, J., DELACHER, M., TRON, K., NIENHAUS, G. U., MUSYANOVYCH, A., MAILANDER, V., LANDFESTER, K. & SIMMET, T. 2011. Differential uptake of functionalized polystyrene nanoparticles by human macrophages and a monocytic cell line. *ACS Nano*, 5, 1657-69.
- MAHMOUDI, M., SAHRAIAN, M. A., SHOKRGOZAR, M. A. & LAURENT, S. 2011. Superparamagnetic iron oxide nanoparticles: promises for diagnosis and treatment of multiple sclerosis. *ACS Chem Neurosci*, 2, 118-40.
- MALEK, A. & BERSINGER, N. A. 2013. Immunology of human pregnancy: Transfer of antibodies and associated placental function. In: NICHOLSON, R. (ed.) *The placenta: Development, function and diseases*. New York: Nova Science Publishers, Inc.
- MALEK, A., WILLI, A., MULLER, J., SAGER, R., HANGGI, W. & BERSINGER, N. 2001. Capacity for hormone production of cultured trophoblast cells obtained from placentae at term and in early pregnancy. *J Assist Reprod Genet*, 18, 299-304.
- MARTIN, A. & HOLLOWAY, K. 2014. 'Something there is that doesn't love a wall': Histories of the placental barrier. *Stud Hist Philos Biol Biomed Sci*, 47 Pt B, 300-10.
- MARUO, T., MATSUO, H., OISHI, T., HAYASHI, M., NISHINO, R. & MOCHIZUKI, M. 1987. Induction of differentiated trophoblast function by epidermal growth factor: relation of immunohistochemically detected cellular epidermal growth factor receptor levels. *J Clin Endocrinol Metab*, 64, 744-50.
- MATHIESEN, L. & KNUDSEN, L. E. 2013. Placental Transport of Environmental Toxicants In: NICHOLSON, R. (ed.) *The Placenta: Development, Function and Diseases*. New York: Nova Science Publishers, Inc.
- MATHIESEN, L., MORCK, T. A., ZURI, G., ANDERSEN, M. H., PEHRSON, C., FREDERIKSEN, M., MOSE, T., RYTTING, E., POULSEN, M. S., NIELSEN, J. K. & KNUDSEN, L. E. 2014. Modelling of human transplacental transport as performed in copenhagen, denmark. *Basic Clin Pharmacol Toxicol*, 115, 93-100.
- MAYNARD, A. D. 2007. Nanotechnology: the next big thing, or much ado about nothing? *Ann Occup Hyg*, 51, 1-12.
- MAYOR, S. & PAGANO, R. E. 2007. Pathways of clathrin-independent endocytosis. *Nat Rev Mol Cell Biol*, 8, 603-12.
- MCMAHON, H. T. & BOUCROT, E. 2011. Molecular mechanism and physiological functions of clathrin-mediated endocytosis. *Nat Rev Mol Cell Biol*, 12, 517-33.

- MEHTA, D. & MALIK, A. B. 2006. Signaling mechanisms regulating endothelial permeability. *Physiol Rev*, 86, 279-367.
- MELNIK, E. A., BUZULUKOV, Y. P., DEMIN, V. F., DEMIN, V. A., GMOSHINSKI, I. V., TYSHKO, N. V. & TUTELYAN, V. A. 2013. Transfer of Silver Nanoparticles through the Placenta and Breast Milk during in vivo Experiments on Rats. *Acta Naturae*, 5, 107-15.
- MENEZES, V., MALEK, A. & KEELAN, J. A. 2011. Nanoparticulate drug delivery in pregnancy: placental passage and fetal exposure. *Curr Pharm Biotechnol*, 12, 731-42.
- MENJOGE, A. R., RINDERKNECHT, A. L., NAVATH, R. S., FARIDNIA, M., KIM, C. J., ROMERO, R., MILLER, R. K. & KANNAN, R. M. 2011. Transfer of PAMAM dendrimers across human placenta: prospects of its use as drug carrier during pregnancy. *J Control Release*, 150, 326-38.
- MERCER, J. & HELENIUS, A. 2009. Virus entry by macropinocytosis. *Nat Cell Biol*, 11, 510-20.
- MILLER, R. K., GENBACEV, O., TURNER, M. A., APLIN, J. D., CANIGGIA, I. & HUPPERTZ, B. 2005. Human placental explants in culture: approaches and assessments. *Placenta*, 26, 439-48.
- MITCHELL, A. A., GILBOA, S. M., WERLER, M. M., KELLEY, K. E., LOUIK, C., HERNANDEZ-DIAZ, S. & NATIONAL BIRTH DEFECTS PREVENTION, S. 2011. Medication use during pregnancy, with particular focus on prescription drugs: 1976-2008. *Am J Obstet Gynecol*, 205, 51 e1-8.
- MONOPOLI, M. P., WALCZYK, D., CAMPBELL, A., ELIA, G., LYNCH, I., BOMBELLI, F. B. & DAWSON, K. A. 2011. Physical-chemical aspects of protein corona: relevance to in vitro and in vivo biological impacts of nanoparticles. *J Am Chem Soc*, 133, 2525-34.
- MYLLYNNEN, P. K., LOUGHRAN, M. J., HOWARD, C. V., SORMUNEN, R., WALSH, A. A. & VAHAKANGAS, K. H. 2008. Kinetics of gold nanoparticles in the human placenta. *Reprod Toxicol*, 26, 130-7.
- NEL, A., XIA, T., MADLER, L. & LI, N. 2006. Toxic potential of materials at the nanolevel. *Science*, 311, 622-7.
- NEL, A. E., MADLER, L., VELEGOL, D., XIA, T., HOEK, E. M., SOMASUNDARAN, P., KLAESSIG, F., CASTRANOVA, V. & THOMPSON, M. 2009. Understanding biophysicochemical interactions at the nano-bio interface. *Nat Mater*, 8, 543-57.
- OBERDORSTER, G. 2002. Toxicokinetics and effects of fibrous and nonfibrous particles. *Inhal Toxicol*, 14, 29-56.
- OBERDORSTER, G., OBERDORSTER, E. & OBERDORSTER, J. 2005. Nanotoxicology: an emerging discipline evolving from studies of ultrafine particles. *Environ Health Perspect*, 113, 823-39.
- ONODA, A., UMEZAWA, M., TAKEDA, K., IHARA, T. & SUGAMATA, M. 2014. Effects of maternal exposure to ultrafine carbon black on brain perivascular macrophages and surrounding astrocytes in offspring mice. *PLoS One*, 9, e94336.
- OWENS, D. E., 3RD & PEPPAS, N. A. 2006. Opsonization, biodistribution, and pharmacokinetics of polymeric nanoparticles. *Int J Pharm*, 307, 93-102.
- PARK, E. J., YI, J., KIM, Y., CHOI, K. & PARK, K. 2010. Silver nanoparticles induce cytotoxicity by a Trojan-horse type mechanism. *Toxicol In Vitro*, 24, 872-8.
- PARTON, R. G. & SIMONS, K. 2007. The multiple faces of caveolae. *Nat Rev Mol Cell Biol*, 8, 185-94.

- PÉREZ-PÉREZ, A., SÁNCHEZ-JIMÉNEZ, F., MAYMÓ, J. L., GAMBINO, Y. P., JOSÉ L. DUEÑAS, VARONE, C. L. & SÁNCHEZ-MARGALET, V. 2013. Leptin Action and Leptin Receptor Signaling in Human Trophoblast *In*: NICHOLSON, R. (ed.) *The Placenta: Development, Function and Diseases*. New York: Nova Science Publishers, Inc.
- PETROFF, M. G., PHILLIPS, T. A., KA, H., PACE, J. L. & HUNT, J. S. 2006. Isolation and culture of term human trophoblast cells. *Methods Mol Med*, 121, 203-17.
- PIETROIUSTI, A. 2012. Health implications of engineered nanomaterials. *Nanoscale*, 4, 1231-47.
- PIETROIUSTI, A., MASSIMIANI, M., FENOGLIO, I., COLONNA, M., VALENTINI, F., PALLESCHI, G., CAMAIONI, A., MAGRINI, A., SIRACUSA, G., BERGAMASCHI, A., SGAMBATO, A. & CAMPAGNOLO, L. 2011. Low doses of pristine and oxidized single-wall carbon nanotubes affect mammalian embryonic development. *ACS Nano*, 5, 4624-33.
- PROUILLAC, C. & LECOEUR, S. 2010. The role of the placenta in fetal exposure to xenobiotics: importance of membrane transporters and human models for transfer studies. *Drug Metab Dispos*, 38, 1623-35.
- QI, W., BI, J., ZHANG, X., WANG, J., WANG, J., LIU, P., LI, Z. & WU, W. 2014. Damaging effects of multi-walled carbon nanotubes on pregnant mice with different pregnancy times. *Sci Rep*, 4, 4352.
- QIU, Y., LIU, Y., WANG, L., XU, L., BAI, R., JI, Y., WU, X., ZHAO, Y., LI, Y. & CHEN, C. 2010. Surface chemistry and aspect ratio mediated cellular uptake of Au nanorods. *Biomaterials*, 31, 7606-19.
- RATTANAPINYOPITUK, K., SHIMADA, A., MORITA, T., SAKURAI, M., ASANO, A., HASEGAWA, T., INOUE, K. & TAKANO, H. 2014. Demonstration of the clathrin- and caveolin-mediated endocytosis at the maternal-fetal barrier in mouse placenta after intravenous administration of gold nanoparticles. *J Vet Med Sci*, 76, 377-87.
- REFUERZO, J. S., GODIN, B., BISHOP, K., SRINIVASAN, S., SHAH, S. K., AMRA, S., RAMIN, S. M. & FERRARI, M. 2011. Size of the nanovectors determines the transplacental passage in pregnancy: study in rats. *Am J Obstet Gynecol*, 204, 546 e5-9.
- REJMAN, J., OBERLE, V., ZUHORN, I. S. & HOEKSTRA, D. 2004. Size-dependent internalization of particles via the pathways of clathrin- and caveolae-mediated endocytosis. *Biochem J*, 377, 159-69.
- RELIENE, R., HLAVACOVA, A., MAHADEVAN, B., BAIRD, W. M. & SCHIESTL, R. H. 2005. Diesel exhaust particles cause increased levels of DNA deletions after transplacental exposure in mice. *Mutat Res*, 570, 245-52.
- RIEHMANN, K., SCHNEIDER, S. W., LUGER, T. A., GODIN, B., FERRARI, M. & FUCHS, H. 2009. Nanomedicine--challenge and perspectives. *Angew Chem Int Ed Engl*, 48, 872-97.
- RINGLER, G. E., KAO, L. C., MILLER, W. L. & STRAUSS, J. F., 3RD 1989. Effects of 8-bromo-cAMP on expression of endocrine functions by cultured human trophoblast cells. Regulation of specific mRNAs. *Mol Cell Endocrinol*, 61, 13-21.
- ROSSANT, J. & CROSS, J. C. 2001. Placental development: lessons from mouse mutants. *Nat Rev Genet*, 2, 538-48.
- ROTHEN-RUTISHAUSER, B. M., SCHURCH, S., HAENNI, B., KAPP, N. & GEHR, P. 2006. Interaction of fine particles and nanoparticles with red blood cells visualized with advanced microscopic techniques. *Environ Sci Technol*, 40, 4353-9.

- SADAUSKAS, E., WALLIN, H., STOLTENBERG, M., VOGEL, U., DOERING, P., LARSEN, A. & DANSCHER, G. 2007. Kupffer cells are central in the removal of nanoparticles from the organism. *Part Fibre Toxicol*, 4, 10.
- SEMMLER-BEHNKE, M., KREYLING, W. G., LIPKA, J., FERTSCH, S., WENK, A., TAKENAKA, S., SCHMID, G. & BRANDAU, W. 2008. Biodistribution of 1.4- and 18-nm gold particles in rats. *Small*, 4, 2108-11.
- SERVICE, R. F. 2004. Nanotoxicology. Nanotechnology grows up. *Science*, 304, 1732-4.
- SHAH, N. B., VERCELLOTTI, G. M., WHITE, J. G., FEGAN, A., WAGNER, C. R. & BISCHOF, J. C. 2012. Blood-nanoparticle interactions and in vivo biodistribution: impact of surface PEG and ligand properties. *Mol Pharm*, 9, 2146-55.
- SHAH, P. S., BALKHAIR, T. & KNOWLEDGE SYNTHESIS GROUP ON DETERMINANTS OF PRETERM, L. B. W. B. 2011. Air pollution and birth outcomes: a systematic review. *Environ Int*, 37, 498-516.
- SHI, Q. J., LEI, Z. M., RAO, C. V. & LIN, J. 1993. Novel role of human chorionic gonadotropin in differentiation of human cytotrophoblasts. *Endocrinology*, 132, 1387-95.
- SHIMIZU, M., TAINAKA, H., OBA, T., MIZUO, K., UMEZAWA, M. & TAKEDA, K. 2009. Maternal exposure to nanoparticulate titanium dioxide during the prenatal period alters gene expression related to brain development in the mouse. *Part Fibre Toxicol*, 6, 20.
- SONNEGAARD POULSEN, M., MOSE, T., LETH MAROUN, L., MATHIESEN, L., EHLERT KNUDSEN, L. & RYTTING, E. 2013. Kinetics of silica nanoparticles in the human placenta. *Nanotoxicology*.
- SOOD, A., SALIH, S., ROH, D., LACHARME-LORA, L., PARRY, M., HARDIMAN, B., KEEHAN, R., GRUMMER, R., WINTERHAGER, E., GOKHALE, P. J., ANDREWS, P. W., ABBOTT, C., FORBES, K., WESTWOOD, M., APLIN, J. D., INGHAM, E., PAPAGEORGIOU, I., BERRY, M., LIU, J., DICK, A. D., GARLAND, R. J., WILLIAMS, N., SINGH, R., SIMON, A. K., LEWIS, M., HAM, J., ROGER, L., BAIRD, D. M., CROMPTON, L. A., CALDWELL, M. A., SWALWELL, H., BIRCHMACHIN, M., LOPEZ-CASTEJON, G., RANDALL, A., LIN, H., SULEIMAN, M. S., EVANS, W. H., NEWSON, R. & CASE, C. P. 2011. Signalling of DNA damage and cytokines across cell barriers exposed to nanoparticles depends on barrier thickness. *Nat Nanotechnol*, 6, 824-33.
- STAPLETON, P. A., MINARCHICK, V. C., YI, J., ENGELS, K., MCBRIDE, C. R. & NURKIEWICZ, T. R. 2013. Maternal engineered nanomaterial exposure and fetal microvascular function: does the Barker hypothesis apply? *Am J Obstet Gynecol*, 209, 227 e1-11.
- SUMNER, S. C., FENNELL, T. R., SNYDER, R. W., TAYLOR, G. F. & LEWIN, A. H. 2010. Distribution of carbon-14 labeled C60 ([<sup>14</sup>C]C60) in the pregnant and in the lactating dam and the effect of C60 exposure on the biochemical profile of urine. *J Appl Toxicol*, 30, 354-60.
- SYME, M. R., PAXTON, J. W. & KEELAN, J. A. 2004. Drug transfer and metabolism by the human placenta. *Clin Pharmacokinet*, 43, 487-514.
- SZEKERES-BARTHO, J., PAR, G., SZEREDAY, L., SMART, C. Y. & ACHATZ, I. 1997. Progesterone and non-specific immunologic mechanisms in pregnancy. *Am J Reprod Immunol*, 38, 176-82.

- TAKEDA, K., SUZUKI, K., ISHIHARA, A., KUBO-IRIE, M., FUJIMOTO, R., TABATA, M., OSHIO, S., NIHEI, Y., IHARA, T. & SUGAMATA, M. 2009. Nanoparticles Transferred from Pregnant Mice to Their Offspring Can Damage the Genital and Cranial Nerve Systems. *Journal of Health Science*, 55, 95 - 102.
- TANG, F., LI, L. & CHEN, D. 2012. Mesoporous silica nanoparticles: synthesis, biocompatibility and drug delivery. *Adv Mater*, 24, 1504-34.
- TIAN, F., RAZANSKY, D., ESTRADA, G. G., SEMMLER-BEHNKE, M., BEYERLE, A., KREYLING, W., NTZIACHRISTOS, V. & STOEGER, T. 2009. Surface modification and size dependence in particle translocation during early embryonic development. *Inhal Toxicol*, 21 Suppl 1, 92-6.
- TIAN, X., ZHU, M., DU, L., WANG, J., FAN, Z., LIU, J., ZHAO, Y. & NIE, G. 2013. Intrauterine inflammation increases materno-fetal transfer of gold nanoparticles in a size-dependent manner in murine pregnancy. *Small*, 9, 2432-9.
- TREUEL, L., JIANG, X. & NIENHAUS, G. U. 2013. New views on cellular uptake and trafficking of manufactured nanoparticles. *J R Soc Interface*, 10, 20120939.
- VERMA, U. & VERMA, N. 2013. An Overview of Development, Function and Diseases of the Placenta In: NICHOLSON, R. (ed.) *The Placenta: Development, Function and Diseases*. New York: Nova Science Publishers, Inc.
- WANG, T., BAI, J., JIANG, X. & NIENHAUS, G. U. 2012. Cellular uptake of nanoparticles by membrane penetration: a study combining confocal microscopy with FTIR spectroelectrochemistry. *ACS Nano*, 6, 1251-9.
- WANG, Z., TIRUPPATHI, C., MINSHALL, R. D. & MALIK, A. B. 2009. Size and dynamics of caveolae studied using nanoparticles in living endothelial cells. *ACS Nano*, 3, 4110-6.
- WICE, B., MENTON, D., GEUZE, H. & SCHWARTZ, A. L. 1990. Modulators of cyclic AMP metabolism induce syncytiotrophoblast formation in vitro. *Exp Cell Res*, 186, 306-16.
- WICK, P., GRAFMUELLER, S., PETRI-FINK, A. & ROTHEN-RUTISHAUSER, B. 2014. Advanced human in vitro models to assess metal oxide nanoparticle-cell interactions. *MRS Bulletin*, 39, 984-989.
- WICK, P., MALEK, A., MANSER, P., MEILI, D., MAEDER-ALTHAUS, X., DIENER, L., DIENER, P. A., ZISCH, A., KRUG, H. F. & VON MANDACH, U. 2010. Barrier capacity of human placenta for nanosized materials. *Environ Health Perspect*, 118, 432-6.
- XIA, T., KOVOCHICH, M., LIONG, M., ZINK, J. I. & NEL, A. E. 2008. Cationic polystyrene nanosphere toxicity depends on cell-specific endocytic and mitochondrial injury pathways. *ACS Nano*, 2, 85-96.
- XIE, G., SUN, J., ZHONG, G., SHI, L. & ZHANG, D. 2010. Biodistribution and toxicity of intravenously administered silica nanoparticles in mice. *Arch Toxicol*, 84, 183-90.
- YAMASHITA, K., YOSHIOKA, Y., HIGASHISAKA, K., MIMURA, K., MORISHITA, Y., NOZAKI, M., YOSHIDA, T., OGURA, T., NABESHI, H., NAGANO, K., ABE, Y., KAMADA, H., MONOBE, Y., IMAZAWA, T., AOSHIMA, H., SHISHIDO, K., KAWAI, Y., MAYUMI, T., TSUNODA, S., ITOH, N., YOSHIKAWA, T., YANAGIHARA, I., SAITO, S. & TSUTSUMI, Y. 2011. Silica and titanium dioxide nanoparticles cause pregnancy complications in mice. *Nat Nanotechnol*, 6, 321-8.
- YANG, H., SUN, C., FAN, Z., TIAN, X., YAN, L., DU, L., LIU, Y., CHEN, C., LIANG, X. J., ANDERSON, G. J., KEELAN, J. A., ZHAO, Y. & NIE, G. 2012. Effects of



- gestational age and surface modification on materno-fetal transfer of nanoparticles in murine pregnancy. *Sci Rep*, 2, 847.
- YOSHIDA, S., HIYOSHI, K., OSHIO, S., TAKANO, H., TAKEDA, K. & ICHINOSE, T. 2010. Effects of fetal exposure to carbon nanoparticles on reproductive function in male offspring. *Fertil Steril*, 93, 1695-9.
- YUI, J., GARCIA-LLORET, M., BROWN, A. J., BERDAN, R. C., MORRISH, D. W., WEGMANN, T. G. & GUILBERT, L. J. 1994. Functional, long-term cultures of human term trophoblasts purified by column-elimination of CD9 expressing cells. *Placenta*, 15, 231-46.
- ZHU, M., NIE, G., MENG, H., XIA, T., NEL, A. & ZHAO, Y. 2013. Physicochemical properties determine nanomaterial cellular uptake, transport, and fate. *Acc Chem Res*, 46, 622-31.



### **3. RESULTS**

**Part I: Determination of the transport rate of xenobiotics and nanomaterials across the placenta using the *ex vivo* human placental perfusion model**

**Part II: Bidirectional transfer study of polystyrene nanoparticles across the placental barrier reveals different transport kinetics**

**Part III: Challenges and common pitfalls in nanoparticle characterization for transport studies across the human placenta**

**Part IV: Evaluation of nanoparticle-placenta interactions *in vitro***



## PART I

### **Determination of the transport rate of xenobiotics and nanomaterials across the placenta using the *ex vivo* human placental perfusion model**

Stefanie Grafmüller, Pius Manser, Harald F. Krug, Peter Wick, Ursula von Mandach

#### ***Author contribution***

In this study, I performed the *ex vivo* placental perfusions, analyzed and summarized the results and wrote the manuscript. Together with Pius Manser, I improved the placenta perfusion technique and the protocol. Ursula von Mandach and Peter Wick conceived and designed the research project. Harald F. Krug provided expertise, guidance and critical reading. All authors contributed to finalize the manuscript.

Published online as video article in the Journal of Visualized Experiments (2013):





Video Article

# Determination of the Transport Rate of Xenobiotics and Nanomaterials Across the Placenta using the *ex vivo* Human Placental Perfusion Model

Stefanie Grafmüller<sup>1,2,3</sup>, Pius Manser<sup>2</sup>, Harald F. Krug<sup>2</sup>, Peter Wick<sup>2</sup>, Ursula von Mandach<sup>1</sup>

<sup>1</sup>Department of Obstetrics, Perinatal Pharmacology, University Hospital Zurich

<sup>2</sup>Laboratory for Materials - Biology Interactions, EMPA Swiss Federal Laboratories for Materials Testing and Research

<sup>3</sup>Graduate School for Cellular and Biomedical Sciences, University of Bern

Correspondence to: Peter Wick at [Peter.Wick@empa.ch](mailto:Peter.Wick@empa.ch)

URL: <http://www.jove.com/video/50401>

DOI: [doi:10.3791/50401](https://doi.org/10.3791/50401)

Keywords: Biomedical Engineering, Issue 76, Medicine, Bioengineering, Anatomy, Physiology, Molecular Biology, Biochemistry, Biophysics, Pharmacology, Obstetrics, Nanotechnology, Placenta, Pharmacokinetics, Nanomedicine, humans, *ex vivo* perfusion, perfusion, biological barrier, xenobiotics, nanomaterials, clinical model

Date Published: 6/18/2013

Citation: Grafmüller, S., Manser, P., Krug, H.F., Wick, P., von Mandach, U. Determination of the Transport Rate of Xenobiotics and Nanomaterials Across the Placenta using the *ex vivo* Human Placental Perfusion Model. *J. Vis. Exp.* (76), e50401, doi:10.3791/50401 (2013).

## Abstract

Decades ago the human placenta was thought to be an impenetrable barrier between mother and unborn child. However, the discovery of thalidomide-induced birth defects and many later studies afterwards proved the opposite. Today several harmful xenobiotics like nicotine, heroin, methadone or drugs as well as environmental pollutants were described to overcome this barrier. With the growing use of nanotechnology, the placenta is likely to come into contact with novel nanoparticles either accidentally through exposure or intentionally in the case of potential nanomedical applications. Data from animal experiments cannot be extrapolated to humans because the placenta is the most species-specific mammalian organ<sup>1</sup>. Therefore, the *ex vivo* dual recirculating human placental perfusion, developed by Panigel *et al.* in 1967<sup>2</sup> and continuously modified by Schneider *et al.* in 1972<sup>3</sup>, can serve as an excellent model to study the transfer of xenobiotics or particles.

Here, we focus on the *ex vivo* dual recirculating human placental perfusion protocol and its further development to acquire reproducible results.

The placentae were obtained after informed consent of the mothers from uncomplicated term pregnancies undergoing caesarean delivery. The fetal and maternal vessels of an intact cotyledon were cannulated and perfused at least for five hours. As a model particle fluorescently labelled polystyrene particles with sizes of 80 and 500 nm in diameter were added to the maternal circuit. The 80 nm particles were able to cross the placental barrier and provide a perfect example for a substance which is transferred across the placenta to the fetus while the 500 nm particles were retained in the placental tissue or maternal circuit. The *ex vivo* human placental perfusion model is one of few models providing reliable information about the transport behavior of xenobiotics at an important tissue barrier which delivers predictive and clinical relevant data.

## Video Link

The video component of this article can be found at <http://www.jove.com/video/50401/>

## Introduction

The placenta is a complex organ which is responsible for the exchange of oxygen, carbon dioxide, nutrients and waste products and at the same time able to keep the two blood circuits of the mother and the growing fetus separated from each other. Additionally, it prevents rejection of the child by the maternal immune system and secretes hormones to maintain pregnancy. The cellular barrier is formed by the cytotrophoblast cells which fuse and form a true syncytium without lateral cell membranes<sup>4,5</sup>. The whole placenta is organized in several cotyledons, which contain one fetal villous tree and represent one functional unit of the placenta.

The study of the placental barrier function was intensified with the discovery of the thalidomide induced malformations in the 1960's. For obvious reasons translocation studies with pregnant women cannot be performed. Consequently, various alternative models have been developed<sup>6,7</sup>. The most promising and probably most clinical relevant model is the *ex vivo* human placental perfusion model developed by Panigel and co-workers<sup>2,3</sup>.

Many women are exposed to different xenobiotics such as drugs or environmental pollutants during their pregnancy<sup>8</sup>. For some drugs which were already administered regularly during pregnancy, *in vivo* studies can be performed by comparison of the maternal blood concentration with that in umbilical cord blood. However, generally there is only limited information about the pharmacokinetics and -dynamics in the fetus and the teratogenicity of these substances.

For example opiates like heroin easily cross the placental barrier and can lead to intrauterine growth restriction, preterm delivery or spontaneous abortion<sup>9,10</sup>. So, in case of missing abstinence during pregnancy a replacement therapy with methadone is recommended. The *ex vivo* human placental perfusion model revealed that the transfer of methadone into the fetal circulation is negligible<sup>11</sup>, which correlates well with the calculated cord blood-to-maternal blood concentration ratio after delivery<sup>12</sup>.

Nanotechnology is a growing field especially in medicine. So, beneath the naturally occurring fine (< 2.5 µm in diameter) and ultrafine particles (< 0.1 µm in diameter) in fumes of forest fires, volcano eruptions and in desert dust, exposure to engineered nanomaterials (at least one dimension < 0.1 µm<sup>13</sup>) is increasing. This raised questions about the toxicological potential of engineered nanomaterials. Although no human hazard could be proved yet, there are principal experimental studies indicating that engineered nanoparticles can cause adverse biological responses leading to toxicological outcomes<sup>14</sup>. Recently, some studies indicated that prenatal exposure to air pollution is linked to a higher respiratory need and airway inflammation in newborns and children<sup>15,16</sup>. In addition, small nanoparticles might be used as drug carriers to specifically treat either the fetus or the mother. Therefore, it becomes evident that extensive studies of distinct xenobiotics or nanomaterials and their ability to cross the placental barrier are required. An actual overview on the current studies on placental permeability to engineered nanomaterials is summarized in Menezes *et al.* 2011<sup>17</sup> and Buerki-Thurnherr *et al.* 2012<sup>7</sup>.

The *ex vivo* dual recirculating human placental perfusion model provides a controlled and reliable system for studying the placental transport of various endogenous and exogenous compounds<sup>3,11,12,18,19</sup> and a wide range of other functions of the placenta like mechanisms responsible for the development of pathological states like preeclampsia<sup>20-22</sup>. In this protocol we focus mainly on the set up, handling and method that allow the study of accumulation, effects and translocation rates of a broad set of xenobiotics or nanoparticles.

## Protocol

### 1. Preparing the Perfusion System

1. Set up the perfusion system consisting of a water bath, a perfusion chamber, two columns for oxygenation, two peristaltic pumps, two bubble traps, two flow heaters and one pressure sensor (**Figure 1**). Connect these components with tubing sections composed of silicone and polyvinyl chloride materials according to the scheme in **Figure 2**. Finally there are two circuits representing the fetal and maternal circuit, respectively.
2. Turn on the water bath, the flow heaters and the heating for the perfusion chamber. The temperature should be 37 °C.
3. Warm up the perfusion medium (NCTC-135 tissue culture medium diluted 1:2 with Earle's buffer (6.8 g/L sodium chloride, 0.4 g/L potassium chloride, 0.14 g/L monosodium phosphate, 0.2 g/L magnesium sulfate, 0.2 g/L calcium chloride, 2 g/L glucose) supplemented with glucose (1 g/L), dextran 40 (10 g/L), bovine serum albumin (10 g/L), sodium heparin (2,500 IU/L), amoxicilline (250 mg/L) and sodium bicarbonate (2.2 g/L); pH 7.4) in the water bath.
4. Consecutively rinse the arterial systems of the fetal and maternal circuit with a) 200 ml distilled water, b) 50 ml 1% sodium hydroxide, c) 1% phosphoric acid and d) again 200 ml distilled water (flow rate: 15 - 20 ml/min).
5. Connect the fetal cannula (Ø 1.2 mm; blunt needle should be attached to a modified winged needle infusion set) to the fetal arterial tubing.
6. Rinse the arterial systems of the fetal and maternal circuit with perfusion medium until all tubes contain medium (flow rate: 15-20 ml/min). During this step fill up the bubble traps and remove all bubbles downstream of the trap. Then stop the pumps. It is really important that the afferent arterial tubes are always free of bubbles; otherwise after cannulation especially the fine fetal vessels can rupture.
7. Turn on the gas flow. The maternal circuit is oxygenated with 5% carbon dioxide and 95% synthetic air and the fetal circuit with 5% carbon dioxide and 95% nitrogen.
8. Start the recording of the pressure sensor.

### 2. Cannulating the Placenta

1. Obtain intact placentae from uncomplicated term pregnancies after primary cesarean section. Written consent has to be given (was obtained in the case of our studies) by the mothers before delivery and the study has to be approved by the local ethics committee (was the case in our studies). First visual control should be done by midwives to assure a healthy and intact placenta.
2. Cannulation of the placenta is a critical step! During perfusion every small disruption in the tissue can lead to a leak between the maternal and fetal circulation. The placenta has to be obtained within 30 min after delivery.
3. Select an intact cotyledon at the marginal zone of the placenta without visible disruptions on the maternal side. At the chorionic plate, tie up both associated branches of the umbilical artery and vein upstream to the later cannulation side (towards the umbilical cord) by using surgical suture material. Make always two knots.
4. Cannulate the fetal artery first. The fetal placental arteries are always smaller and thinner than the veins.
5. Make a suture around the fetal artery, but do not tie it up immediately. Hold the vessel with a forceps, cut the vessel carefully and put the small cannula (Ø 1.2 mm) in the artery. Then tie up the suture (two knots).
6. Proceed with the fetal vein in the same manner but use a bigger cannula (Ø 1.5-1.8 mm; blunt needle should be attached to a modified winged needle infusion set).
7. Turn on the fetal pump (2 ml/min). If there is no visible leak and blood emanates out of the fetal vein cannula, slowly increase the flow up to 4 ml/min. Observe the pressure in the fetal artery, it should not exceed 70 mmHg. If fluid leaks out at the fetal or maternal cannula fix them with another suture.
8. Place the placenta on the tissue holder with the fetal side up and pull the placental membrane and tissue over the spikes. In the end the perfused cotyledon should be in the middle of the hole in the tissue holder.
9. Stabilize the part where only the membrane holds the placenta with a silicone membrane (Ø 1 mm) or alternatively two parafilm pieces.
10. Assemble the complete tissue holder, tighten the screws and cut the overhanging tissue. Please note that the venous and arterial cannulae are not pinched but instead lay in the small channels of the tissue holder.



11. Turn the tissue holder upside down, put it into the perfusion chamber and add the cover. Now, the maternal side should be at the top. Check always if the fetal circuit is still intact and the medium is flowing out of the fetal vein tubing.
12. Turn on the maternal pump (12 ml/min). Introduce the three blunt cannulae ( $\varnothing$  0.8 mm) at the end of the maternal artery tube into the intervillous space by penetrating the decidual plate. To return the perfusate to the maternal circuit put one tube as venous drain which is also connected with the maternal pump to the lowest position in the upper part of the perfusion chamber.
13. Connect the fetal vein cannula to the fetal vein tube.

### 3. Executing the Pre- and Experimental Phase of Perfusion

1. To allow the tissue to recover from the ischemic period after delivery and to flush out the blood in the intervillous space, an open pre-phase of 20 min is necessary. That means the maternal and fetal vein are not leading back to the arterial reservoir containing the perfusion medium. Collect the fetal and maternal venous outflow in a bottle and discard it after the pre-phase.
2. To assess the integrity of the perfusion perform another pre-phase of 20 min but in a closed circuit. Use two separate reservoirs with perfusion medium for the fetal and maternal circuit and close the circuits by leading the fetal venous outflow back in the fetal reservoir and the maternal venous outflow back in the maternal reservoir.
3. For the main perfusion experiment prepare two flasks with 120 ml perfusion medium (one for the maternal and one for the fetal reservoir). Add the radiolabeled  $^{14}\text{C}$ -antipyrine (4 nCi/ml; serves as positive control; CAUTION: radioactive substance) and the fluorescently labeled xenobiotic or nanoparticles which one wants to analyze to the maternal reservoir. Mix the maternal perfusate well.
4. Start the experiment by exchanging the pure perfusion medium with the two prepared flasks (fetal and maternal reservoirs). Close the circuits by leading the fetal venous outflow back in the fetal reservoir and the maternal venous outflow back in the maternal reservoir.
5. Continue the perfusion for 6 hr and take samples regularly. Always resuspend the medium in the fetal and maternal reservoir before withdrawal.
6. Control the pressure in the fetal artery (should not exceed 70 mmHg), pH in both circuits (should be in a physiological range 7.2-7.4) and the volume of both reservoirs (fetal volume loss should not exceed 4 ml/hr) during perfusion. If necessary adjust the pH values using either hydrochloric acid or sodium hydroxide.
7. If the volume loss in the fetal reservoir exceeds 4 ml/hr there is a leak in the tissue and one has to stop the perfusion. The success rate of a perfusion for 6 hr without leak is about 15-20%.
8. Stop the perfusion after 6 hr. Turn out the pumps, water bath, flow heaters and gas flow.
9. Remove the placenta from the tissue holder, cut the perfused cotyledon (brighter than the unperfused tissue) and weigh it.
10. Take samples from unperfused (part of the placenta which was cut in the beginning; could be already taken during the pre-phase) and perfused tissue (each about 1 g) and store them at  $-20\text{ }^{\circ}\text{C}$  until homogenization or in liquid nitrogen for later analysis. Fix another tissue sample in 4% formalin for histopathological evaluation. The samples should include all layers of the placenta.
11. Clean the tubes after perfusion by successively rinsing the arterial systems of the fetal and maternal circuit with a) 200 ml distilled water, b) 50 ml 1% sodium hydroxide, c) 50 ml 1% phosphoric acid and d) again 200 ml distilled water (flow: 15-20 ml/min).

The entire working procedure of the placenta perfusion experiment is depicted in **Figure 3**.

### 4. Analyzing the Samples

1. Centrifuge the perfusate samples for 10 min at 800 x g before analysis to remove residual erythrocytes. Take the supernatant for the further analysis. The samples can be left overnight at  $4\text{ }^{\circ}\text{C}$ . For the analysis of leptin and hCG production the samples can be stored at  $-20\text{ }^{\circ}\text{C}$ .
2. To evaluate the permeability of the placenta analyze the  $^{14}\text{C}$ -antipyrine by liquid scintillation. Mix 300  $\mu\text{l}$  of the fetal and maternal samples with 3 ml scintillation cocktail and measure for 5 min in a beta counter.
3. To assess the transfer of the fluorescent nanoparticles or the xenobiotic of interest read the fluorescence at 485 nm excitation and 528 nm emission in a microplate reader (indicated wavelengths are for analysis of the yellow green label which we used for the nanoparticles).
4. To determine the viability of the placental tissue during perfusion measure the glucose consumption and lactate production in the fetal and maternal circuit with an automated blood gas system. Additionally, evaluate the production of the placental hormones human choriongonadotropin (hCG) and leptin in the homogenized tissue samples and the perfusates by enzyme-linked immunosorbent assay (ELISA).

## Representative Results

**Figure 4A** shows the perfusion profiles of small polystyrene particles (80 nm) which were transported across the placenta compared to bigger polystyrene particles (500 nm) which were not transferred to the fetal compartment. Each data point represents the mean particle concentration to the given time point of at least 3 independent experiments. For polystyrene nanoparticles the placental transfer is size-dependent<sup>19</sup>. After 3 hr of placenta perfusion already 20-30% of the initially added 80 nm polystyrene particles were transferred from the maternal to the fetal circuit, while the 500 nm polystyrene particles were not appearing in the fetal circuit even after 6 hr of perfusion. Nevertheless, the maternal concentration of the 500 nm particles is decreasing. Fluorescence images on histological section of the tissue after perfusion showed that these particles accumulate in the villi of the placenta (data not shown). **Figure 4B** depicts a characteristic perfusion profile of the radiolabeled  $^{14}\text{C}$ -antipyrine. Antipyrine as a small lipophilic molecule is distributed over the placental barrier via passive diffusion and serves as control for the integrity of the circuits. After 4-6 hr of perfusion an equilibrium between the fetal and maternal antipyrine concentration should be built<sup>23</sup>. To assess and compare the placental transport rate of xenobiotics the fetal-to-maternal drug concentration (F/M) ratio is usually displayed (**Figure 5**).

Through the analysis of lactate and placental hormone (human choriongonadotropin and leptin) production as well as glucose consumption the viability and functionality of the placental tissue during the perfusion could be monitored (**Figure 6**). The values for the perfusions with xenobiotic should always be in the same range as the values from control perfusion without xenobiotic. In addition, histopathological evaluation of the

perfused placental tissue could be performed. A comparison with non-perfused placental tissue could then reveal pathological changes due to perfusion (e.g. bacterial contamination) and therefore could serve as another quality control parameter.

Further representative results obtained with the *ex vivo* dual recirculating human placental perfusion model were published recently<sup>11,19</sup>.

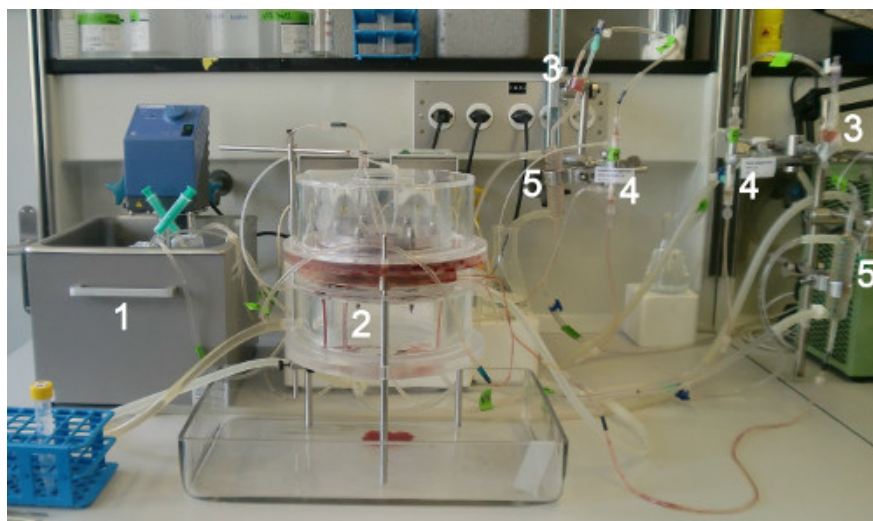


**Figure 1. *Ex vivo* human placental perfusion set-up.** 1) Water bath with maternal and fetal reservoirs, 2) perfusion chamber, 3) bubble trap, 4) oxygenator columns, and 5) flow heater.

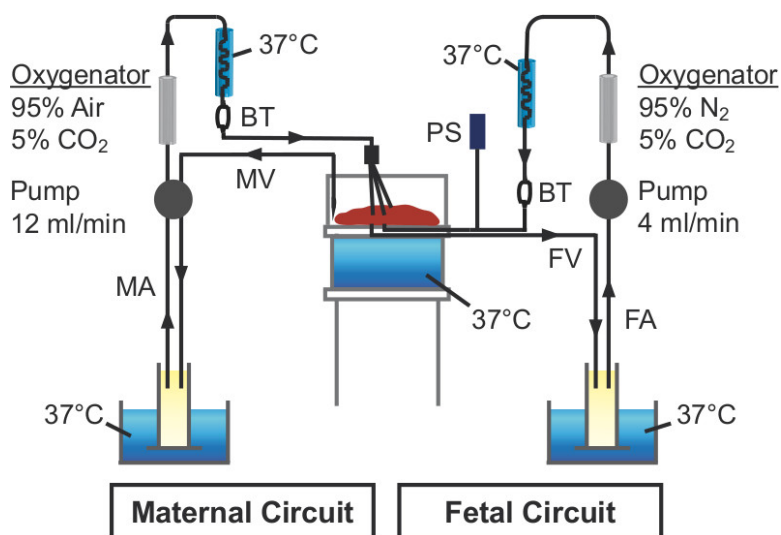


**Figure 2. Schematic illustration of the *ex vivo* human placental perfusion model.** FA: fetal artery; FV: fetal vein; MA: maternal artery; MV: maternal vein; BT: bubble trap; PS: pressure sensor

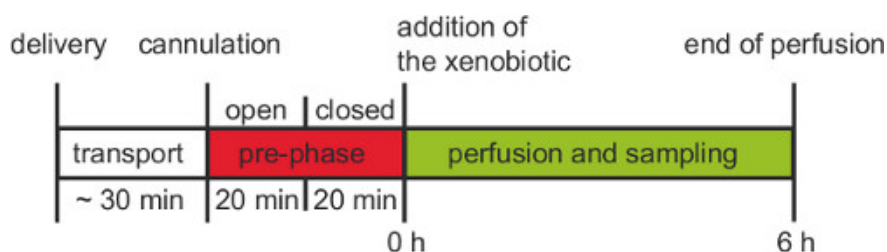


**Figure 3. Working procedure of an *ex vivo* human placental perfusion experiment.** After delivery the placenta has to be cannulated within 30 min. Before the 6 hr experimental phase with recirculation an open pre-phase and closed pre-phase should be performed for at least 20 min each.

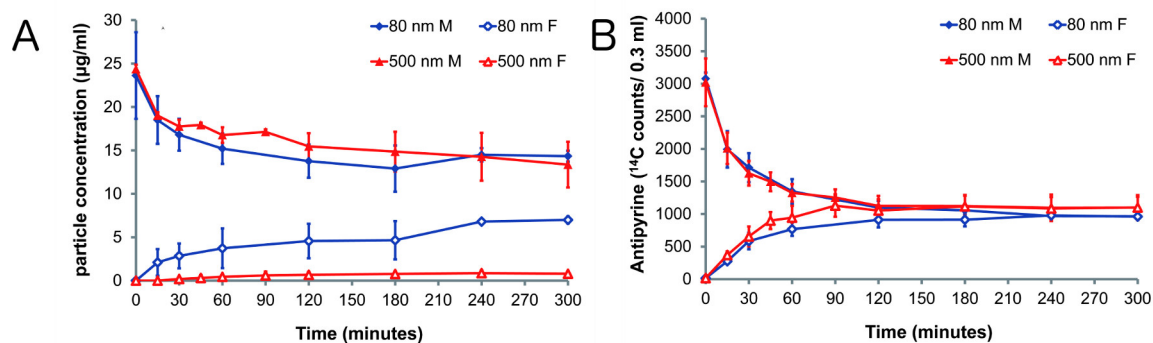


**Figure 4. Perfusion profiles of polystyrene particles and  $^{14}\text{C}$ -antipyrine <sup>19</sup>.** Perfusion profile of polystyrene particles in the sizes 80 nm (n=4) and 500 nm (n=3). Initially 25 µg/ml particles and 4.2 nCi/ml  $^{14}\text{C}$ -antipyrine were added to the maternal circuit. The amount of particles (A) and  $^{14}\text{C}$ -antipyrine (B) were measured in the maternal (M, solid symbols) and fetal (F, open symbols) circuits after the indicated time points. Displayed is the mean concentration  $\pm$  SE. [Click here to view larger figure.](#)

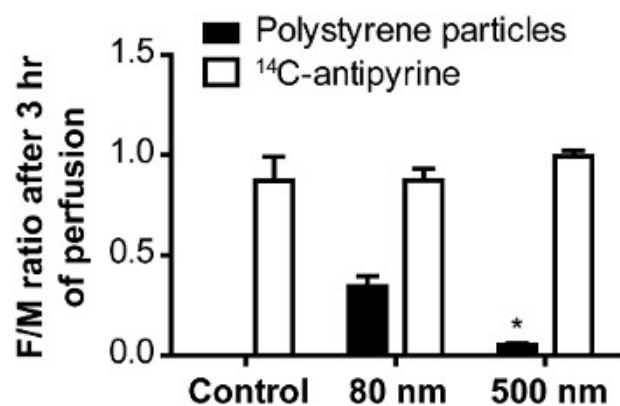


**Figure 5. Size-dependent transfer of polystyrene particles across the human placenta <sup>19</sup>.** The ratios between fetal and maternal concentrations of  $^{14}\text{C}$ -antipyrine and polystyrene particles were calculated after 180 min of placenta perfusion. Data represent the mean  $\pm$  SE of at least 3 independent experiments. The control column depicts perfusions without particles but with  $^{14}\text{C}$ -antipyrine. (\* p < 0.05 compared with 80 nm ratio value).

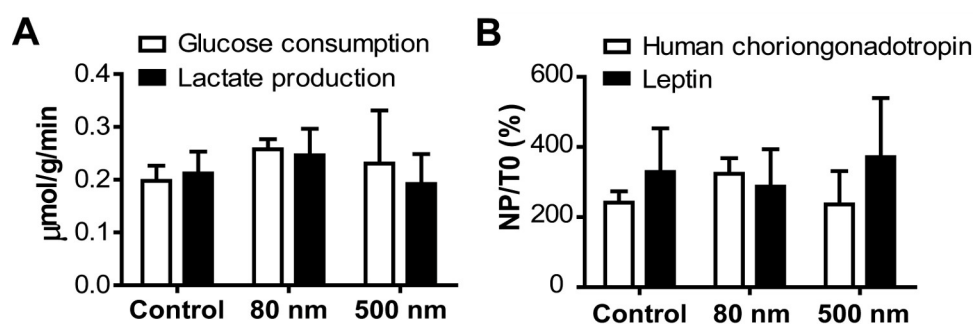


**Figure 6. Viability of the placental tissue during perfusion <sup>19</sup>.** (A) Glucose consumption and lactate production in the perfused placenta. Displayed is the sum of changes in total content in the circuits (fetal and maternal) over time divided by the weight of the perfused cotyledon. (B) Normalized net production (NP divided by initial tissue content T0) of the placental hormones human choriongonadotropin and leptin. Data represent the mean  $\pm$  SE of at least 3 independent experiments.

## Discussion

Beneath the dual recirculating perfusion showed here, there are several other experimental configurations possible depending on the question which has to be answered. Particularly open placental perfusions are commonly used to assess the drug clearance at steady-state concentration <sup>3</sup>. The recirculating perfusion set-up can be also applied to confirm active transport of endogenous or exogenous substances. For this approach the same concentration of the xenobiotic has to be added to the maternal and the fetal circulation. Assumed that there is active transport against

the concentration gradient, accumulation of the test substance in either one of the both circuits may be observed <sup>24</sup>. Of note, the addition of the test substance only to the fetal circuit is also feasible and can reveal the mechanism of transport across the placental barrier of this particular substance <sup>25</sup>.

The protocol has evolved over time and can vary between different research groups especially concerning the flow rate, composition of perfusion medium, form of oxygenation and heating <sup>26,27</sup>. Especially the flow rate can influence the time at which transplacental transfer occurs. To control this, the addition of a passively transported reference compound like antipyrine is important. The transfer rate of the xenobiotic can be always compared to the transfer rate of antipyrine (F/M ratio should be above 0.75) <sup>26</sup>. Since the antipyrine transfer is mainly limited by the flow and exchange surface, this comparison takes differences in the flow and the size of the perfused cotyledon into account which could vary between the experiments. In addition, FITC-dextran could be added to the fetal circuit to serve as control for the integrity of the barrier <sup>26</sup>. Fetal volume loss is also used as marker for the barrier integrity. Usually a fetal fluid loss up to 4 ml/hr is allowed <sup>28</sup>, but there is no generally accepted limit.

Obviously, there are some disadvantages of the *ex vivo* human placental perfusion method like inter-individual variations and a low success rate (15-20%). Moreover, a perfusion period of 6 hr cannot simulate a chronic drug treatment and therefore can't completely exclude the transfer of a xenobiotic after long-term exposure. Another limitation of the model is that mainly the transplacental transfer at term is assessed while the transport rate at early gestational ages when the barrier is thicker remains still unknown. Indeed, perfusion of first trimester placentae is possible but the availability of these placentae is rather limited. Nevertheless, up to now the *ex vivo* placental perfusion method is the only model to study the transport of various xenobiotics or nanoparticles in organized human placental tissue. While toxicodynamics in the *ex vivo* human perfusion model can be analyzed only in the placental tissue, animal experiments can indeed provide also information about the embryotoxicity. Though, because of the anatomic differences of the placental barrier between humans and rodents these results cannot be extrapolated to humans <sup>4,5</sup>. Another possibility to investigate transplacental transfer may be cell culture models like primary cytotrophoblasts, choriocarcinoma cell lines, isolated plasma membrane vesicles or placental tissue explants <sup>29</sup>. The most used model is the BeWo cell line; these cells are derived from a malignant gestational choriocarcinoma and can form a confluent monolayer on a permeable membrane, so transport studies can be performed. Results of transport studies using the BeWo cell model correlate well with results obtained in the *ex vivo* human placental perfusion <sup>30</sup>. However, to study the details of drug transport (e.g. contribution of a specific transport protein) and metabolism, the BeWo cell model may be more feasible primarily because it is easier to handle and susceptible to manipulation like expression of genetically altered transporters or enzymes, but regarding general drug transfer studies the reliability of this model is limited. It lacks blood flow and the integrity of the monolayer has to be evaluated carefully since it depends on several factors like cell culture conditions, seeding density, exposure duration and the membrane insert <sup>6,29</sup>.

Different xenobiotics and also nanoparticles bind to various plasma proteins which can significantly influence the transplacental transfer <sup>31</sup>; considering the binding to plasma proteins is therefore important. The perfusion medium contains bovine serum albumin, the most frequent plasma protein. Recently, a study showed that the transfer ratios of various substances obtained with the *ex vivo* human placental perfusion model correlate well with the *in vivo* cord blood to maternal blood concentration ratios when the transfer ratios were adjusted according to the extent of plasma protein binding <sup>12</sup>.

Overall, the *ex vivo* placental perfusion model is a valid and reliable method to study the transport across the human placenta and to predict the *in vivo* transplacental passage of xenobiotics and nanoparticles.

## Disclosures

The authors declare that they have no competing financial interests.

## Acknowledgements

This work is financially supported by the Swiss National Foundation, (NRP 64 program, grant no 4064-131232).

## References

1. Ala-Kokko, T.I., Myllynen, P., & Vahakangas, K. *Ex vivo* perfusion of the human placental cotyledon: implications for anesthetic pharmacology. *Int. J. Obstet. Anesth.* **9**, 26-38 (2000).
2. Panigel, M., Pascaud, M., & Brun, J.L. [Radioangiographic study of circulation in the villi and intervillous space of isolated human placental cotyledon kept viable by perfusion]. *J. Physiol. (Paris)*. **59**, 277 (1967).
3. Schneider, H., Panigel, M., & Dancis, J. Transfer across the perfused human placenta of antipyrine, sodium and leucine. *Am. J. Obstet. Gynecol.* **114**, 822-828 (1972).
4. Enders, A.C. & Blankenship, T.N. Comparative placental structure. *Adv. Drug Deliv. Rev.* **38**, 3-15 (1999).
5. Takata, K. & Hirano, H. Mechanism of glucose transport across the human and rat placental barrier: a review. *Microsc. Res. Tech.* **38**, 145-152, doi:10.1002/(SICI)1097-0029(19970701/15)38:1/2<145::AID-JEMT15>3.0.CO;2-P (1997).
6. Saunders, M. Transplacental transport of nanomaterials. *Wiley Interdiscip. Rev. Nanomed. Nanobiotechnol.* **1**, 671-684, doi:10.1002/wnan.53 (2009).
7. Buerki-Thurnherr, T., von Mandach, U., & Wick, P. Knocking at the door of the unborn child: engineered nanoparticles at the human placental barrier. *Swiss Med. Wkly.* **142**, w13559, doi:10.4414/smw.2012.13559 (2012).
8. Gendron, M.P., Martin, B., Oraichi, D., & Berard, A. Health care providers' requests to Teratogen Information Services on medication use during pregnancy and lactation. *Eur. J. Clin. Pharmacol.* **65**, 523-531, doi:10.1007/s00228-008-0611-6 (2009).

9. Burns, L., Mattick, R.P., Lim, K., & Wallace, C. Methadone in pregnancy: treatment retention and neonatal outcomes. *Addiction*. **102**, 264-270, doi:10.1111/j.1360-0443.2006.01651.x (2007).
10. von Mandach, U. [Drug use in pregnancy]. *Ther. Umsch.* **62**, 29-35 (2005).
11. Malek, A., Obrist, C., Wenzinger, S., & von Mandach, U. The impact of cocaine and heroin on the placental transfer of methadone. *Reprod. Biol. Endocrinol.* **7**, 61, doi:10.1186/1477-7827-7-61 (2009).
12. Hutson, J.R., Garcia-Bourmissen, F., Davis, A., & Koren, G. The human placental perfusion model: a systematic review and development of a model to predict in vivo transfer of therapeutic drugs. *Clin. Pharmacol. Ther.* **90**, 67-76, doi:10.1038/clpt.2011.66clpt201166 (2011).
13. International Organization for Standardization (ISO). Technical Specification (ISO/TS) 27687. Nanotechnologies – Terminology and definitions for nano-objects – Nanoparticles, nanofibre and nanoplate (2008).
14. Pietroiusti, A. Health implications of engineered nanomaterials. *Nanoscale*. **4**, 1231-1247, doi:10.1039/c2nr11688j (2012).
15. Latzin, P., Roosli, M., Huss, A., Kuehni, C.E., & Frey, U. Air pollution during pregnancy and lung function in newborns: a birth cohort study. *Eur. Respir. J.* **33**, 594-603, doi:10.1183/09031936.00084008 (2009).
16. Lacasana, M., Esplugues, A., & Ballester, F. Exposure to ambient air pollution and prenatal and early childhood health effects. *Eur. J. Epidemiol.* **20**, 183-199 (2005).
17. Menezes, V., Malek, A., & Keelan, J.A. Nanoparticulate drug delivery in pregnancy: placental passage and fetal exposure. *Curr. Pharm. Biotechnol.* **12**, 731-742 (2011).
18. Muhlemann, K., Menegus, M.A., & Miller, R.K. Cytomegalovirus in the perfused human term placenta *in vitro*. *Placenta*. **16**, 367-373 (1995).
19. Wick, P., *et al.* Barrier capacity of human placenta for nanosized materials. *Environ. Health Perspect.* **118**, 432-436, doi:10.1289/ehp.0901200 (2010).
20. Dancis, J. Why perfuse the human placenta. *Contrib. Gynecol. Obstet.* **13**, 1-4 (1985).
21. May, K., *et al.* Perfusion of human placenta with hemoglobin introduces preeclampsia-like injuries that are prevented by alpha1-microglobulin. *Placenta*. **32**, 323-332, doi:10.1016/j.placenta.2011.01.017 (2011).
22. Guller, S., *et al.* Protein composition of microparticles shed from human placenta during placental perfusion: Potential role in angiogenesis and fibrinolysis in preeclampsia. *Placenta*. **32**, 63-69, doi:10.1016/j.placenta.2010.10.011 (2011).
23. Challier, J.C. Criteria for evaluating perfusion experiments and presentation of results. *Contrib. Gynecol. Obstet.* **13**, 32-39 (1985).
24. Kraemer, J., Klein, J., Lubetsky, A., & Koren, G. Perfusion studies of glyburide transfer across the human placenta: implications for fetal safety. *Am. J. Obstet. Gynecol.* **195**, 270-274, doi:10.1016/j.ajog.2005.12.005 (2006).
25. Ieal, J.K., *et al.* Modification of fetal plasma amino acid composition by placental amino acid exchangers *in vitro*. *J. Physiol.* **582**, 871-882, doi:10.1113/jphysiol.2007.130690 (2007).
26. Mathiesen, L., *et al.* Quality assessment of a placental perfusion protocol. *Reprod. Toxicol.* **30**, 138-146, doi:10.1016/j.reprotox.2010.01.006 (2010).
27. Myllynen, P. *et al.* Preliminary interlaboratory comparison of the ex vivo dual human placental perfusion system. *Reprod. Toxicol.* **30**, 94-102, doi:10.1016/j.reprotox.2010.04.006 (2010).
28. Malek, A., Sager, R., & Schneider, H. Maternal-fetal transport of immunoglobulin G and its subclasses during the third trimester of human pregnancy. *Am. J. Reprod. Immunol.* **32**, 8-14 (1994).
29. Prouillac, C. & Lecoeur, S. The role of the placenta in fetal exposure to xenobiotics: importance of membrane transporters and human models for transfer studies. *Drug Metab. Dispos.* **38**, 1623-1635, doi:10.1124/dmd.110.033571 (2010).
30. Poulsen, M.S., Rytting, E., Mose, T., & Knudsen, L.E. Modeling placental transport: correlation of *in vitro* BeWo cell permeability and *ex vivo* human placental perfusion. *Toxicol. In Vitro*. **23**, 1380-1386, doi:10.1016/j.tiv.2009.07.028 (2009).
31. Mathiesen, L., Rytting, E., Mose, T., & Knudsen, L.E. Transport of benzo[alpha]pyrene in the dually perfused human placenta perfusion model: effect of albumin in the perfusion medium. *Basic Clin. Pharmacol. Toxicol.* **105**, 181-187, doi:10.1111/j.1742-7843.2009.00431.x (2009).





Materials List for:

# Determination of the Transport Rate of Xenobiotics and Nanomaterials Across the Placenta using the *ex vivo* Human Placental Perfusion Model

Stefanie Grafmüller<sup>1,2,3</sup>, Pius Manser<sup>2</sup>, Harald F. Krug<sup>2</sup>, Peter Wick<sup>2</sup>, Ursula von Mandach<sup>1</sup>

<sup>1</sup>Department of Obstetrics, Perinatal Pharmacology, University Hospital Zurich

<sup>2</sup>Laboratory for Materials - Biology Interactions, EMPA Swiss Federal Laboratories for Materials Testing and Research

<sup>3</sup>Graduate School for Cellular and Biomedical Sciences, University of Bern

Correspondence to: Peter Wick at [Peter.Wick@empa.ch](mailto:Peter.Wick@empa.ch)

URL: <http://www.jove.com/video/50401>

DOI: [doi:10.3791/50401](https://doi.org/10.3791/50401)

## Materials

| Name   | Company                               | Catalog Number  | Comments  |
|--|---------------------------------------|-----------------|---|
| NCTC-135 medium  | ICN Biomedicals, Inc.                 | 10-911-22C      | could be replaced by Medium 199 from Sigma (M3769)            |
| Sodium chloride (NaCl)   | Sigma-Aldrich, Fluka                  | 71381           |   |
| Potassium chloride (KCl)   | Hospital pharmacy                     |                 | also possible: Sigma (P9541)                                  |
| Monosodium phosphate (NaH <sub>2</sub> PO <sub>4</sub> · H <sub>2</sub> O) | Merck                                 | 106346          |   |
| Magnesium sulfate (MgSO <sub>4</sub> · H <sub>2</sub> O)                   | Sigma-Aldrich, Fluka                  | 63139           |   |
| Calcium chloride (CaCl <sub>2</sub> , anhydrous)                           | Merck                                 | 102388          |   |
| D(+) Glucose (anhydrous)   | Sigma-Aldrich, Fluka                  | 49138           |   |
| Sodium bicarbonate (NaHCO <sub>3</sub> )                                   | Merck                                 | 106329          |   |
| Dextran from Leuconostoc spp.  | Sigma-Aldrich                         | 31389           |   |
| Bovine serum albumin (BSA)   | Applichem                             | A1391           |   |
| Amoxicilline (Clamoxyl)  | GlaxoSmithKline AG                    | 2021101A        |   |
| Sodium heparin   | B. Braun Medical AG                   | 3511014         |   |
| Sodium hydroxide (NaOH) pellets  | Merck                                 | 106498          | CAUTION: corrosive  |
| Ortho-phosphoric acid 85% (H <sub>3</sub> PO <sub>4</sub> )                | Merck                                 | 100573          | CAUTION: corrosive  |
| Maternal gas mixture: 95% synthetic air, 5% CO <sub>2</sub>                | PanGas AG                             |                 |   |
| Fetal gas mixture: 95% N <sub>2</sub> , 5% CO <sub>2</sub>                 | PanGas AG                             |                 |   |
| Antipyrine (N-methyl- <sup>14</sup> C)                                     | American Radiolabeled Chemicals, Inc. | ARC 0108-50 µCi | CAUTION: radioactive material (specific activity: 55mCi/mmol) |
| Scintillation cocktail (IrgaSafe Plus)                                     | Zinsser Analytic GmbH                 | 1003100         |   |
| Polystyrene particles 80 nm  | Polyscience, Inc.                     | 17150           |   |
| Polystyrene particles 500 nm   | Polyscience, Inc.                     | 17152           |   |
| <b>EQUIPMENT</b>   |                                       |                 |   |
| Water bath   | VWR                                   | 462-7001        |   |
| Thermostat   | IKA-Werke GmbH & Co. KG               | 3164000         |   |
| Peristaltic pumps  | Ismatec                               | ISM 833         |   |
| Bubble traps (glass)   | UNI-GLAS Laborbedarf                  |                 |   |
| Flow heater  | UNI-GLAS Laborbedarf                  |                 |   |

|   |                                |                       |   |
|---|--------------------------------|-----------------------|---|
| Pressure sensor + Software for analyses           | MSR Electronics GmbH           | 145B5                 |   |
| Notebook  | Hewlett Packard                |                       |   |
| Miniature gas exchange oxygenator                 | Living Systems Instrumentation | LSI-OXR               |   |
| Tygon Tube (ID: 1.6 mm; OD: 4.8 mm)               | Ismatec                        | MF0028                |   |
| Tubes for pumps (PharMed BPT; ID: 1.52 mm)        | Ismatec                        | SC0744                |   |
| Blunt cannulae ( 0.8 mm)                          | Polymed Medical Center         | 03.592.81             |   |
| Blunt cannulae ( 1.2 mm)                          | Polymed Medical Center         | 03.592.90             |   |
| Blunt cannulae ( 1.5 mm)                          | Polymed Medical Center         | 03.592.94             |   |
| Blunt cannulae ( 1.8 mm)                          | Polymed Medical Center         | 03.952.82             |   |
| Parafilm  | VWR                            | 291-1212              |   |
| Perfusion chamber with tissue holder (plexiglass) | Internal technical department  |                       | Similar equipment is available from Hemotek Limited, UK |
| Surgical suture material (PremiCron)              | B. Braun Medical AG            | C0026005              |   |
| Winged Needle Infusion Set (21G Butterfly)        | Hospira, Inc.                  | ASN 2102              |   |
| Multidirectional stopcock (Discofix C-3)          | B. Braun Medical AG            | 16494C                |   |
| Surgical scissors                                 | B. Braun Medical AG            | BC304R                |   |
| Dissecting scissors                               | B. Braun Medical AG            | BC162R                |   |
| Needle holder                                     | B. Braun Medical AG            | BM200R                |   |
| Dissecting forceps                                | B. Braun Medical AG            | BD215R                |   |
| Automated blood gas system                        | Radiometer Medical ApS         | ABL800 FLEX           |   |
| Multi-mode microplate reader                      | BioTek                         | Synergy HT            |   |
| Liquid scintillation analyzer                     | GMI, Inc.                      | Packard Tri-Carb 2200 |   |
| Scintillation tubes 5.5 ml                        | Zinsser Analytic GmbH          | 3020001               |   |
| Tissue Homogenizer                                | OMNI, Inc.                     | TH-220                |   |
| pH meter + electrode                              | VWR                            | 662-2779              |   |



## PART II

### **Bidirectional transfer study of polystyrene nanoparticles across the placental barrier reveals different transport kinetics**

Stefanie Grafmueller, Pius Manser, Liliane Diener, Pierre-André Diener, Xenia Maeder-Althaus, Lionel Maurizi, Wolfram Jochum, Harald F. Krug, Tina Buerki-Thurnherr, Ursula von Mandach, Peter Wick

#### ***Author contribution***

In this study, I measured the size distribution, determined the detection limit and the stability of the NPs. I analyzed and summarized the results. I performed all the *ex vivo* placental perfusions from M to F direction and some from F to M direction. Most reverse *ex vivo* placental perfusions were performed by Pius Manser. I also performed the analysis of hormone and lactate secretion, as well as glucose consumption during perfusion. Furthermore, I analyzed all perfusate samples for their antipyrine content. Liliane Diener performed TEM analysis of NP suspensions and perfusate samples after perfusion. Xenia Maeder-Althaus performed the MTS assay with BeWo cells. Fluorescence microscopy was conducted by the Team of Wolfram Jochum and Pierre-André Diener at the Institute of Pathology at the Kantonsspital St. Gallen. The zeta potential of the polystyrene beads was measured by Lionel Maurizi at EPFL. Ursula von Mandach and Peter Wick conceived and designed the research project. Ursula von Mandach, Tina Buerki-Thurnherr, Peter Wick and Harald Krug helped me to interpret the data. Tina Buerki-Thurnherr and Harald F. Krug provided expertise, guidance and critical reading. All authors contributed to finalize the manuscript. A manuscript with these results was submitted to Environmental Health Perspectives.



## **Bidirectional transfer study of polystyrene nanoparticles across the placental barrier reveals different transport kinetics**

Stefanie Grafmueller<sup>1,2,3</sup>, Pius Manser<sup>1</sup>, Liliane Diener<sup>1</sup>, Pierre-André Diener<sup>4</sup>, Xenia Maeder-Althaus<sup>1</sup>, Lionel Maurizi<sup>5</sup>, Wolfram Jochum<sup>4</sup>, Harald F. Krug<sup>6</sup>, Tina Buerki-Thurnherr<sup>1</sup>, Ursula von Mandach<sup>2</sup>, Peter Wick<sup>1</sup>

<sup>1</sup>Laboratory for Materials-Biology Interactions, Empa, St. Gallen, Switzerland

<sup>2</sup>Perinatal Pharmacology, Department of Obstetrics, University Hospital Zurich, Zurich, Switzerland

<sup>3</sup>Graduate School for Cellular and Biomedical Sciences, University of Berne, Berne, Switzerland

<sup>4</sup>Institute of Pathology, Cantonal Hospital St. Gallen, St. Gallen, Switzerland

<sup>5</sup>Powder Technology Laboratory, Ecole Polytechnique Federale de Lausanne, Lausanne, Switzerland

<sup>6</sup>Empa, International Research Cooperations Manager, St. Gallen Switzerland

### ***Corresponding Author:***

Dr. Peter Wick

Empa, Swiss Federal Laboratories for Materials Science and Technology

Laboratory for Materials-Biology Interactions

Lerchenfeldstrasse 5

9014 St. Gallen

Switzerland

Phone: +41 58 765 76 84

Fax: +41 58 765 76 99

Email: [peter.wick@empa.ch](mailto:peter.wick@empa.ch)

***Running title:*** Placental transfer of polystyrene nanoparticles

***Acknowledgments:*** This work was financially supported by the Swiss National Foundation, (NRP 64 program, grant no 4064-131232). This project has received funding from the European Union's Seventh Framework Programme for research, technological development and demonstration under grant agreement no 263215 (MARINA) and no 309329 (NANOSOLUTIONS).

We thank M. Roesslein for technical support in measurement of particle size distribution.

***Disclosures:*** The authors declare that they have no competing financial interests.

## Abstract

**Background:** Nanoparticle exposure *in utero* might not be a major concern yet, but could become more important with the increasing application of nanomaterials in consumer and medical products. Several epidemiologic and *in vitro* studies have shown that nanoparticles can have potential toxic effects. However, nanoparticles also offer the opportunity to develop new therapeutic strategies to treat specifically either the pregnant mother or the fetus. Previous studies mainly addressed whether nanoparticles are able to cross the placental barrier or not. Though, the transport mechanisms underlying nanoparticle translocation across the placenta are still unknown.

**Objectives:** In this study we examined which transport mechanisms underlie the placental transfer of nanoparticles.

**Methods:** We used the *ex vivo* human placental perfusion model to analyze the bidirectional transfer of plain and carboxylate modified polystyrene particles in a size range between 50 to 300 nm.

**Results:** We showed that the transport of polystyrene particles in the fetal to maternal direction was significantly higher than for the maternal to fetal direction. Regardless of their ability to cross the placental barrier and the direction of perfusion, all polystyrene particles accumulated in the syncytiotrophoblast of the placental tissue.

**Conclusions:** Our results indicate that the syncytiotrophoblast is the key player in regulating nanoparticle transport across the human placenta. The mechanism underlying this translocation is not based on passive diffusion, but involves active, energy-dependent transport pathways. These findings will be important for reproductive toxicology as well as for pharmaceutical engineering of new drug carriers.

## Introduction

Currently the application of engineered nanoparticles (NP) in industrial and consumer products is increasing continuously. Epidemiological as well as *in vitro* studies showed that these NPs could have adverse health effects in humans (Oberdorster et al., 2005, Pietroiusti, 2012). However, to cause damage *in vivo*, NPs have to cross highly protective biological barriers. Besides the intestine and skin, the air-blood barrier of the lung is an important entry site for NPs. Multiple studies have shown that NPs are able to cross this protective barrier *in vitro* and *in vivo* (Geiser et al., 2005, Kreyling et al., 2009, Rothen-Rutishauser et al., 2007). Furthermore, NPs are applied in various medical products like contrast agents for imaging or metal oxide particles for cancer therapy (Gupta and Gupta, 2005, Rasmussen et al., 2010). Since these medical NPs need to be injected, they get direct access to the blood circulation. Therefore it will be increasingly important to investigate NP transport across internal barriers such as the placenta barrier between the mother and the unborn child.

The placenta is responsible for the supply of nutrients, the removal of waste products and the protection of the fetus against harmful substances. It is organized in cotyledons, which represent the functional units of the placenta. Each cotyledon is formed by a fetal villous tree. Due to the extensive division of the villous trees the total exchange surface area at term is about 13 m<sup>2</sup> (Larsen et al., 1995, Syme et al., 2004). The maternal blood is released into the intervillous space and separated from the fetal circulation by the syncytiotrophoblast layer, some few cytotrophoblast cells and the endothelial cell layer of the fetal capillaries, which are surrounded by stromal fibroblasts and fetal macrophages. The thickness of this barrier decreases during pregnancy to allow an increased maternal-fetal exchange at late gestational ages (Juch et al., 2013, Syme et al., 2004). The syncytiotrophoblast layer as key barrier is built from cytotrophoblast cells which fuse during development and form a true syncytium without lateral cell membranes (Enders and Blankenship, 1999). The plasma membrane of the syncytiotrophoblast is highly polarized and consists of two membranes. The basal membrane is in contact with the villous stroma which surrounds the fetal capillaries while the brush border membrane with its many microvilli faces the maternal blood stream. The polarity of the syncytiotrophoblast is based on a different repertoire of transport proteins for each of these membranes. Furthermore, there is a huge variety of transporters, which act in both directions (importer and exporter), to ensure an optimal supply with nutrients and an efficient efflux of waste products or harmful drugs (Ganapathy et al., 2000). The placental transfer of such substances depends on four different mechanisms: passive diffusion, active transport,

phagocytosis/ pinocytosis and biotransformation through metabolic enzymes (Syme et al., 2004).

Several animal studies showed that different NPs like gold, silica or titanium dioxide can cross the placental barrier and some of them can even impair fetal development (Semmler-Behnke et al., 2008, Yamashita et al., 2011). However, the placenta is the most species-specific organ and data obtained in rodent models cannot be simply extrapolated to the human system (Enders and Blankenship, 1999, Takata and Hirano, 1997). The *ex vivo* human placental perfusion provides an ethically accepted model, close to the *in vivo* situation, to investigate placental transport of xenobiotics as well as NPs (Grafmüller et al., 2013, Malek et al., 2009, Panigel et al., 1967, Schneider et al., 1972). Using this model it has been shown that 25 and 50 nm silica particles are transported across the human placental barrier while pegylated 10 – 30 nm gold particles were retained in the maternal circulation and the placental tissue (Myllynen et al., 2008, Sonnegaard Poulsen et al., 2013). Previous work performed by our group revealed a size-dependent translocation of polystyrene (PS) particles with placental passage of PS particles up to 240 nm in diameter (Wick et al., 2010). Though there is an increasing number of *in vivo* and *in vitro* studies about placental NP transport (Buerki-Thurnherr et al., 2012, Saunders, 2009), the transport mechanisms for NPs across the placental barrier are largely unknown. Knowledge about the route of NP transport across the placenta barrier and about its dependency on NPs physicochemical properties is a prerequisite for future development of NPs as drug carriers to either specifically treat the mother without affecting the fetus or even to treat placental dysfunctions. To assess the contribution of the physicochemical properties of NPs to placental NP transfer and the transport mechanisms underlying this process, we performed and analyzed bidirectional transfer studies of fluorescently labeled PS particles with different sizes and surface modifications in the *ex vivo* human placental perfusion model.

## Materials and Methods

**Particles.** Yellow-green-labeled PS beads without functionalization (plain) with the size of 50 and 240 nm from Spherotech (Lake Forest, IL, USA) were used. Yellow-green-labeled, carboxylate-modified (COOH) 50 and 300 nm PS beads were purchased from Polysciences (Warrington, PA, USA).

**Particle characterization.** The zeta potential in 10 mM sodium chloride and perfusion medium at pH between 6.8 and 7.2 was determined with a Zetasizer NanoZS (Malvern Instruments, Worcestershire, UK).

Particle size distribution in double distilled (DD) water and perfusion medium (PM) was determined by nanoparticle tracking analysis (NTA; NanoSight LM 20 System, NanoSight Ltd., Amesbury, UK) as described previously (Hole et al., 2013). The ingredients of the PM are described in the Supplemental Material, p. 73 - 74. The DD water and PM were filtered through a 0.02  $\mu\text{m}$  Anotop® 25 syringe filter (Whatman GmbH, Germany) prior to analysis. For each particle size the results were normalized to the area under the NP concentration/size curve.

The detection limit of the PS beads fluorescence was determined by making a serial dilution in the range of 0.02 – 10  $\mu\text{g/mL}$  of each PS particle in perfusion medium. The detection limit was defined as the minimum concentration of PS particles in perfusion medium which showed a significant increase in fluorescence intensity as compared to pure perfusion medium.

To assess the stability of fluorescence the loss of fluorescence intensity was analyzed after incubation of the PS beads in perfusion medium at 37 °C for 3, 6, 24, 48 and 72 hrs using a microplate reader (Biotek Synergy HT, Winooski, VT, USA) with excitation and emission wavelengths of 485 and 528 nm. The leakage of fluorescence was assessed by measuring the fluorescence before and after filtration through a 0.1  $\mu\text{m}$  syringe filter at the end of the indicated incubation periods.

**Ex vivo human placental perfusion model.** The placentas were obtained from uncomplicated term pregnancies after caesarean section at the Department of Obstetrics at the University Hospital Zurich, the Kantonsspital and the Klinik Stephanshorn in St. Gallen. Written informed consent was obtained prior to delivery. The project was approved by the local ethics committee and performed in accordance with the principles of the Declaration of Helsinki. The placenta perfusion was performed as described previously (Wick et al., 2010, Grafmuller et al., 2013). For a brief description see Supplemental Material, p. 73 - 74.



**Fluorescence microscopy.** Unstained paraffin sections of non-perfused (negative control) and perfused placenta were deparaffinized with xylene followed by 100 % ethanol. Afterwards the slides were air-dried, covered with VECTASHIELD® Mounting Medium containing DAPI (Vector Laboratories, Burlingame, CA, USA) on a glass slide and the coverslips were sealed with nail polish. The slides were analysed with a Leica DM6000B fluorescence microscope system (Leica Microsystems, Heerbrugg, Switzerland) equipped with a triple band pass filter set (DAPI/Spectrum Green/Spectrum Orange). All cases were photographed for documentation using a Leica DFC420C Camera.

**Transmission electron microscopy (TEM).** Particle suspensions as supplied by the manufacturer were applied onto a carbon-coated copper grid and processed for TEM analysis (Zeiss 900 TEM, Carl Zeiss MicroImaging, Oberkochen, Germany). Samples from fetal or maternal circulation after 1.5 - 6 hrs of perfusion were centrifuged twice for 30 minutes at 25000 g and 4 °C. The pellets were resuspended in DD water and processing for TEM analysis was performed as described for the particle suspensions.

**Statistical analysis.** Data are shown as mean  $\pm$  standard deviation (SD) from at least three independent experiments. Unpaired Student's t-test was performed using GraphPad Prism software, version 6 (GraphPad Software, La Jolla, CA, USA). Differences were considered statistically significant at a p-value below 0.05.

## Results

### *Particle characterization and cytotoxicity evaluation*

The fluorescently labeled PS beads were extensively characterized and the results are summarized in Table 1 and Figure 1. All PS particles suspended in 10 mM sodium chloride solution were negatively charged, but the zeta potential of the carboxylate-modified PS beads was significantly lower than the one of plain PS beads in the same size range. Analysis of the size distribution by nanoparticle tracking analysis confirmed that the plain 50 nm and carboxylate-modified 50 nm PS beads were relatively monodisperse (Figure 1A, B). However, the plain 240 nm and carboxylate-modified 300 nm PS beads contained an additional fraction of smaller beads around 100 nm which were not observed to that extent in the corresponding TEM micrographs (Figure 1D, F). Furthermore, TEM images demonstrated that the plain and carboxylate-modified 50 nm PS beads contained some smaller particles of around 20 nm in diameter (Figure 1C, E). As expected, the hydrodynamic diameter for all PS beads in perfusion medium was higher than in water.

Since a few studies showed a leakage of the fluorescence dye from NPs (Pietzonka et al., 2002, Tenuta et al., 2011), their stability in perfusion medium was tested over a time period of 72 hrs at 37 °C. After 3 hrs fluorescence intensity decreased to  $75 \pm 4$  % of the initial signal for the plain 50 nm,  $76 \pm 2$  % for the plain 240 nm,  $83 \pm 4$  % for the carboxylate-modified 50 nm and  $84 \pm 5$  % for the carboxylate-modified 300 nm PS beads, but there was no further decline after 72 hrs (see Supplemental Material, Figure S1A). This slight decrease in fluorescence intensity was not due to a loss of fluorescence dye from the particles, as mean leakage of the dye was below 0.52 % for the plain 240 nm and 2.3 % for the carboxylate-modified 300 nm PS beads (see Supplemental Material, Figure S1B). Filtration of the smaller beads through a 20 nm syringe filter was attempted, but failed due to the high viscosity of the perfusion medium and the obstruction of the filter. Therefore leakage of the dye could not be assessed in these samples. However, since the 50 nm beads were obtained from the same supplier as the larger particles, we assumed that they were produced with similar quality standards.

To confirm the absence of cytotoxic effects of the PS beads an MTS viability assay was performed on BeWo cells. These cells were used as a model of the syncytiotrophoblast which will get into contact with NPs in the *ex vivo* perfusion system first. None of the PS particles decreased significantly cell viability even at higher concentrations and longer exposure time than those used in the *ex vivo* perfusion experiments (see Supplemental Material, Figure S2).

**Table 1. Summary of PS beads characteristics**

|   | plain       |             | carboxylate-modified |              |
|---|-------------|-------------|----------------------|--------------|
|   | 50 nm       | 240 nm      | 50 nm                | 300 nm       |
| Diameter (nm) <sup>a</sup>                                | 49          | 240         | 42.5                 | 302.7        |
| Diameter (nm) <sup>b</sup> in TEM                         | 43.7 ± 8    | 220.5 ± 5.1 | 44.1 ± 7.1           | 289.4 ± 10.2 |
| Hydrodynamic diameter in DD water (nm) <sup>c</sup>       | 88 ± 79.5   | 230 ± 65.3  | 68 ± 19.2            | 283 ± 85.2   |
| Hydrodynamic diameter in PM (nm) <sup>c</sup>             | 104 ± 74.7  | 273 ± 95.4  | 114 ± 49.1           | 359 ± 101.2  |
| Initial no. of particles/mL in PM <sup>d</sup>            | 5.45E+11    | 4.24E+09    | 5.30E+11             | 1.88E+09     |
| Particle surface (nm <sup>2</sup> )/mL in PM <sup>d</sup> | 3.27E+15    | 6.48E+14    | 3.24E+15             | 4.94E+14     |
| Detection limit in PM (μg/mL)                             | < 1.25      | < 0.63      | < 0.078              | < 0.078      |
| Zeta potential in 10 mM NaCl (mV) <sup>b</sup>            | -19.8 ± 4.0 | -20.5 ± 2.7 | -34.7 ± 7.1          | -55.6 ± 6.1  |
| Zeta potential in PM (mV) <sup>b</sup>                    | -11.3 ± 6.5 | -13.7 ± 5.8 | -11.9 ± 11.2         | -13.9 ± 7.4  |

Abbreviations: DD double distilled; PM perfusion medium; TEM transmission electron microscopy

<sup>a</sup>according to the manufacturer's information; <sup>b</sup>experimentally determined (mean ± SD); <sup>c</sup>experimentally determined (mode ± SD); <sup>d</sup>calculated values

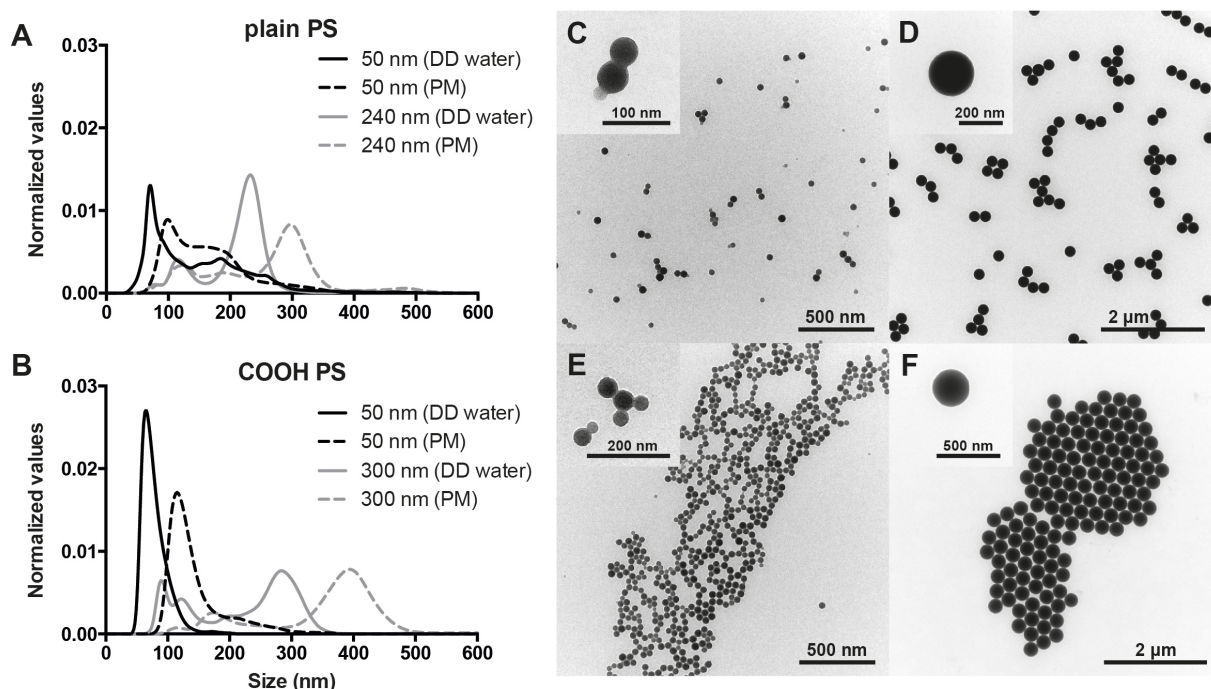


**Figure 1:** (A + B) Particle size distribution of plain (A) and carboxylate-modified (B) PS beads was measured in DD water (solid line) and PM (dashed line) by nanoparticle tracking analysis. (C – F) TEM micrographs of plain 50 nm (C), plain 240 nm (D), carboxylate-modified 50 nm (E) and carboxylate-modified 300 nm (F) polystyrene beads in DD water.

#### ***Placental transfer***

In a previous study we observed a size-dependent transfer of PS beads after 3 hrs of *ex vivo* human placental perfusion in maternal to fetal direction with the highest transfer rate for plain 50 nm PS beads (Wick et al. 2010). In the current study we investigated the bidirectional placental transfer of plain 50 and 240 nm as well as carboxylate-modified 50 and 300 nm PS particles by either adding 25  $\mu\text{g/mL}$  PS beads to the maternal (M) or to the fetal (F) circulation. After 6 hrs of perfusion, the concentration of all PS beads was increased in reverse direction (F to M) as compared to normal perfusions (M to F direction) (Figure 2A, B). We observed a significant difference in placental transfer between normal and reverse perfusions for the plain 50 nm (M to F  $13.7 \pm 8.4$  % versus F to M  $23.7 \pm 5.8$  %), the carboxylate-modified 50 nm (M to F  $1.4 \pm 0.5$  % versus F to M  $7.2 \pm 1.3$  %) and carboxylate-modified 300 nm PS beads (M to F  $1.2 \pm 0.7$  % versus F to M  $5.3 \pm 0.5$  %) (Figure 2C). Plain 240 nm PS beads also showed a tendency for a higher transfer in the reverse direction (M to F  $2.4 \pm 0.7$  % versus F to M  $6.1 \pm 4.1$  %) indicating a generally increased placental permeability in the F to M direction. In addition, we showed an increased translocation of non-functionalized 50 nm PS beads as compared to carboxylate-modified 50 nm PS particles in both directions indicating that the surface charge or modification of NPs could also influence placental NP transfer (Figure 2C). For the particles in the size range between 240 and 300 nm a significant difference between plain and carboxylate-modified beads was also observed but only in perfusions from M to F direction (Figure 2C). To ensure that we did not measure placental transfer of detached fluorescence dye, we wanted to recover the PS beads from the fetal (in case of normal perfusions) or the maternal (reverse perfusions) perfusates after *ex vivo* perfusion. In TEM micrographs both large (240 and 300 nm) and the plain 50 nm PS beads were found in the maternal perfusate after reverse perfusions, whereas in the fetal perfusate after normal perfusions only the plain 50 nm PS beads were detected (see Supplemental Material, Figure S1C). Transfer of the plain 240 nm and both carboxylate-modified beads from M to F direction was too low ( $< 0.8$   $\mu\text{g/mL}$ ) for detection by TEM, but still within the detection limit of the more sensitive fluorescence measurement. Moreover, during *ex vivo* placental perfusion a great amount of other electron dense substances such as proteins or sugars were released in both circulations, which made it especially difficult to find the small 50 nm PS beads via TEM analysis. Therefore, only the plain 50 nm PS beads were detectable in TEM micrographs due to their high transfer in both directions.

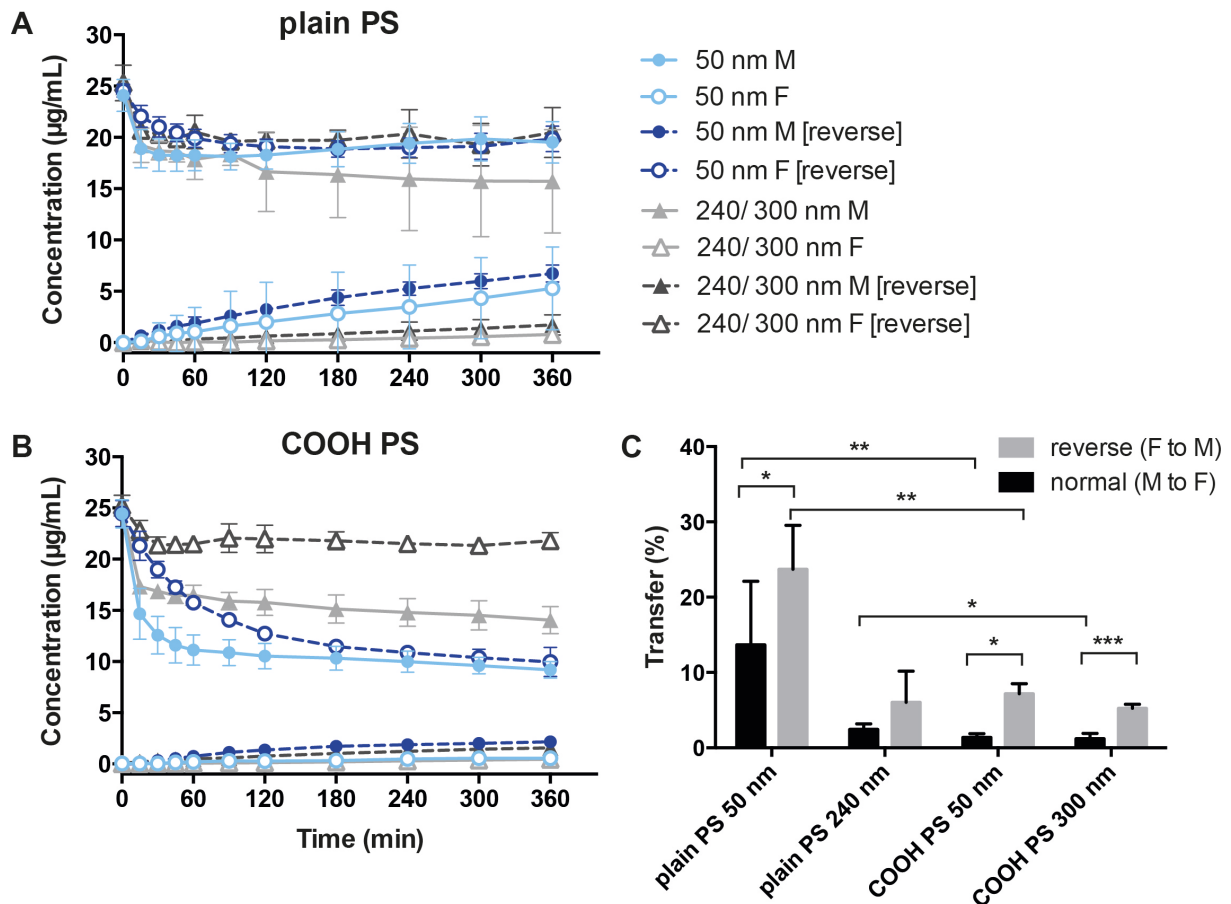


**Figure 2:** Perfusion profiles and transfer rates of PS beads during *ex vivo* human placental perfusion. Transplacental transport of plain (A) and carboxylate-modified (B) PS beads over a time period of 6 hrs either from the maternal to fetal (M to F) or reverse from the fetal to maternal (F to M) circulation. Initially 25  $\mu\text{g/mL}$  beads were added to the maternal (normal perfusions; continuous line) or fetal (reverse perfusions; dashed line) circulation, respectively. The amount of particles was determined by fluorescence measurement in the maternal (M, solid symbols) and fetal (F, open symbols) circuit at several time points. Data represents the mean particle concentration  $\pm$  SD of at least 3 independent experiments. (C) Transfer of PS beads calculated after 6 hrs of perfusion. Data is expressed as mean percentage of the initially added amount of PS beads  $\pm$  SD of at least 3 independent experiments. (\*)  $p < 0.05$ , (\*\*)  $p < 0.01$ , (\*\*\*)  $p < 0.001$

As control for a passively transported substance across the placental barrier, radiolabeled  $^{14}\text{C}$ -antipyrine was added to each perfusion. After 4 - 6 hrs equal concentrations should be reached in both circulations (Challier et al., 1983) and F to M or M to F concentration ratios should be around 1. This criterion was fulfilled in all perfusions demonstrating that the PS beads had no effect on barrier permeability itself (see Supplemental Material, Figure S3). Of note, the development of the concentration equilibrium of antipyrine in reverse perfusions was decelerated compared to perfusions in M to F direction (see Supplemental Material, Figure S3A). During the perfusion process there was no influence of the PS beads on viability (glucose consumption and lactate production) and functionality (human chorionic gonadotropin and leptin secretion) of the placenta (see Supplemental Material, Figure S3B, C). Moreover, no

visible structural changes to the placental tissue after perfusion with or without particles were identified in histological tissue sections (data not shown).

Despite there was only little transfer of the plain 240 nm, carboxylate-modified 50 nm and 300 nm PS beads in both directions, the maternal (normal perfusions) or fetal (reverse perfusions) concentration of these beads was declining (Figure 2A, B). Fluorescence microscopic images showed that these particles accumulated in the placental tissue (Figure 3). PS beads were mainly found in the syncytiotrophoblast layer of the placental villi independent of particle size, functionalization or mode of perfusion (Figure 3A, B). Unfortunately a reliable quantification of the PS beads in the tissue based on the fluorescence images was not possible because resolution is not sufficient to visualize single particles and small agglomerates which would lead to an underestimation of NP tissue content. Therefore we calculated the theoretical amount of PS beads in the tissue by subtracting the measured concentration in the fetal and maternal circuit from the initially added concentration (Figure 3C). After 6 hrs of perfusion the tissue content of the PS beads with a higher transfer rate (plain 50 nm F to M and M to F; plain 240 nm F to M; COOH 300 nm F to M) was significantly lower as compared to the PS beads (COOH 50 nm M to F and F to M; plain 240 nm M to F, COOH 300 nm M to F) with only low placental transfer (Figure 3C).

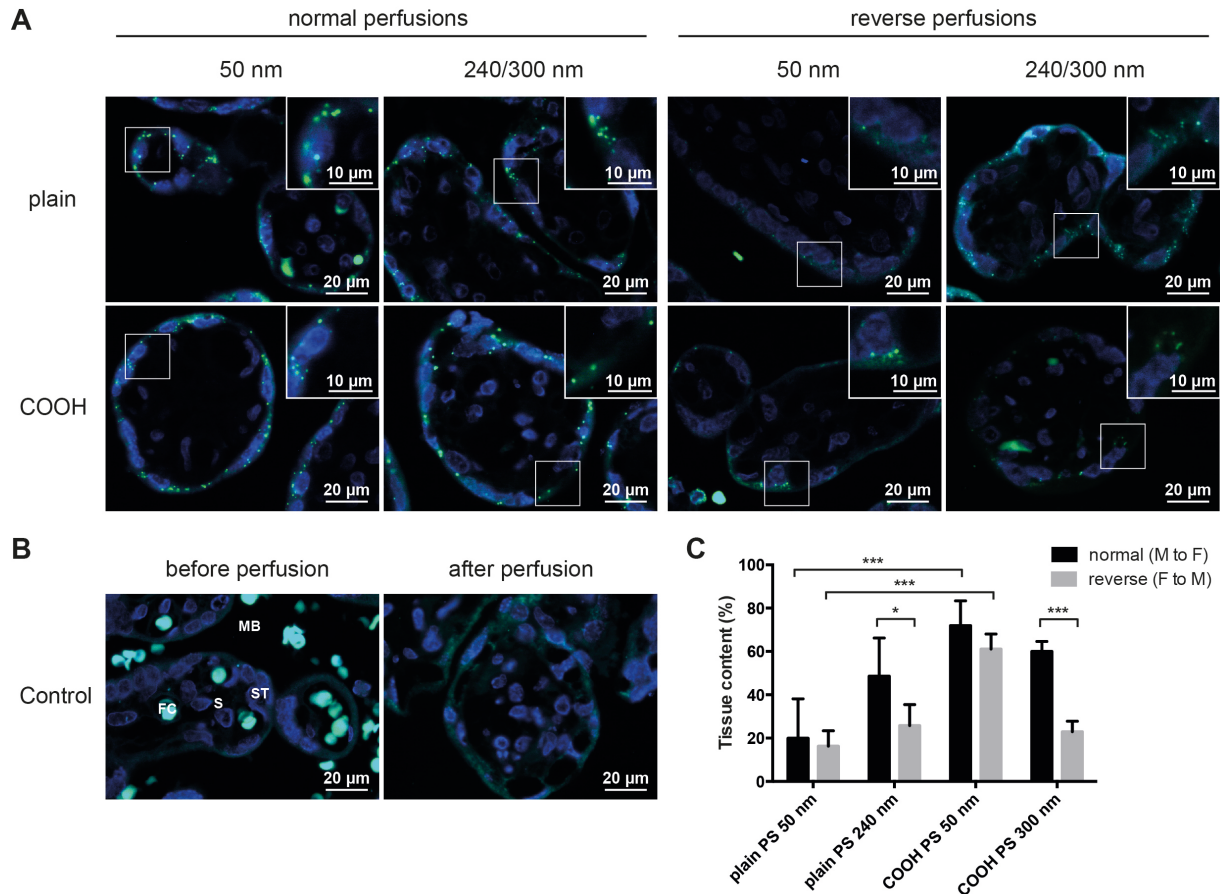


**Figure 3:** Localization (A + B) and quantification (C) of PS beads in the placental tissue. (A) Fluorescence microscope images of placental tissue after 6 hrs of perfusion in normal and reverse direction with plain 50 nm, plain 240 nm, carboxylate-modified 50 nm and carboxylate-modified 300 nm PS beads (green). Nuclei were stained with DAPI (blue). (B) Fluorescence microscope images of placental tissue before and after control perfusions without particles. (C) Theoretical NP tissue content after 6 hrs of perfusion. Displayed is the percentage of initially added PS beads after subtraction of the PS fractions in fetal and maternal circuits after 6 hrs (mean  $\pm$  SD of at least 3 independent experiments). (\*)  $p < 0.05$ , (\*\*\*)  $p < 0.001$

ST: syncytiotrophoblast; S: Stroma; FC: fetal capillary; MB: maternal blood space)

## Discussion

In this study we showed a bidirectional transfer of plain and carboxylate-modified PS beads up to a size of 300 nm using the *ex vivo* human placental perfusion model. The placental transport was increased in reverse perfusions from the fetal to the maternal side indicating that there are different transport mechanisms for PS particles on the fetal and maternal side of the human placenta. Although transport in the reverse direction is physiologically not relevant regarding *in vivo* exposure to NPs, which will only occur in the maternal circulation, reverse *ex vivo* placental perfusion is a common method to evaluate the mode of transport of many drugs across the human placenta (Nanovskaya et al., 2012, Nekhayeva et al., 2005, Sudhakaran et al., 2005). For example a study about bidirectional placental transfer of antibiotics revealed that telavancin has a higher placental transfer in the reverse direction suggesting a translocation not simply by passive diffusion, but indicates that specific transporters may be involved (Nanovskaya et al., 2012). However, it is rather unlikely that NPs in general are transported via such transporters across the placenta (Menezes et al., 2011). Nevertheless our results demonstrate that passive diffusion is not the key mechanism underlying placental translocation of PS particles, because concentration equilibrium was not achieved after 4 – 6 hours as compared to the passively transported antipyrine. According to Fick's law, diffusion of a substance mainly depends on the permeability of the membrane for this substance, the concentration gradient across the membrane and the membrane surface area. In our study placental transfer kinetics of antipyrine from F to M direction was significantly delayed as compared to M to F direction which was likely due to the lower exchange surface from the fetal direction (inner surface of the fetal capillaries versus the very large brush border membrane of the syncytiotrophoblast for the maternal direction) and the reduced fetal perfusion flow (3 - 4 mL/min compared to 12 mL/min for the maternal circuit) (Challier et al., 1983). Thus, NP transfer in the reverse direction should be reduced if it would be based predominantly on a passive transport mechanism. However, we even observed an augmented transfer in F to M direction (compared to M to F) of PS particles independent of their physicochemical properties, suggesting an energy-dependent transport mechanism for PS particle translocation across the human placenta. Phagocytosis is one example of an energy-dependent mechanism proposed for NP uptake into cells especially in phagocytes (Jud et al., 2013). It has been shown that primary human macrophages engulf carboxylate-modified PS beads via this pathway whereas THP-1 cells, a human monocytic leukemia cell line, use an endocytosis pathway (Lunov et al., 2011). During phagocytosis vesicles with a diameter



> 0.5  $\mu\text{m}$  are formed, whereas the diameter of endocytotic vesicles is considerably smaller (Aderem and Underhill, 1999). Caveolin coated vesicles are defined as membrane invaginations with a diameter of 60 to 80 nm and vesicles arising from clathrin-dependent endocytosis are described to have a diameter of approximately 120 to 150 nm e.g. in human epithelial cells (McMahon and Boucrot, 2011, Parton and Simons, 2007). A study using specific transport pathway inhibitors revealed that A549 cells, a human alveolar epithelial cell line, take up gold NPs with a diameter of 15 nm mainly by endocytosis (Brandenberger et al., 2010). Moreover, endo- and transcytosis are also proposed as the most common transport mechanisms for NPs at the blood-brain barrier (Kreuter, 2014).

Most of the studies about NP uptake mechanism were performed on non-polarized cells or cell lines, which do not resemble a typical polarized barrier as the placental syncytiotrophoblast. The different membrane properties and receptor repertoires on the apical and basal side may allow different transport mechanisms depending on the site of exposure. So far most groups observed NP uptake in the syncytiotrophoblast after *ex vivo* human placental perfusion even if NP translocation to the fetal circulation was absent or below detection limit (Menjoge et al., 2011, Myllynen et al., 2008, Sonnegaard Poulsen et al., 2013). We also observed most of the PS particles accumulated predominantly in the syncytiotrophoblast layer, which indicates that the syncytium is a major determinant of NP transfer. Besides the syncytiotrophoblast the endothelial cells of the fetal capillaries are also part of the placental barrier. It has been shown that these cells contribute to the barrier function and mostly act as a molecular sieve for larger hydrophilic molecules (Firth and Leach, 1996). However, to evaluate the definite contribution of the fetal endothelium to placental NP transfer, *in vitro* co-culture models including trophoblasts as well as endothelial cells are necessary and currently under development (Levkovitz et al., 2013).

Nanoparticle uptake into cells also depends on the physicochemical properties of the materials (Lunov et al., 2011). We demonstrated that carboxylate-modified PS beads were transferred across the placenta in significantly lower amounts than plain particles. The carboxylate-modified PS beads had a lower zeta potential than the plain beads indicating that the surface charge of NPs can have an impact on placental transfer. Indeed, such a surface charge-dependent placental translocation has been demonstrated in pregnant rats where amine-modified PS beads showed a stronger translocation than carboxylate-modified PS beads (Tian et al., 2009). Similar observations have been made with NPs at other biological barriers. The accumulation of negatively charged gold NPs in secondary organs after oral exposure in rats

was higher than for positively charged particles (Schleh et al., 2012). Furthermore, studies of NP uptake at the air-blood barrier revealed that the surface charge of NPs below a size threshold of 34 nm is the most critical factor for translocation (Choi et al., 2010). Differently charged NPs acquire a distinct protein corona after contact with serum or biological fluids (Hirsch et al., 2013, Lundqvist et al., 2008, Monopoli et al., 2011). The protein corona can influence the biological fate of NPs through alteration of their hydrodynamic diameter or surface properties. In addition, serum proteins can also influence directly the uptake mechanism of NPs by binding to their specific receptors on the cell surface, thereby mediating endocytosis (Monopoli et al., 2012). Several groups observed that albumin concentration in the perfusion medium determines the transplacental transfer of several drugs in the *ex vivo* human placental perfusion model (Mathiesen et al., 2009, Nanovskaya et al., 2008). The perfusion medium used in our study was supplemented with albumin only and not with complete serum. However, many other proteins are produced by placental cells during perfusion and are released into the circulation where they can get in contact with the PS beads. Interestingly, many hormones produced in the placenta are secreted asymmetrically into the maternal and the fetal circulation (Linnemann et al., 2000, Malek et al., 2001). Therefore adsorption of different proteins in fetal and maternal circulation may also provide an explanation for the differential transport in normal and reverse perfusions in our study. To corroborate this hypothesis, further studies with a broad variety of differently charged NPs as well as on the composition of the NP protein corona are required.

Studies using the *ex vivo* human placental perfusion model are limited to a few hours of perfusion due to tissue degradation (Panigel et al., 1967, Schneider et al., 1972), and only reflect placental transport at late pregnancy. To assess long-term effects of NP exposure and transport during early stages of pregnancy, when the placental barrier is much thicker (Nikitina et al., 2013), *in vitro* studies are indispensable. In addition, *in vitro* studies would allow a higher throughput than *ex vivo* perfusions. So, involvement of specific transport pathways could be tested first *in vitro* and could be subsequently confirmed in the *ex vivo* placental perfusion model which is closer to the *in vivo* situation. Overall, development of more advanced and carefully validated *in vitro* models, which include also flow and several placental cell types, are expected to lead to a better understanding of NP transport mechanisms across the placental barrier and their dependence on the physicochemical properties of NPs.

## Conclusions

Our study is the first approach to investigate the transport mechanism of NPs by studying bidirectional transfer of PS particles in the *ex vivo* human placental perfusion model. We demonstrated an increased transfer of PS beads in reverse (F to M direction) perfusions and an accumulation of PS beads in the syncytiotrophoblast layer of the placental tissue. Based on our findings we can exclude a transfer via passive diffusion. We propose an energy-dependent placental translocation pathway and the polarized syncytiotrophoblast as the main contributor to NP transfer in the placenta. Though, for development and safe use of NPs in nanomedicine, transport mechanisms of NPs across the placental barrier need to be determined precisely in further studies.

## References

- ADEREM, A. & UNDERHILL, D. M. 1999. Mechanisms of phagocytosis in macrophages. *Annu Rev Immunol*, 17, 593-623.
- BRANDENBERGER, C., MUHLFELD, C., ALI, Z., LENZ, A. G., SCHMID, O., PARAK, W. J., GEHR, P. & ROTHEN-RUTISHAUSER, B. 2010. Quantitative evaluation of cellular uptake and trafficking of plain and polyethylene glycol-coated gold nanoparticles. *Small*, 6, 1669-78.
- BUERKI-THURNHERR, T., VON MANDACH, U. & WICK, P. 2012. Knocking at the door of the unborn child: engineered nanoparticles at the human placental barrier. *Swiss Med Wkly*, 142, w13559.
- CHALLIER, J. C., D'ATHIS, P., GUERRE-MILLO, M. & NANDAKUMARAN, M. 1983. Flow-dependent transfer of antipyrine in the human placenta in vitro. *Reprod Nutr Dev*, 23, 41-50.
- CHOI, H. S., ASHITATE, Y., LEE, J. H., KIM, S. H., MATSUI, A., INSIN, N., BAWENDI, M. G., SEMMLER-BEHNKE, M., FRANGIONI, J. V. & TSUDA, A. 2010. Rapid translocation of nanoparticles from the lung airspaces to the body. *Nat Biotechnol*, 28, 1300-3.
- ENDERS, A. C. & BLANKENSHIP, T. N. 1999. Comparative placental structure. *Adv Drug Deliv Rev*, 38, 3-15.
- FIRTH, J. A. & LEACH, L. 1996. Not trophoblast alone: a review of the contribution of the fetal microvasculature to transplacental exchange. *Placenta*, 17, 89-96.
- GANAPATHY, V., PRASAD, P. D., GANAPATHY, M. E. & LEIBACH, F. H. 2000. Placental transporters relevant to drug distribution across the maternal-fetal interface. *J Pharmacol Exp Ther*, 294, 413-20.
- GEISER, M., ROTHEN-RUTISHAUSER, B., KAPP, N., SCHURCH, S., KREYLING, W., SCHULZ, H., SEMMLER, M., IM HOF, V., HEYDER, J. & GEHR, P. 2005. Ultrafine particles cross cellular membranes by nonphagocytic mechanisms in lungs and in cultured cells. *Environ Health Perspect*, 113, 1555-60.
- GRAFMULLER, S., MANSER, P., KRUG, H. F., WICK, P. & VON MANDACH, U. 2013. Determination of the transport rate of xenobiotics and nanomaterials across the placenta using the ex vivo human placental perfusion model. *J Vis Exp*.
- GUPTA, A. K. & GUPTA, M. 2005. Synthesis and surface engineering of iron oxide nanoparticles for biomedical applications. *Biomaterials*, 26, 3995-4021.
- HIRSCH, V., KINNEAR, C., MONIATTE, M., ROTHEN-RUTISHAUSER, B., CLIFT, M. J. & FINK, A. 2013. Surface charge of polymer coated SPIONs influences the serum protein adsorption, colloidal stability and subsequent cell interaction in vitro. *Nanoscale*, 5, 3723-32.
- HOLE, P., SILLENCE, K., HANNELL, C., MAGUIRE, C. M., ROESSLEIN, M., SUAREZ, G., CAPRACOTTA, S., MAGDOLENOVA, Z., HOREV-AZARIA, L., DYBOWSKA, A., COOKE, L., HAASE, A., CONTAL, S., MANO, S., VENNEMANN, A., SAUVAIN, J. J., STAUNTON, K. C., ANGUISSOLA, S., LUCH, A., DUSINSKA, M., KORENSTEIN, R., GUTLEB, A. C., WIEMANN, M., PRINA-MELLO, A., RIEDIKER, M. & WICK, P. 2013. Interlaboratory comparison of size measurements on nanoparticles using nanoparticle tracking analysis (NTA). *J Nanopart Res*, 15, 2101.

- JUCH, H., NIKITINA, L., DEBBAGE, P., DOHR, G. & GAUSTER, M. 2013. Nanomaterial interference with early human placenta: Sophisticated matter meets sophisticated tissues. *Reprod Toxicol*, 41, 73-9.
- JUD, C., CLIFT, M. J., PETRI-FINK, A. & ROTHEN-RUTISHAUSER, B. 2013. Nanomaterials and the human lung: what is known and what must be deciphered to realise their potential advantages? *Swiss Med Wkly*, 143, w13758.
- KREUTER, J. 2014. Drug delivery to the central nervous system by polymeric nanoparticles: what do we know? *Adv Drug Deliv Rev*, 71, 2-14.
- KREYLING, W. G., SEMMLER-BEHNKE, M., SEITZ, J., SCYMCZAK, W., WENK, A., MAYER, P., TAKENAKA, S. & OBERDORSTER, G. 2009. Size dependence of the translocation of inhaled iridium and carbon nanoparticle aggregates from the lung of rats to the blood and secondary target organs. *Inhal Toxicol*, 21 Suppl 1, 55-60.
- LARSEN, L. G., CLAUSEN, H. V., ANDERSEN, B. & GRAEM, N. 1995. A stereologic study of postmature placentas fixed by dual perfusion. *Am J Obstet Gynecol*, 172, 500-7.
- LEVKOVITZ, R., ZARETSKY, U., GORDON, Z., JAFFA, A. J. & ELAD, D. 2013. In vitro simulation of placental transport: part I. Biological model of the placental barrier. *Placenta*, 34, 699-707.
- LINNEMANN, K., MALEK, A., SAGER, R., BLUM, W. F., SCHNEIDER, H. & FUSCH, C. 2000. Leptin production and release in the dually in vitro perfused human placenta. *J Clin Endocrinol Metab*, 85, 4298-301.
- LUNDQVIST, M., STIGLER, J., ELIA, G., LYNCH, I., CEDERVALL, T. & DAWSON, K. A. 2008. Nanoparticle size and surface properties determine the protein corona with possible implications for biological impacts. *Proc Natl Acad Sci U S A*, 105, 14265-70.
- LUNOV, O., SYROVETS, T., LOOS, C., BEIL, J., DELACHER, M., TRON, K., NIENHAUS, G. U., MUSYANOVYCH, A., MAILANDER, V., LANDFESTER, K. & SIMMET, T. 2011. Differential uptake of functionalized polystyrene nanoparticles by human macrophages and a monocytic cell line. *ACS Nano*, 5, 1657-69.
- MALEK, A., OBRIST, C., WENZINGER, S. & VON MANDACH, U. 2009. The impact of cocaine and heroin on the placental transfer of methadone. *Reprod Biol Endocrinol*, 7, 61.
- MALEK, A., SAGER, R., LANG, A. B. & SCHNEIDER, H. 1997. Protein transport across the in vitro perfused human placenta. *Am J Reprod Immunol*, 38, 263-71.
- MALEK, A., WILLI, A., MULLER, J., SAGER, R., HANGGI, W. & BERSINGER, N. 2001. Capacity for hormone production of cultured trophoblast cells obtained from placentae at term and in early pregnancy. *J Assist Reprod Genet*, 18, 299-304.
- MATHIESEN, L., RYTTING, E., MOSE, T. & KNUDSEN, L. E. 2009. Transport of benzo[alpha]pyrene in the dually perfused human placenta perfusion model: effect of albumin in the perfusion medium. *Basic Clin Pharmacol Toxicol*, 105, 181-7.
- MCCMAHON, H. T. & BOUCROT, E. 2011. Molecular mechanism and physiological functions of clathrin-mediated endocytosis. *Nat Rev Mol Cell Biol*, 12, 517-33.
- MENEZES, V., MALEK, A. & KEELAN, J. A. 2011. Nanoparticulate drug delivery in pregnancy: placental passage and fetal exposure. *Curr Pharm Biotechnol*, 12, 731-42.
- MENJOGE, A. R., RINDERKNECHT, A. L., NAVATH, R. S., FARIDNIA, M., KIM, C. J., ROMERO, R., MILLER, R. K. & KANNAN, R. M. 2011. Transfer of PAMAM dendrimers across human placenta: prospects of its use as drug carrier during pregnancy. *J Control Release*, 150, 326-38.

- MONOPOLI, M. P., ABERG, C., SALVATI, A. & DAWSON, K. A. 2012. Biomolecular coronas provide the biological identity of nanosized materials. *Nat Nanotechnol*, 7, 779-86.
- MONOPOLI, M. P., WALCZYK, D., CAMPBELL, A., ELIA, G., LYNCH, I., BOMBELLI, F. B. & DAWSON, K. A. 2011. Physical-chemical aspects of protein corona: relevance to in vitro and in vivo biological impacts of nanoparticles. *J Am Chem Soc*, 133, 2525-34.
- MYLLYNEN, P. K., LOUGHRAN, M. J., HOWARD, C. V., SORMUNEN, R., WALSH, A. A. & VAHAKANGAS, K. H. 2008. Kinetics of gold nanoparticles in the human placenta. *Reprod Toxicol*, 26, 130-7.
- NANOVSKAYA, T., PATRIKEEVA, S., ZHAN, Y., FOKINA, V., HANKINS, G. D. & AHMED, M. S. 2012. Transplacental transfer of vancomycin and telavancin. *Am J Obstet Gynecol*, 207, 331 e1-6.
- NANOVSKAYA, T. N., PATRIKEEVA, S., HEMAUER, S., FOKINA, V., MATTISON, D., HANKINS, G. D., AHMED, M. S. & NETWORK, O. 2008. Effect of albumin on transplacental transfer and distribution of rosiglitazone and glyburide. *J Matern Fetal Neonatal Med*, 21, 197-207.
- NEKHAYEVA, I. A., NANOVSKAYA, T. N., DESHMUKH, S. V., ZHARIKOVA, O. L., HANKINS, G. D. & AHMED, M. S. 2005. Bidirectional transfer of methadone across human placenta. *Biochem Pharmacol*, 69, 187-97.
- NIKITINA, L., DOHR, G. & JUCH, H. 2013. Studying nanoparticle interaction with human placenta: Festina lente! *Nanotoxicology*.
- OBERDORSTER, G., OBERDORSTER, E. & OBERDORSTER, J. 2005. Nanotoxicology: an emerging discipline evolving from studies of ultrafine particles. *Environ Health Perspect*, 113, 823-39.
- PANIGEL, M., PASCAUD, M. & BRUN, J. L. 1967. [Radioangiographic study of circulation in the villi and intervillous space of isolated human placental cotyledon kept viable by perfusion]. *J Physiol (Paris)*, 59, 277.
- PARTON, R. G. & SIMONS, K. 2007. The multiple faces of caveolae. *Nat Rev Mol Cell Biol*, 8, 185-94.
- PIETROIUSTI, A. 2012. Health implications of engineered nanomaterials. *Nanoscale*, 4, 1231-47.
- PIETZONKA, P., ROTHEN-RUTISHAUSER, B., LANGGUTH, P., WUNDERLI-ALLENSPACH, H., WALTER, E. & MERKLE, H. P. 2002. Transfer of lipophilic markers from PLGA and polystyrene nanoparticles to caco-2 monolayers mimics particle uptake. *Pharm Res*, 19, 595-601.
- RASMUSSEN, J. W., MARTINEZ, E., LOUKA, P. & WINGETT, D. G. 2010. Zinc oxide nanoparticles for selective destruction of tumor cells and potential for drug delivery applications. *Expert Opin Drug Deliv*, 7, 1063-77.
- ROTHEN-RUTISHAUSER, B., MUHLFELD, C., BLANK, F., MUSSO, C. & GEHR, P. 2007. Translocation of particles and inflammatory responses after exposure to fine particles and nanoparticles in an epithelial airway model. *Part Fibre Toxicol*, 4, 9.
- SAUNDERS, M. 2009. Transplacental transport of nanomaterials. *Wiley Interdiscip Rev Nanomed Nanobiotechnol*, 1, 671-84.
- SCHLEH, C., SEMMLER-BEHNKE, M., LIPKA, J., WENK, A., HIRN, S., SCHAFFLER, M., SCHMID, G., SIMON, U. & KREYLING, W. G. 2012. Size and surface charge of

- gold nanoparticles determine absorption across intestinal barriers and accumulation in secondary target organs after oral administration. *Nanotoxicology*, 6, 36-46.
- SCHNEIDER, H., PANIGEL, M. & DANCIS, J. 1972. Transfer across the perfused human placenta of antipyrine, sodium and leucine. *Am J Obstet Gynecol*, 114, 822-8.
- SEMMLER-BEHNKE, M., KREYLING, W. G., LIPKA, J., FERTSCH, S., WENK, A., TAKENAKA, S., SCHMID, G. & BRANDAU, W. 2008. Biodistribution of 1.4- and 18-nm gold particles in rats. *Small*, 4, 2108-11.
- SONNEGAARD POULSEN, M., MOSE, T., LETH MAROUN, L., MATHIESEN, L., EHLERT KNUDSEN, L. & RYTTING, E. 2013. Kinetics of silica nanoparticles in the human placenta. *Nanotoxicology*.
- SUDHAKARAN, S., GHABRIAL, H., NATION, R. L., KONG, D. C., GUDE, N. M., ANGUS, P. W. & RAYNER, C. R. 2005. Differential bidirectional transfer of indinavir in the isolated perfused human placenta. *Antimicrob Agents Chemother*, 49, 1023-8.
- SYME, M. R., PAXTON, J. W. & KEELAN, J. A. 2004. Drug transfer and metabolism by the human placenta. *Clin Pharmacokinet*, 43, 487-514.
- TAKATA, K. & HIRANO, H. 1997. Mechanism of glucose transport across the human and rat placental barrier: a review. *Microsc Res Tech*, 38, 145-52.
- TENUTA, T., MONOPOLI, M. P., KIM, J., SALVATI, A., DAWSON, K. A., SANDIN, P. & LYNCH, I. 2011. Elution of labile fluorescent dye from nanoparticles during biological use. *PLoS One*, 6, e25556.
- TIAN, F., RAZANSKY, D., ESTRADA, G. G., SEMMLER-BEHNKE, M., BEYERLE, A., KREYLING, W., NTZIACHRISTOS, V. & STOEGER, T. 2009. Surface modification and size dependence in particle translocation during early embryonic development. *Inhal Toxicol*, 21 Suppl 1, 92-6.
- WICK, P., MALEK, A., MANSER, P., MEILI, D., MAEDER-ALTHAUS, X., DIENER, L., DIENER, P. A., ZISCH, A., KRUG, H. F. & VON MANDACH, U. 2010. Barrier capacity of human placenta for nanosized materials. *Environ Health Perspect*, 118, 432-6.
- YAMASHITA, K., YOSHIOKA, Y., HIGASHISAKA, K., MIMURA, K., MORISHITA, Y., NOZAKI, M., YOSHIDA, T., OGURA, T., NABESHI, H., NAGANO, K., ABE, Y., KAMADA, H., MONOBE, Y., IMAZAWA, T., AOSHIMA, H., SHISHIDO, K., KAWAI, Y., MAYUMI, T., TSUNODA, S., ITOH, N., YOSHIKAWA, T., YANAGIHARA, I., SAITO, S. & TSUTSUMI, Y. 2011. Silica and titanium dioxide nanoparticles cause pregnancy complications in mice. *Nat Nanotechnol*, 6, 321-8.

## **Supplemental Material**

### **Bidirectional transfer study of polystyrene nanoparticles across the placental barrier reveals different transport kinetics**

Stefanie Grafmueller, Pius Manser, Liliane Diener, Pierre-André Diener,  
Xenia Maeder-Althaus, Lionel Maurizi, Wolfram Jochum, Harald F. Krug,  
Tina Buerki-Thurnherr, Ursula von Mandach, Peter Wick



## Materials and Methods

**Cell culture.** BeWo cells (b30 clone), a cell line derived from human choriocarcinoma, were obtained from Prof. Dr. Ursula Graf-Hausner (Zurich University of Applied Sciences, Waedenswil, Switzerland) with permission of Dr. Alan L. Schwartz (Washington University School of Medicine, MO, USA) and cultured in Ham's F-12K medium (Gibco, Thermo Fisher Scientific Inc., Waltham, MA, USA) supplemented with 1 % penicillin-streptomycin and 10 % fetal calf serum (FCS) at 37°C and 5 % carbon dioxide (CO<sub>2</sub>).

**MTS viability assay.** The *in vitro* cytotoxicity of the different PS beads was tested using the MTS viability assay. 24 hrs before treatment BeWo cells were seeded in a 96-well plate (8000 cells per well). Different concentrations of PS beads were applied. As negative control, cells without treatment were used and as positive control 1, 10, 100 and 1000 µM CdSO<sub>4</sub> was applied. After 3 or 24 hrs of incubation at 37 °C and 5 % CO<sub>2</sub>, an MTS assay (CellTiter96® AQueous One Solution Cell Proliferation Assay; Promega, Madison, WI, USA) was performed according to the manufacturer's instructions. Results were presented as mean percentage of the untreated control from three independent experiments.

**Ex vivo human placental perfusion model.** A fetal artery and vein of an intact cotyledon were cannulated. Afterwards the placenta was fixed in a tissue holder and placed into a perfusion chamber. To connect the maternal side three blunt cannulas were introduced in the intervillous space and a venous drain was introduced to return the fluid to the maternal circuit. Two peristaltic pumps maintained the fetal flow at 3 - 4 mL/min and the maternal flow at 12 mL/min. A water bath kept the temperature of both circuits at 37 °C. For the fetal side one oxygenator with 95 % N<sub>2</sub> and 5 % CO<sub>2</sub> and for the maternal side one oxygenator with 95 % synthetic air and 5 % CO<sub>2</sub> were applied. To flush out the blood and allow a recovery of the tissue from the ischemic period after the delivery, the experiment started with an open perfusion (both circuits) for 20 minutes using only perfusion medium. The perfusion medium contained M199 tissue culture medium (Sigma, St. Louis, MO, USA) diluted with Earl's buffer (dilution 1 : 2), 1 g/L glucose (Sigma, St. Louis, MO, USA), 10 g/L bovine serum albumin (AppliChem GmbH, Darmstadt, Germany), 10 g/L dextran 40 (Sigma, St. Louis, MO, USA), 2500 IU/L sodium heparin (B.Braun Medical AG, Melsungen, Germany), 250 mg/L amoxicillin (GlaxoSmithKline AG, Brentford, UK) and 2.2 g/L sodium bicarbonate (Merck, Darmstadt, Germany). After closing of the fetal and maternal circulation by leading the venous outflow back to the corresponding reservoir, the PS particles were added either to the maternal

(M) or the fetal (F) reservoir at a final concentration of 25 µg/mL. The concentration of the PS beads in the fetal and maternal circuit was determined by fluorescence measurement in a microplate reader (Biotek Synergy HT, Winooski, VT, USA) after centrifugation at 800 x g to remove residual erythrocytes. Particle concentrations were corrected for the PM volume in the tubes and volume loss due to sampling before placental transfer was calculated as percentage of transferred PS beads compared to the initially added particle amount. As control radiolabeled <sup>14</sup>C-antipyrine (50 nCi/mL, specific activity: 4.7 mCi/mmol; American Radiolabeled Chemicals Inc., St. Louis, MO, USA) was also added to the maternal or fetal circuit. The criteria for a successful perfusion were visual control (intact membranes, no lesion, no disruption of the placenta), leak from fetal to maternal side < 4 ml/hr (for reverse perfusions < 1 ml/hr), an equilibrium of <sup>14</sup>C-antipyrine between maternal and fetal circuit after 4 - 6 hrs, a fetal perfusion pressure < 70 mmHg and fetal pH at a physiological range of 7.2 - 7.4.

***Antipyrine transfer.*** Perfusate samples were mixed with scintillation cocktail (Irgasafe Plus Scintillation Cocktail, Zinsser Analytic, Frankfurt, Germany) and measured in a liquid scintillation analyzer (Packard Tri-Carb 2200; GMI, Ramsey, MN, USA).

***Viability and functionality of the placenta.*** Glucose and lactate concentration in the fetal and maternal circuit were determined with an automated blood gas system (ABL800 FLEX automated benchtop analyzer, Radiometer Medical ApS, Copenhagen, Denmark). The placental hormones human chorionic gonadotropin (hCG) and leptin in the fetal and maternal circuit before and after perfusion were determined by enzyme-linked immunosorbent assay (ELISA) as described previously (Malek et al., 1997, Malek et al., 2001). The hormone production was calculated by dividing the amount released in both circulations after 6 hrs of perfusion by the weight of perfused tissue.

***Histopathological evaluation.*** Tissue samples of non-perfused (negative control) and perfused placentas were fixed in 4 % formaldehyde (Formafix AG, Hittnau, Switzerland). After standardized dehydration of the tissue overnight in a Medite Tissue Processor TPC 15 the probes were embedded in paraffin blocks with the Medite Tissue Embedding System TES 99. Using a microtome, 4 µm thick sections were obtained, mounted and air dried on glass slides and stained with haematoxylin and eosin in a Tissue-Tek® Prisma™. The slides were examined at a Leica DMLB microscope.

## References

Malek A, Sager R, Lang AB, Schneider H. 1997. Protein transport across the in vitro perfused human placenta. *American journal of reproductive immunology* 38:263-271.

Malek A, Willi A, Muller J, Sager R, Hanggi W, Bersinger N. 2001. Capacity for hormone production of cultured trophoblast cells obtained from placentae at term and in early pregnancy. *Journal of assisted reproduction and genetics* 18:299-304.

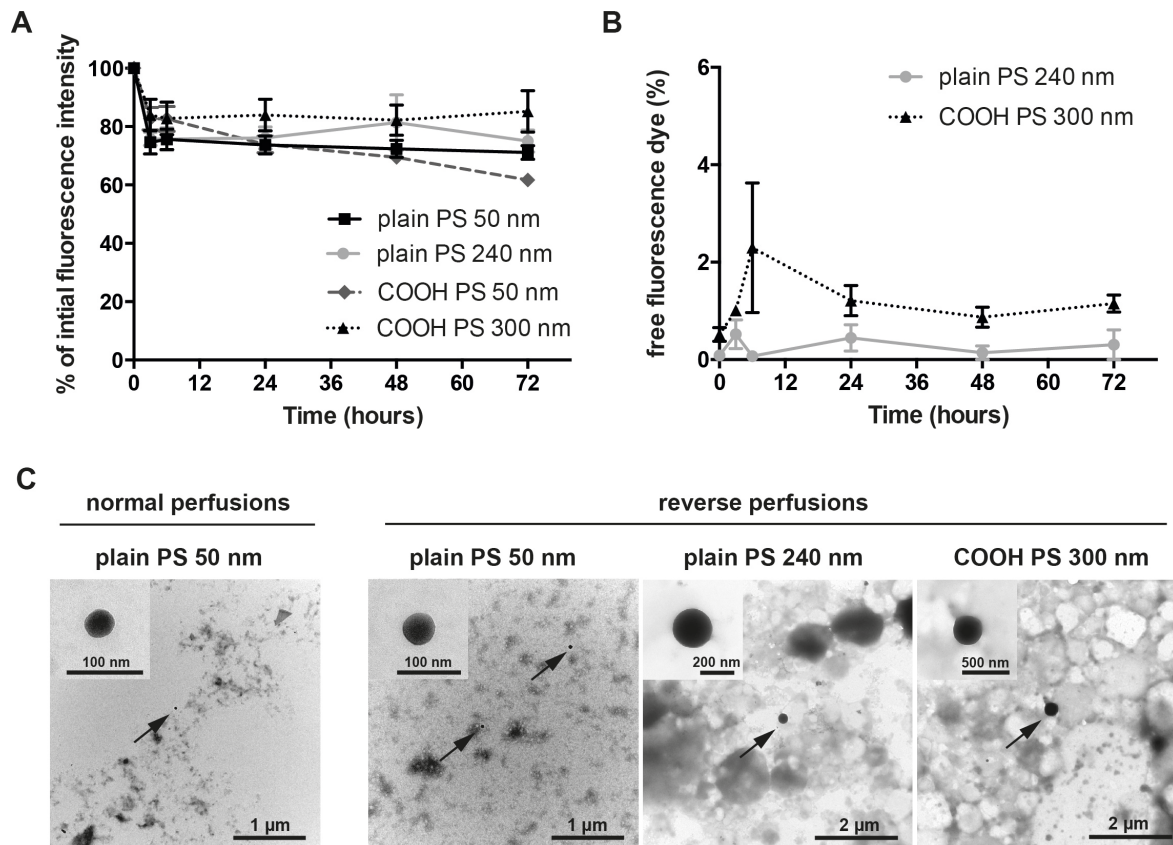


**Figure S1.** Stability (A) and leakage (B) of the fluorescence dye was assessed after 3, 6, 24, 48 and 72 hrs of incubation at 37°C in perfusion medium. Shown are the mean percentages of initial (time point 0) fluorescence intensity  $\pm$  SD (A) and the free fluorescence of the large PS particles as percentage of total fluorescence intensity  $\pm$  SD (B),  $n=3$ . (C) Representative TEM micrographs of plain 50 nm, 240 nm and carboxylate-modified 300 nm PS beads in the fetal or maternal circulation after 1.5 - 6 hrs of normal (M to F direction) or reverse (F to M direction) perfusion.

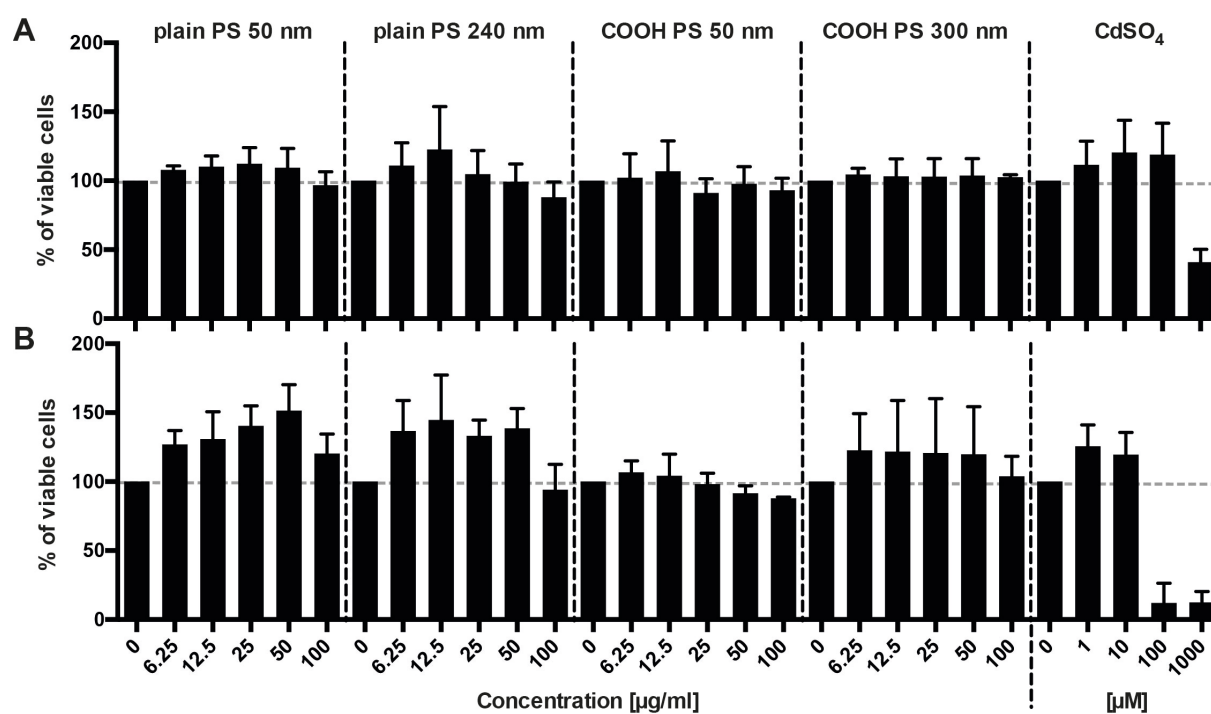


**Figure S2.** BeWo cell viability after 3 (A) and 24 hrs (B) of exposure to PS beads measured with a MTS assay. CdSO<sub>4</sub> served as positive control for cytotoxicity. Data represent the mean percentages of viable cells compared to the untreated control  $\pm$  SD of at least 3 independent experiments.

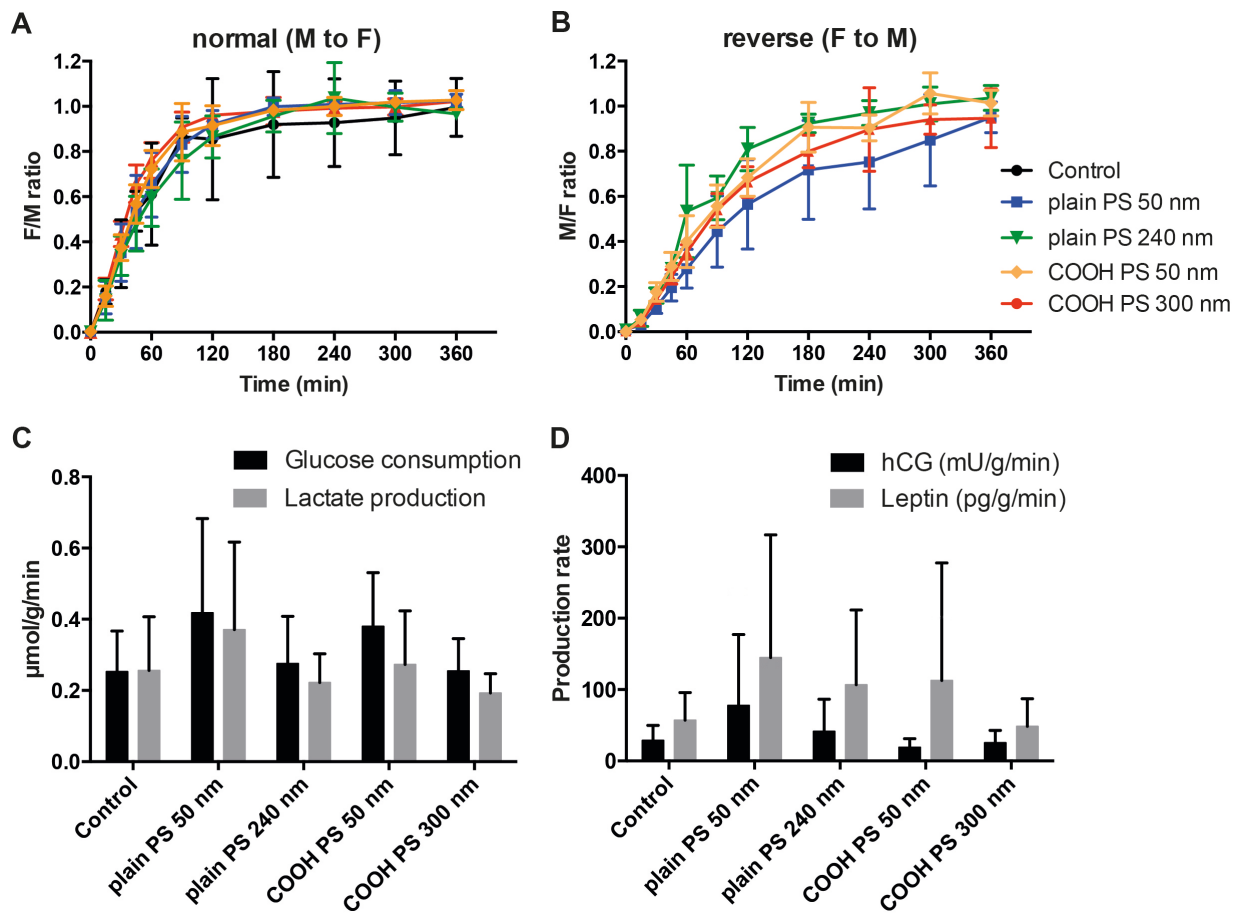


**Figure S3.** (A) Fetal-to-maternal (F/M) or maternal-to-fetal transfer ratio (M/F) of radiolabeled  $^{14}\text{C}$ -antipyrine over a time period of 6 hrs of normal or reverse placenta perfusion with or without PS beads. (B + C) Glucose consumption and lactate production (B) and human chorionic gonadotropin (hCG) and leptin hormone production rate (C) during *ex vivo* human placental perfusion with or without particles (control). All data is expressed as the mean  $\pm$  SD of at least 3 independent experiments.

## PART III

### **Challenges and common pitfalls in nanoparticle characterization for transport studies across the human placenta**

Stefanie Grafmueller, Pius Manser, Liliane Diener, Lionel Maurizi, Heinrich Hofmann, Pierre-André Diener, Wolfram Jochum, Harald F. Krug, Tina Buerki-Thurnherr, Ursula von Mandach, Peter Wick

#### ***Author contribution***

In this study, I measured the size distribution, determined the detection limit and the stability of the NPs. I assessed the dye elution, performed most *ex vivo* placental perfusions and the ninhydrin assay. In addition, I analyzed and summarized the results. The *ex vivo* placenta perfusion with silica-SPIONs, intended for tissue analysis in TEM, was performed by Pius Manser. Preparation of nanoparticle suspensions for TEM, tissue sample fixation and TEM analysis was performed by Liliane Diener. Fluorescence microscopy was conducted by the Team of Wolfram Jochum and Pierre-André Diener at the Institute of Pathology at the Kantonsspital St. Gallen. The zeta potential measurement of the polystyrene beads as well as the synthesis of the silica-SPIONs was performed by Lionel Maurizi and Heinrich Hofmann at EPFL. Ursula von Mandach and Peter Wick conceived and designed the research project. Tina Buerki-Thurnherr and Harald F. Krug provided expertise, guidance and critical reading. A manuscript including parts of these results is in preparation.





## **Challenges and common pitfalls in nanoparticle characterization for transport studies across the human placenta**

Stefanie Grafmueller<sup>1,2,3</sup>, Pius Manser<sup>1</sup>, Liliane Diener<sup>1</sup>, Lionel Maurizi<sup>4</sup>, Heinrich Hofmann<sup>4</sup>, Pierre-André Diener<sup>5</sup>, Wolfram Jochum<sup>5</sup>, Harald F. Krug<sup>6</sup>, Tina Buerki-Thurnherr<sup>1</sup>, Ursula von Mandach<sup>2</sup>, Peter Wick<sup>1</sup>

<sup>1</sup>Laboratory for Materials-Biology Interactions, Empa, St. Gallen, Switzerland

<sup>2</sup>Perinatal Pharmacology, Department of Obstetrics, University Hospital Zurich, Zurich, Switzerland

<sup>3</sup>Graduate School for Cellular and Biomedical Sciences, University of Berne, Berne, Switzerland

<sup>4</sup>Powder Technology Laboratory, Ecole Polytechnique Federale de Lausanne, Lausanne, Switzerland

<sup>5</sup>Institute of Pathology, Cantonal Hospital St. Gallen, St. Gallen, Switzerland

<sup>6</sup>Empa, International Research Cooperations Manager, St. Gallen Switzerland

### **Abstract**

Nanotechnology is an expanding field not only in medicine. So, besides the naturally occurring fine and ultrafine particles, exposure to engineered nanoparticles is steadily increasing. This raises questions about the safety of such engineered nanoparticles. Thus, many researchers are investigating cellular responses to nanoparticles. Additionally to the toxicological know-how, an extensive particle characterization is fundamental to receive meaningful and comparable results in such studies. In this case report we present common issues, which we encountered during the evaluation of nanoparticles in order to determine the physicochemical properties responsible for placental transfer. We highlighted various challenges, for example in the measurement of particle size, functionalization and stability of a label such as a fluorescent dye. In conclusion, a careful assessment of nanoparticle properties in a physiologically relevant milieu is as challenging and important than the study dealing with nanoparticle-cell interactions itself.

## Introduction

The field of nanotechnology is growing continuously and there is intensive research particularly in the area of nanomedicine (Riehemann et al., 2009). To understand the interactions of nanoparticles (NP) with cells and their biodistribution is a pre-requisite for medical applications such as using NPs as carriers to deliver a drug to a specific target cell or organ. It has been shown that the physicochemical properties of NPs determine their fate in biological systems (Kreyling et al., 2010). Different NP characteristics could lead to selective coating with various biomolecules and therefore lead to altered cellular responses (Nel et al., 2009). Therefore, an extensive particle characterization is indispensable. Researchers suggested analyzing particle size, size distribution, agglomeration state, stability, NP composition, endotoxin contamination, sample purity, batch-to-batch consistency, surface coating and reactivity (Crist et al., 2013, Warheit, 2008). There is already an increased awareness that all these features should be examined not only in water, but also in the physiologically relevant media, which are used in the respective experimental set-ups (Crist et al., 2013, Warheit, 2008). However, in many cases properties such as dye elution, agglomeration behavior or NP stability *in vivo* cannot be predicted by *in vitro* testing using cell culture medium, because the composition of biological fluids outside and inside cells is more complex. In such situations, NP stability has to be assessed directly in the desired biological model.

Here, we want to present a brief case report about the practical challenges which emerged during our investigations of NP transport across the human placenta. To assess transplacental translocation of NPs across the human placenta and to determine the physicochemical properties responsible for placental transfer, NPs with different characteristics are required. We chose polystyrene (PS) beads as model particles because they are commercially available in numerous sizes and with different surface modifications. The use of such commercial PS beads is widely established and the manufacturers already provide information about the NP characteristics. So, it is assumed that confirmation of such information for one random sample of one supplier is sufficient. Furthermore, to visualize and measure particle concentrations in a biologic environment such as that of the human placenta an easy detectable label is highly convenient. PS beads are available labeled with a range of different fluorescent dyes of high intensity and photostability. We evaluated plain, carboxylate- and amine-modified PS beads with different fluorescent labels to study placental translocation in the human *ex vivo* placental perfusion model.

## Materials and Methods

**Particles.** An overview of all fluorescently labeled PS beads used in this study is provided in Table 1. Numbers were assigned to each type of beads according to its functionalization. Yellow-green-labeled non-functionalized (plain) PS beads with sizes of 87 (P1) and 504 nm (P2), and carboxylated (COOH) PS beads with sizes of 100.8 (C1) and 533.8 nm (C2) were purchased from Polysciences Inc. (Warrington, PA, USA). GreenF-labeled, amine-modified (NH<sub>2</sub>) 100 (N1) and 250 nm (N3) PS beads were purchased from mircomod Partikeltechnologie GmbH (Rostock, D). Yellow-labeled, amine-modified 170 (N2) and 530 nm (N4) PS beads were purchased from SpheroTech (Lake Forest, IL, USA). Envy-green-labeled, amine-modified 60 (N5), 250 (N6) and 510 nm (N7) PS beads were customized synthesized from Bangs Laboratories Inc. (Fishers, IN, USA). Orange amine-modified 110 nm (N8) PS beads were purchased from Sigma (St. Louis, MO, USA).

Silica-SPIONs (superparamagnetic iron oxide nanoparticles) were kindly provided by Lionel Maurizi and Heinrich Hofmann (Powder Technology Laboratory, Ecole Polytechnique Federale de Lausanne, CH). Particle characteristics are summarized in Table 3.

**Particle characterization.** The zeta potential of the PS beads in 10 mM sodium chloride and perfusion medium (PM) at pH between 6.8 and 7.2 was determined with a Zetasizer NanoZS (Malvern Instruments, Worcestershire, UK). Particle size distribution of PS beads and silica-SPIONs in double distilled (DD) water and PM was determined by nanoparticle tracking analysis (NTA; NanoSight LM 20 System, software version 2.3.5, NanoSight Ltd., Amesbury, UK) as described previously (Hole et al., 2013). The DD water and PM were filtered through a 0.02 µm Anotop® 25 syringe filter (Whatman GmbH, Germany) prior to analysis. For comparison of the different NPs the results were normalized to the area under the NP concentration/size curve.

**Stability of fluorescent dye.** The detection limit of the fluorescence of PS beads was determined as described previously (Wick et al., 2010). To assess the stability of fluorescence the loss of fluorescence intensity was analyzed after incubation of the PS beads in PM at 37 °C for 3, 6, 24, 48 and 72 hours using a microplate reader (Biotek Synergy HT, Winooski, VT, USA) with excitation and emission wavelengths as indicated in Table 1. The leakage of fluorescence was assessed at the indicated time points during 72 hours at 37 °C in PM and in samples from the maternal circulation after 3 and 6 hours of placenta perfusion by measuring the fluorescence before and after filtration through a 0.1 µm syringe filter.

**Transmission electron microscopy (TEM).** Polystyrene beads and silica-SPION suspensions as supplied by the manufacturer were applied onto a carbon-coated copper grid and incubated processed for TEM analysis. Images were taken with a Zeiss EM 900 TEM (Zeiss SMT, Oberkochen, Germany) at 80 kV. Tissue samples (before and after perfusion) were fixed in a 0.1 M sodium cacodylate buffer containing 3 % glutaraldehyde. After a post-fixation step in 2 % osmium tetroxide in 0.1 M sodium cacodylate buffer, samples were dehydrated through a graded ethanol series followed by acetone and embedded in epon resin (Sigma, St. Louis, MO, USA). Ultrathin sections were contrasted with 2 % uranyl acetate and lead citrate (Reynolds, 1963) before analysis in a Zeiss EM 900 TEM (Zeiss SMT, Oberkochen, Germany) at 80 kV.

**Ex vivo human placental perfusion model.** The placentas were obtained from uncomplicated term pregnancies after caesarean section at the Department of Obstetrics, Zurich University Hospital. Written informed consent was obtained prior to delivery. The project was approved by the local ethics committee and performed in accordance with the principles of the Declaration of Helsinki. The placenta perfusion was performed as described previously (Grafmüller et al., 2013, Wick et al., 2010). The PM contained M199 tissue culture medium (Sigma, St. Louis, MO, USA) diluted with Earl's buffer (dilution 1 : 2), 1 g/L glucose (Sigma, St. Louis, MO, USA), 10 g/L bovine serum albumin (AppliChem GmbH, Darmstadt, Germany), 10 g/L dextran 40 (Sigma, St. Louis, MO, USA), 2500 IU/L sodium heparin (B.Braun Medical AG, Melsungen, Germany), 250 mg/L amoxicillin (GlaxoSmithKline AG, Brentford, UK) and 2.2 g/L sodium bicarbonate (Merck, Darmstadt, Germany). Placental perfusion was started by adding 25 µg/mL PS beads or 25 µg/mL silica-SPIONs into the maternal circulation. The concentration of the PS beads in the fetal and maternal circuit was determined by fluorescence measurement in a microplate reader (Biotek Synergy HT, Winooski, VT, USA). Particle concentrations were corrected for the PM volume in the tubes and volume loss due to sampling before placental transfer was calculated as percentage of transferred PS beads compared to the initially added particle amount. The concentration of silica-SPIONs was measured after acidic digestion of the samples by analyzing iron and silicon concentration via inductively coupled plasma mass spectrometry (ICP-MS; Elan 6000, Perkin Elmer-Sciex, Waltham, MA, USA).

**Fluorescence microscopy.** Tissue samples of perfused placentas were fixed in 4 % formaldehyde (Formafix AG, Hittnau, Switzerland), dehydrated overnight in a Medite Tissue Processor TPC 15 and embedded in paraffin blocks with the Medite Tissue Embedding System TES 99. Unstained 4 µm thick paraffin sections of perfused placenta were deparaffinized with

xylene followed by ethanol 100 %. Afterwards the slides were air-dried, covered with VECTASHIELD<sup>®</sup> Mounting Medium containing DAPI (Vector Laboratories, Burlingame, CA, USA) on a glass slide and the coverslips were sealed with nail polish. The slides were analysed with a Leica DM6000B fluorescence microscope system (Leica Microsystems, Heerbrugg, Switzerland) equipped with a triple band pass filter set (DAPI/Spectrum Green/Spectrum Orange).

***Ninhydrin assay.*** 20 mM ninhydrin (Fluka, Buchs, CH) solution in ethanol was added to 1 mg/mL PS bead suspension. After 30 min at 80°C and 300 rpm absorption at 550 nm was measured in a microplate reader (Biotek Synergy HT, Winooski, VT, USA) (Hwang and Ederer, 1975).

***Statistical analysis.*** Data are shown as mean  $\pm$  standard deviation (SD) from at least three independent experiments. Unpaired Student's t-test was performed using GraphPad Prism software, version 6 (GraphPad Software, La Jolla, CA, USA). Differences were considered statistically significant at a p-value below 0.05.

**Table 1: Summary of PS beads characteristics**

|   | plain        |              | carboxylate-modified |              | amine-modified |             |              |              |             |              |             |             |
|---|--------------|--------------|----------------------|--------------|----------------|-------------|--------------|--------------|-------------|--------------|-------------|-------------|
|   | P1           | P2           | C1                   | C2           | N1             | N2          | N3           | N4           | N5          | N6           | N7          | N8          |
| Diameter (nm) <sup>a</sup>                                | 87           | 504          | 100.8                | 533.8        | 100            | 170         | 250          | 530          | 60          | 250          | 510         | 110         |
| Diameter (nm) <sup>b</sup> in TEM                         | 78.1 ± 20.5  | 455.1 ± 32   | 88.8 ± 3             | 499.1 ± 8.3  | 88.4 ± 7.2     | 159.9 ± 5.2 | 224.4 ± 16.7 | 493.7 ± 28.7 | 62.5 ± 10   | 181.1 ± 10.7 | 450.7 ± 28  | 70.7 ± 10.8 |
| Hydrodynamic diameter in DD water (nm) <sup>c</sup>       | 97 ± 0.8     | 445 ± 133.2  | 89 ± 0.7             | 475 ± 143.2  | n.d.           | n.d.        | n.d.         | n.d.         | 78 ± 1.0    | 202 ± 2.1    | 445 ± 143.4 | n.d.        |
| Hydrodynamic diameter in PM (nm) <sup>c</sup>             | 132 ± 2.9    | 621 ± 157.1  | 130 ± 1.4            | 619 ± 186.6  | n.d.           | n.d.        | n.d.         | n.d.         | 112 ± 0.9   | 328 ± 2.2    | 658 ± 9.1   | n.d.        |
| Initial no. of particles/mL in PM <sup>d</sup>            | 9.55E+10     | 4.82E+08     | 6.49E+10             | 3.66E+08     | 6.58E+10       | 1.11E+10    | 4.02E+09     | 3.78E+08     | 1.86E+11    | 7.66E+09     | 4.97E+08    | 1.29E+11    |
| Particle surface (nm <sup>2</sup> )/mL in PM <sup>d</sup> | 1.83E+09     | 3.14E+08     | 1.61E+09             | 2.86E+08     | 1.62E+09       | 8.93E+08    | 6.37E+08     | 2.89E+08     | 2.29E+09    | 7.89E+08     | 3.17E+08    | 2.02E+09    |
| Detection limit in PM (µg/mL)                             | < 0.078      | < 0.21       | < 0.078              | < 0.039      | n.d.           | n.d.        | < 2.5        | < 0.02       | < 0.078     | < 0.078      | < 0.039     | n.d.        |
| Zeta potential in 10 mM NaCl (mV) <sup>b</sup>            | -50 ± 9.7    | -46.9 ± 4.0  | -38.2 ± 10.4         | -55.6 ± 4.3  | n.d.           | n.d.        | n.d.         | n.d.         | -30.2 ± 8.2 | -36.2 ± 4.4  | -38.9 ± 2.7 | n.d.        |
| Zeta potential in PM (mV) <sup>b</sup>                    | -13.1 ± 7.2  | -14.5 ± 6.6  | -13.1 ± 10.1         | -15.3 ± 8.3  | n.d.           | n.d.        | n.d.         | n.d.         | -12.7 ± 5.4 | -14.1 ± 9.9  | -17.3 ± 5.7 | n.d.        |
| Fluorescent dye   | Yellow green | Yellow green | Yellow green         | Yellow green | GreenF         | Yellow      | GreenF       | Yellow       | Envy green  | Envy green   | Envy green  | Orange      |
| Dye excitation/emission (nm)                              | 485/528      | 485/528      | 485/528              | 485/528      | 475/510        | 485/520     | 475/510      | 485/520      | 525/565     | 525/565      | 525/565     | 481/644     |
| Number of perfusions                                      | 3            | 3            | 4                    | 4            | 1              | 0           | 4            | 3            | 3           | 3            | 3           | 1           |

Abbreviations: DD double distilled; PM perfusion medium; TEM transmission electron microscopy; n.d. not determined

<sup>a</sup>according to the manufacturer's information; <sup>b</sup>experimentally determined (mean ± SD); <sup>c</sup>experimentally determined (mode ± SD); <sup>d</sup>calculated values

## Results and Discussion

NPs were carefully characterized and their properties are displayed in **Fehler! Verweisquelle konnte nicht gefunden werden.** During our investigations we encountered different problems, which did not allow conducting a reasonable NP translocation study. A brief overview of the practical challenges during evaluation of different NP types is provided in Table 2 and the topics, size, surface modification and charge as well as dye stability will be discussed extensively.

**Table 1: Summary of the encountered problems for each PS bead type**

| PS beads | Size                               | Surface modification/charge                 | Fluorescent dye  |
|----------|------------------------------------|---|--|
| P1       | Mixture of differently sized beads |   |  |
| P2       | Bimodal size distribution          |   |  |
| N1       |                                    |   | Dye leakage after <i>ex vivo</i> placental perfusion   |
| N2       | Mixture of differently sized beads |   |  |
| N3       |                                    |   | Dye elution after 24 and 72 hours at 37°C in PM;<br>Dye leakage after <i>ex vivo</i> placental perfusion (> 20 % fluorescence from free dye) |
| N4       |                                    |   | Dye leakage after <i>ex vivo</i> placental perfusion (> 20 % fluorescence from free dye)   |
| N5       | Mixture of differently sized beads | Negative instead of positive surface charge |  |
| N6       |                                    | Negative instead of positive surface charge | Dye elution only after 24 hours at 37°C in PM  |
| N7       |                                    | Negative instead of positive surface charge | Little dye leakage after <i>ex vivo</i> placental perfusion (about 11 % fluorescence from free dye)  |
| N8       | Mixture of differently sized beads |   |  |

*Note: For C1 and C2 no problems were found regarding the tested properties.*

#### ***Size***

To unambiguously identify the influence of NP size on placental translocation, a monodisperse suspension is a prerequisite. During evaluation of PS beads for our study, we experienced that obtaining PS beads with a narrow size distribution is quite challenging. Often particle suspensions are contaminated to some extent with beads of a smaller diameter than stated by the manufacturer (Figure 1). The TEM micrographs in Figure 1A illustrate that the PS beads P1, P2, N2, N5 and N8 actually contained particles with various sizes whereas the manufacturer declared one size determined by dynamic light scattering (DLS). DLS measures the average hydrodynamic diameter ( $d$ ) of particles and the intensity of the scattered light is proportional to  $d^6$  (the diameter raised to the power of 6). This term means that a 500 nm particle will scatter  $10^6$  times more light than a 50 nm particle. Therefore, DLS measurement is usually biased towards large particles and often prevents the detection of small NPs in polydisperse mixtures. An alternative method for such mixtures is the nanoparticle tracking analysis (Nanosight). This method doesn't determine the average particle size, but tracks the movement of individual particles in a fluid on a particle-by-particle basis and thus allows a discrimination of differently sized particles in a polydisperse suspension. However, analyzing particle size distribution by nanoparticle tracking analysis only detected the contamination with smaller beads for larger beads such as P2 (about 500 nm), while PS beads with a diameter around 50 nm such as N5 were already at the detection limit of this method (Figure 1B). For the latter a contamination with smaller beads could only be detected by another method such as TEM analysis. Similar observations that the manufacturer's size information needs to be confirmed preferably by a complimentary technique have been made for other NPs. Some silver NPs showed significant differences in size between the information from the manufacturer and TEM analysis (Zheng et al., 2011). Besides the measuring technique also the conditions during the measurements have an impact on the results. For example the hydrodynamic diameter of gold particles determined by DLS increased after contact with human plasma (Dobrovolskaia et al., 2009). Consequently, to assess the diameter also in a physiological relevant medium is crucial for experiments carried out in a biological environment.



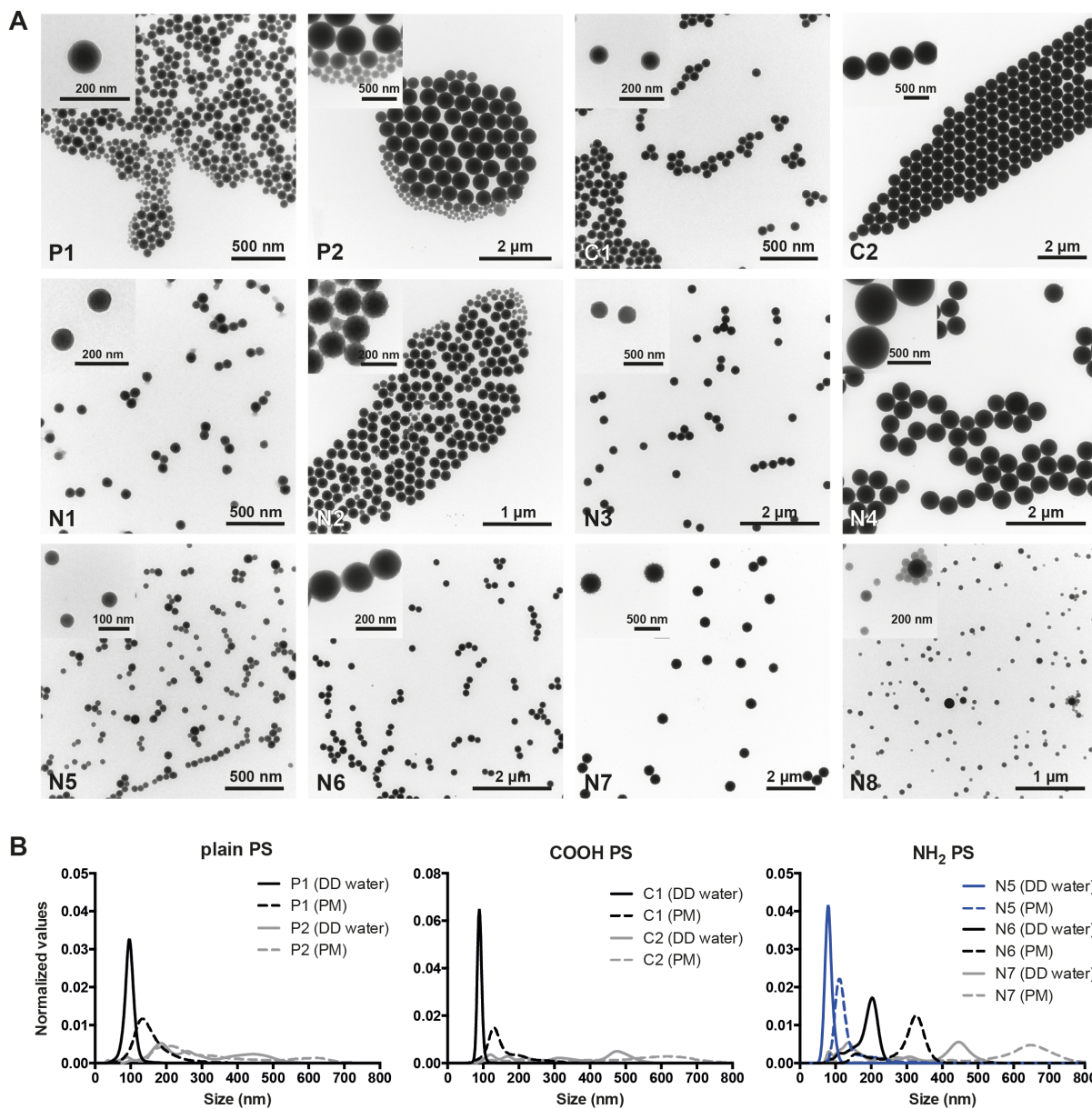


**Figure 1:** (A) TEM micrographs of PS bead suspensions in DD water with low and high magnification (upper left corner). (B) Size distribution of PS beads was determined by nanoparticle tracking analysis.

#### ***Surface modification and charge***

Specific particle shells or surface coatings are added to NPs for example to prevent aggregation or to provoke a specific effect *in vivo*. In addition, such coatings are also important parameters to induce toxicity or accelerate transport into cells or across barriers (Oberdorster et al., 2005). In order to determine the influence of NP surface modification and charge on placental transfer, it is crucial to confirm the presence of these functionalized groups. In *ex vivo* placenta perfusion experiments, we observed a difference in placental transport between plain, carboxylate-modified and amine-modified PS beads (Figure 4). Plain PS beads (P1 and P2) but not amine-modified N5, N6 and N7 PS beads were transported across the placental barrier suggesting that the surface modification is a major determinant of placental translocation (Figure 4D). Zeta potential measurements revealed that contrary to expectations, these amine-modified NPs were strongly negatively charged. Since the fluorescent dye in the particles is slightly negatively charged, it might be that the density of the amine functionalization on the PS beads was not high enough to cause a positive zeta potential. Besides an insufficient functionalization, the particle suspensions could also contain residues of sodium dodecyl sulfate (SDS). SDS is used as surfactant during synthesis of PS beads and is negatively charged. Normally SDS is removed after NP synthesis by dialysis against water. However, small residual amounts of SDS in combination with a low amine group density could explain the negative zeta potential. Hence, a direct detection of the chemical amine group would be required, but the attempt to detect the amine groups on the particle surface by the colorimetric ninhydrin assay failed due to NP interference with the assay. Primary amine groups react with ninhydrin and form a purple compound, which leads to an increased absorbance at 570 nm. The internal fluorescence of the PS beads caused a false positive signal and, thus, a difference in intensity before and after ninhydrin treatment could not be observed (Figure 2). Consequently, the ninhydrin assay is not suitable to confirm the presence of functional amine groups attached to fluorescently labeled NPs and analytical methods such as infrared spectroscopy may be considered for further studies.

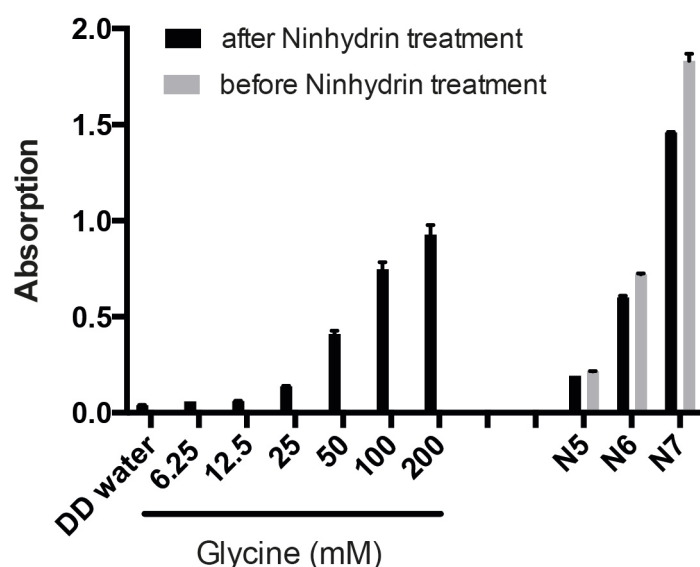


**Figure 2:** To assess the presence of amino groups on the surface of PS beads N5, N6 and N7, a ninhydrin assay was performed. The amino acid glycine served as positive control. Absorption was determined at 550 nm and mean  $\pm$  SD of 2 technical replicates is displayed.

### *In vitro and ex vivo elution of fluorescent dyes*

Several studies demonstrate that a fluorescent dye can elute from NPs after contact with biological fluids (Pietzonka et al., 2002, Salvati et al., 2011, Tenuta et al., 2011, Mahon et al., 2012). Therefore, we tested the fluorescent dye stability of the PS beads after incubation at 37 °C for up to 72 hours in PM. The fluorescence intensity of the greenF-labeled N3 and the yellow-green C1 PS beads remained completely stable over 72 hours and only the N3 PS beads showed an elution of fluorescent dye from the particles ( $43.1 \pm 9.3$  % of total fluorescence intensity was from free fluorescent dye after 24 hours) (Figure 3A, B). For all other PS beads the fluorescence intensity decreased to 60 – 80 % of the initial signal after 72 hours (Figure 3A). Figure 3B indicates that this loss in fluorescence intensity was not due to a significant leakage of fluorescent dye except for the envy green-labeled N6 PS beads, which showed a transient release of dye after 24 hours ( $25.3 \pm 5.2$  %). Due to technical issues, PS beads with a diameter of 100 nm and below could not be analyzed for fluorescence leakage. Syringe filters with a smaller pore size than 0.1  $\mu$ m, which are required to separate the free fluorescent dye from the particles, were not applicable because components of the PM lead to a clogging of the filter. The overall reduction of the measured fluorescence intensity for most of the PS beads (P1, P2, C2, N4, N5, N6, N7) after incubation in PM might be caused by adsorption of albumin or other components of the medium to the NPs, which might impair the fluorescence signal. The adsorption or binding of proteins and other molecules to NPs occurs usually rapidly and is saturated after a certain time point (Cedervall et al., 2007, Tenzer et al., 2013). Thus, the fact

that the fluorescence intensities are not further declining after 3 – 6 hours would corroborate this hypothesis. However, whether a shell of adsorbed molecules is the cause of the fluorescence intensity loss in PM remains to be determined in additional studies.

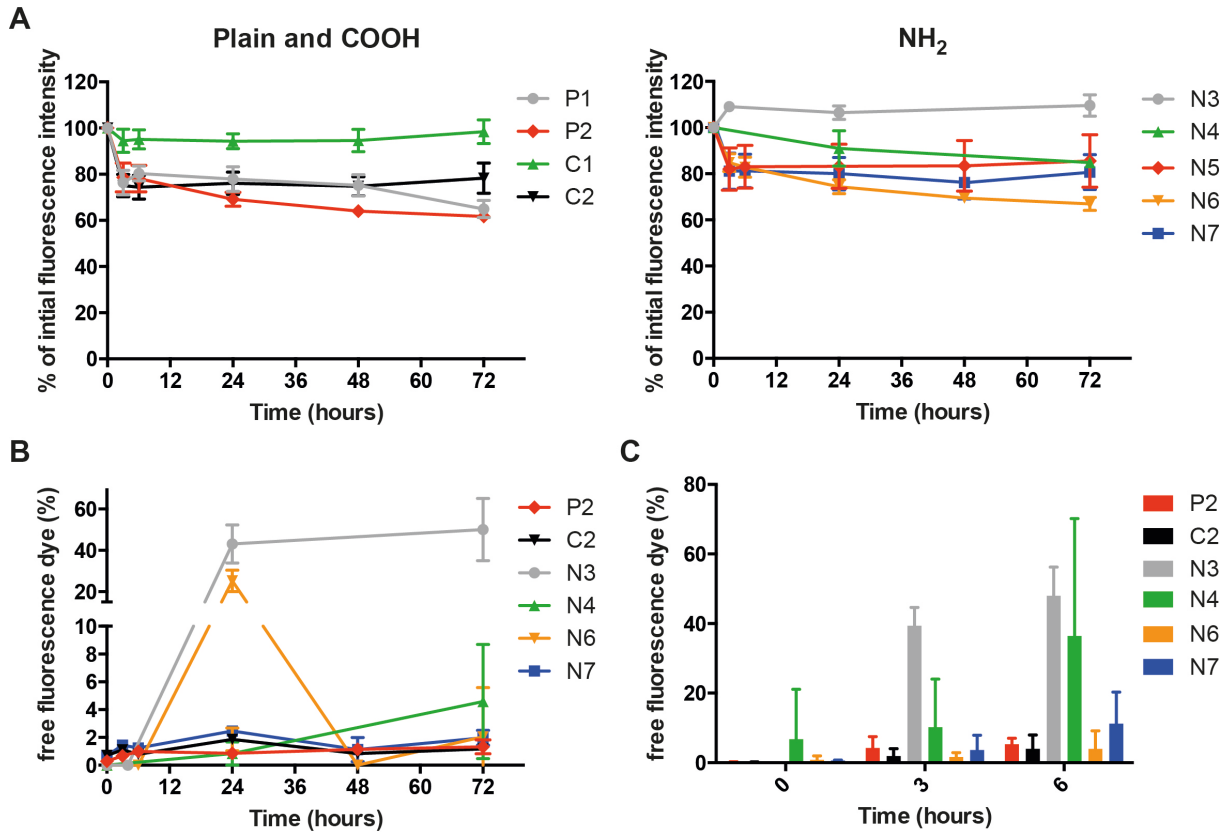


**Figure 3:** (A) Fluorescent dye stability of PS beads in perfusion medium at 37 °C over 72 hours. Displayed is the percentage of initial fluorescence intensity at several time point compared to time point at 0 hours (mean  $\pm$  SD; n=3). (B) Leakage of the fluorescent dye of the large PS beads during 72 hours at 37 °C in perfusion medium. Data is expressed as percentage of free fluorescence of total fluorescence intensity (mean  $\pm$  SD; n=3). (C) Elution of fluorescent dye of the large PS beads after 3 and 6 hours of *ex vivo* placental perfusion. Data is expressed as percentage of free fluorescence of total fluorescence intensity (mean  $\pm$  SD of at least 2 independent experiments).

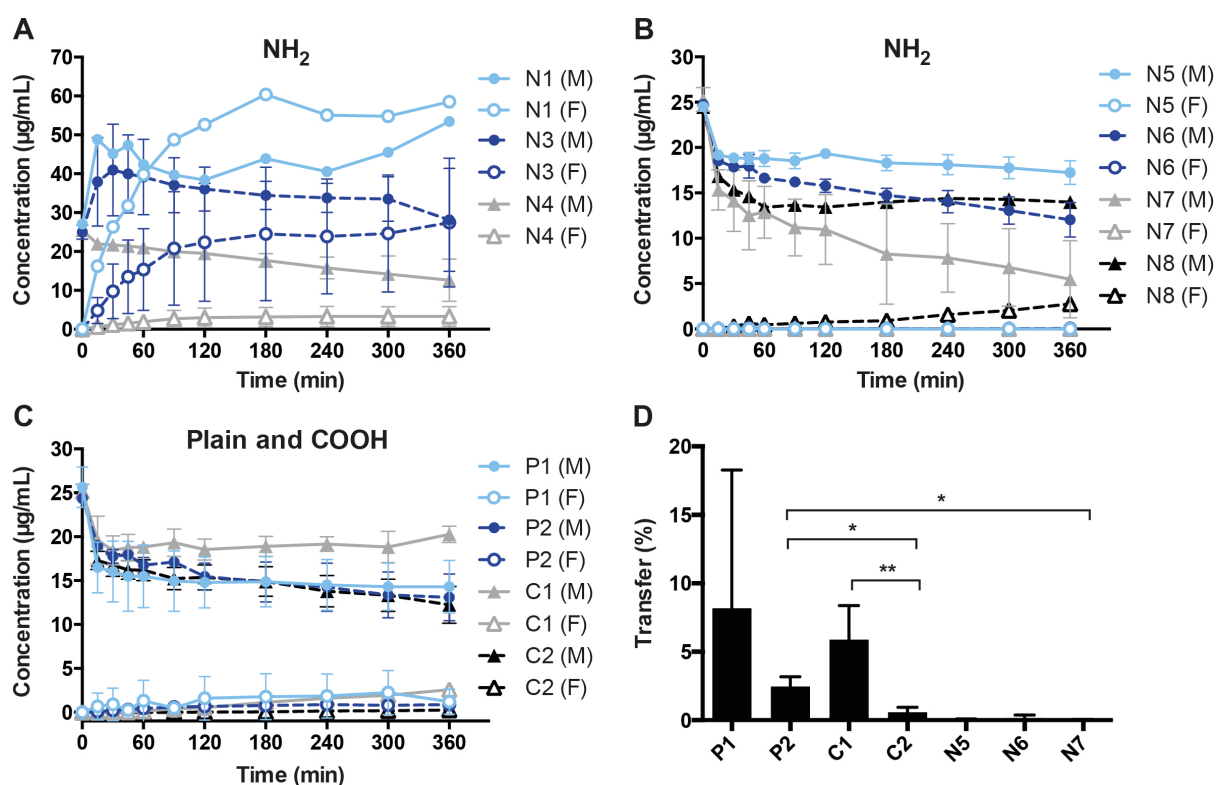


**Figure 4:** (A + B) Perfusion profiles after *ex vivo* human placental perfusion of amine-modified PS beads N1 (n=1), N3 (n=4), N4 (n=3), N5, N6, N7 (all n=3), N8 (n=1). (C) Perfusion profiles of plain and carboxylate-modified PS beads P1, P2, C1 and C2 of at least 3 independent experiments. Data is expressed as mean particle concentration (µg/mL) in the fetal (F) and maternal (M) circulation determined by fluorescence measurement at the indicated time points ± SD. (D) Percentage of plain and carboxylate-modified PS beads (P1, P2, C1, C2) in the fetal circulation after 6 hours of perfusion compared to the initially added particle amount (mean ± SD of at least 3 independent experiments). (\*)  $p < 0.05$ , (\*\*)  $p < 0.01$

Although dye elution was not a major problem for most PS beads after incubation in PM, it became an important issue after contact with the human placenta. During placenta perfusion the greenF-labeled N1 and N3 PS beads showed an unexpected perfusion profile (Figure 4A). After addition of 25 µg/mL PS bead into the maternal circulation, the total concentration (fetal and maternal circuit) seemed to increase above the initially added amount during placental perfusion. Further analysis of samples from the fetal and maternal circulation after 6 hours of perfusion revealed that  $47.9 \pm 8.3$  % of the fluorescent dye was leaking out of the greenF-labeled N3 PS particles (Figure 3C). Although the perfusion profile of the yellow-labeled N4 PS particles appeared more rational, the filtration also showed  $36.4 \pm 33.8$  % leakage of the fluorescent dye after 6 hours of perfusion (Figure 3C, and 4A). According to the particle supplier, the fluorescence in the particles is partially quenched because of the heavy dye-loading, thus we suggest that the perfusion profile showed an increased fluorescence in the maternal circuit due to the fact that the free dye generates a higher fluorescence. Consequently,

the increased fluorescence intensity in the fetal circulation was likely due to the rapid transfer of the free dye across the placental barrier. GreenF and yellow are fluorescein derivatives and it has been shown that such small hydrophobic chemical compounds can easily cross the placenta (Menezes et al., 2011). Regardless of the fluorescence leakage, analysis of histological sections of placental tissue after perfusion by fluorescence microscopy still showed some fluorescent particles in the syncytiotrophoblast and the villous mesenchyme (N3 and N4 in Figure 5 compared to stable particles N5, N6, N7 and P1, P2, C1, C2 in Figure 6). We were not able to detect a difference in fluorescence distribution within the cells as described previously for rhodamine labeled N-isopropylacrylamide (NIPAM) NPs which were found to elute dye and the free dye was spread in the whole cell and particle-bound dye was only restricted to organelles such as lysosomes (Tenuta et al., 2011). According to the NP suppliers the water insoluble fluorescent dyes were incorporated in the glassy polymer matrix after swelling in an appropriate solvent and are not chemically bound in the particle or to the surface. Therefore all dyes should remain entrapped in an aqueous environment. However, as every biological environment the placental tissue consists of several compartments with different pH values and containing different proteins or lipids. It is known that dyes can elute from NPs after contact with a hydrophobic milieu in a cell (Pietzonka et al., 2002, Salvati et al., 2011). The plasma membrane of a cell retains an enormous hydrophobic area which is especially enlarged in the human placenta compared to other organs. The brush border membrane of the placental syncytiotrophoblast, which is in contact with the maternal blood, forms numerous microvilli to gain a huge surface for effective exchange of nutrients and waste products. Hence, the possibility of NP contact with hydrophobic membrane in the placenta is much higher than in other biological tissues and therefore the probability of dye elution is increased. Of note, the placenta is an organ with an increased enzymatic and metabolic activity due to its physiological function to protect the fetus and detoxify harmful substances (Prouillac and Lecoeur, 2010, Aye and Keelan, 2013). So it could also be conceivable that parts of the greenF and yellow amine-modified PS particles were degraded by the placental cells which lead to the release of the fluorescent dye. Since this phenomenon could not be observed with the non-functionalized and carboxylate-modified PS beads this fluorescence leakage seems to be dependent on the surface modification. However, examinations with amine-modified N5, N6, N7 and N8 PS beads containing a different fluorescent dye (envy green and orange) revealed a fraction of only  $3.9 \pm 5.2 \%$  and  $11.2 \pm 9.1 \%$  free dye after 6 hours of perfusion for N6 and N7 nm PS beads, respectively, indicating that dye elution depends mainly on the properties of the fluorescent dye (Figure 3C and 4B).



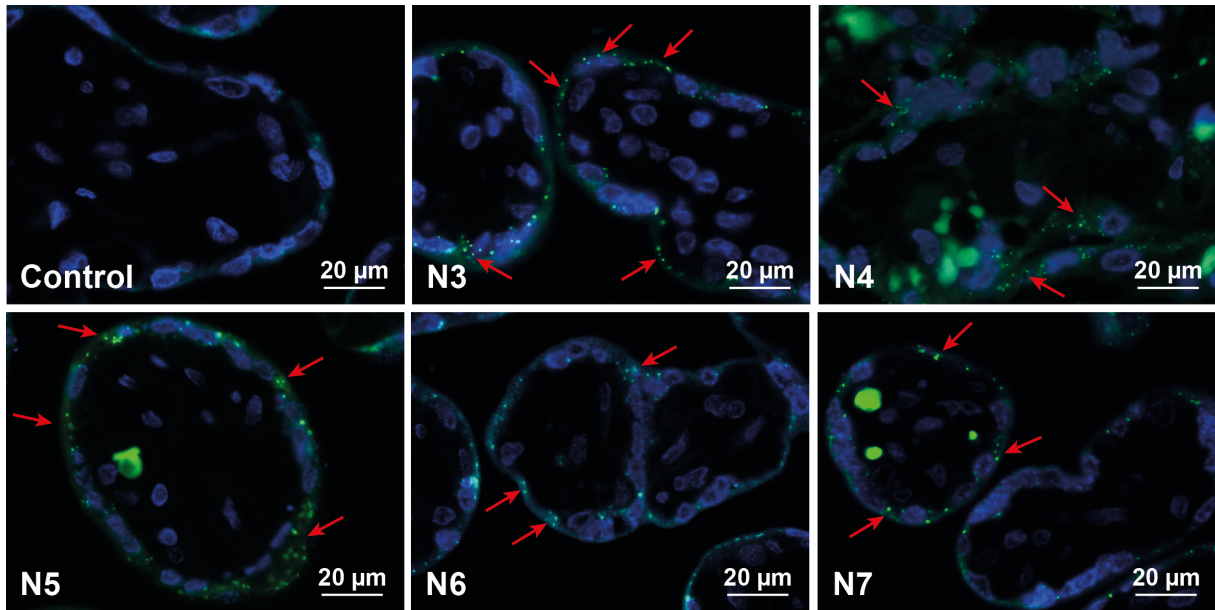


**Figure 5:** Representative fluorescence microscope images of amine-modified PS beads in placental tissue after 6 hours of *ex vivo* perfusion. As control placental perfusion without addition of particles was performed. PS particles are displayed in green and nuclei are stained with DAPI (blue). Due to autofluorescence erythrocytes appear also in green. Red arrows indicate accumulated PS beads.

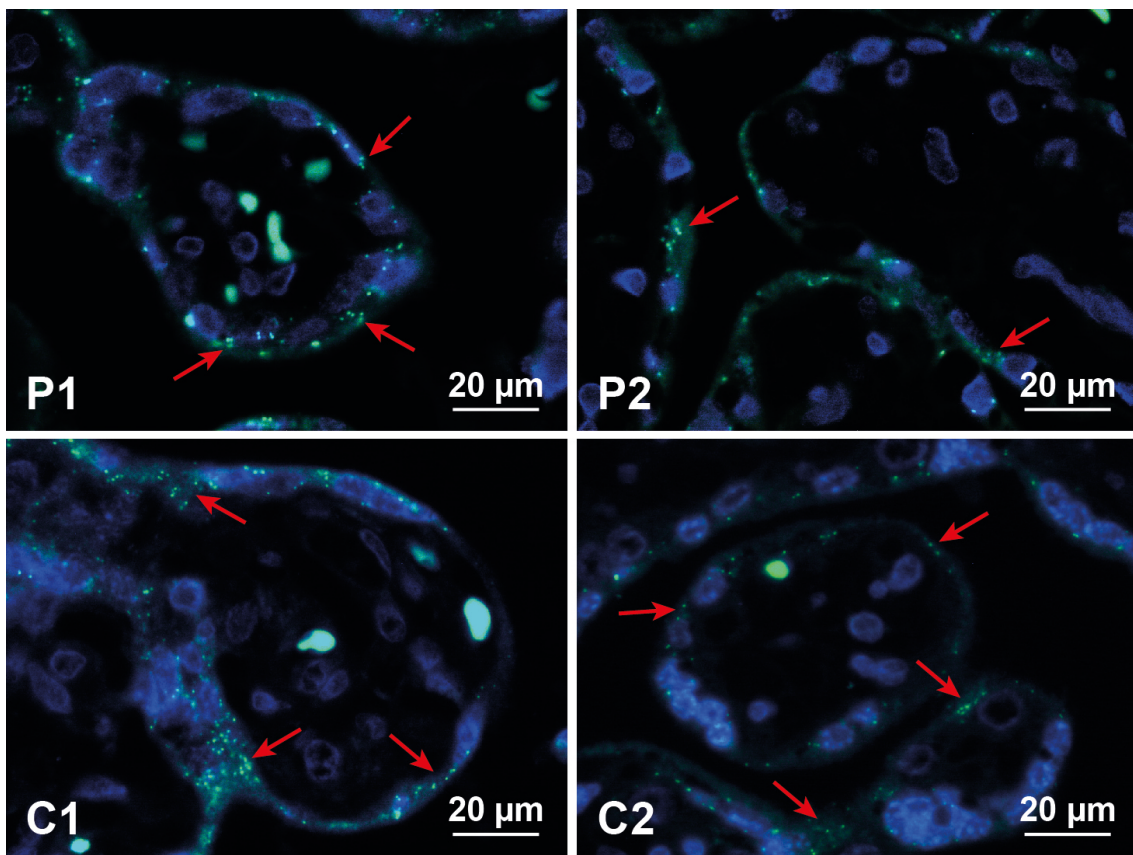


**Figure 6:** Representative fluorescence microscope images of plain and carboxylate-modified PS beads in placental tissue after 6 hours of *ex vivo* perfusion. PS particles are displayed in green and nuclei are stained with DAPI (blue). Due to autofluorescence erythrocytes appear also in green. Red arrows indicate accumulated PS beads.

To avoid the problem of dye leaching, we wanted to use silica-iron core-shell nanoparticles (silica-SPIONs) instead of polystyrene (Table 3, Figure 7). The elements silicon and iron in these particles can be directly detected by ICP-MS analysis. Unfortunately, first measurements indicated that these elements are already present in the placental tissue and the perfusion system itself (Figure 8). Therefore it will be very difficult to interpret the diverse results obtained after *ex vivo* placental perfusion especially if only low placental transfer is expected (Figure 9A). Indeed, TEM micrographs of placental tissue after perfusion implied such a low transport rate, because silica-SPIONs were exclusively found in the maternal part of the placenta mainly in macrophages lying in the intervillous space or near the brush border membrane of the syncytiotrophoblast (Figure 9B). Overall, using nanoparticles without fluorescent label for transport studies in a biological context requires a careful evaluation of the background levels of the respective elements in this environment and the experimental system prior to analysis.

**Table 2: Summary of silica-SPIONs characteristics**

|  | Silica-SPIONs |
|--|---------------|
| Diameter (nm) <sup>a</sup> in TEM                    | 46 ± 10       |
| Hydrodynamic diameter in DD water (nm) <sup>b</sup>  | 125 ± 68.6    |
| Hydrodynamic diameter in PM (nm) <sup>b</sup>        | 145 ± 66.9    |
| Zeta potential in DD water (mV) <sup>a</sup>         | -33 ± 0.6     |
| Iron content (mgFe/mL) <sup>a</sup>                  | 0.42          |
| Silica content (mgSiO <sub>2</sub> /mL) <sup>c</sup> | 6.84          |

Abbreviations: SPION superparamagnetic iron oxide nanoparticles

<sup>a</sup>according to the manufacturer's information; <sup>b</sup>experimentally determined (mode ± SD); <sup>c</sup>calculated values



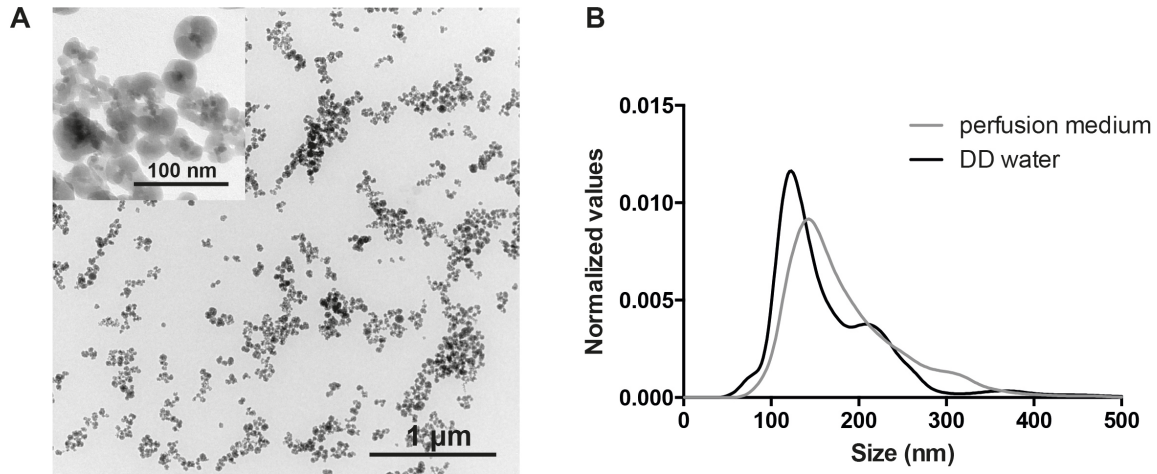


**Figure 7:** (A) TEM micrographs of silica-SPIONs in DD water. (B) Size distribution of silica-SPIONs in DD water and perfusion medium.

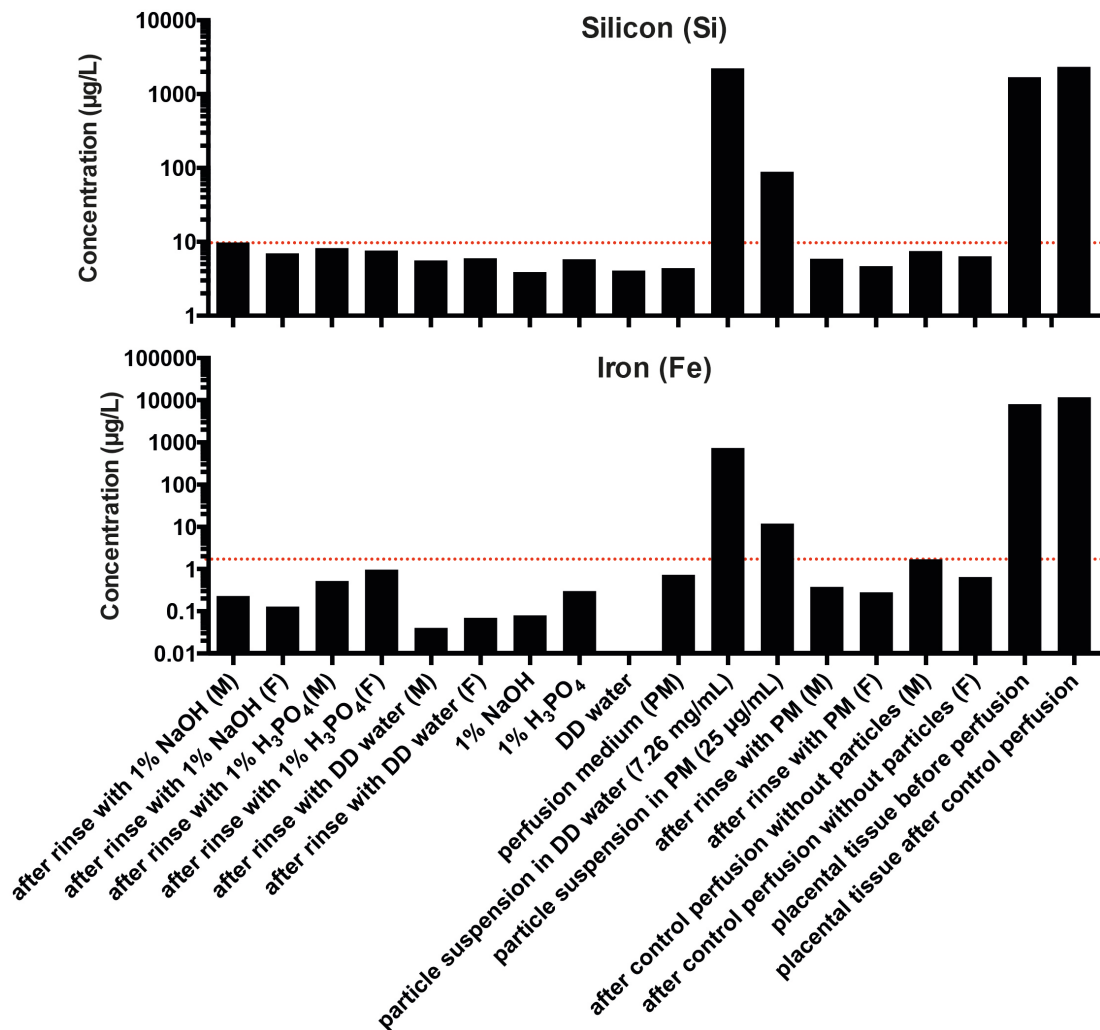


**Figure 8:** Background levels of silicon (Si) and iron (Fe) in the perfusion system and placental tissue. Si and Fe concentrations of solutions (1 % NaOH, 1 % H<sub>3</sub>PO<sub>4</sub>, DD water) used to clean the perfusion system, perfusion medium (PM), silica-SPION suspensions, control perfusions (without particles) as well as tissue samples were measured by ICP-MS.

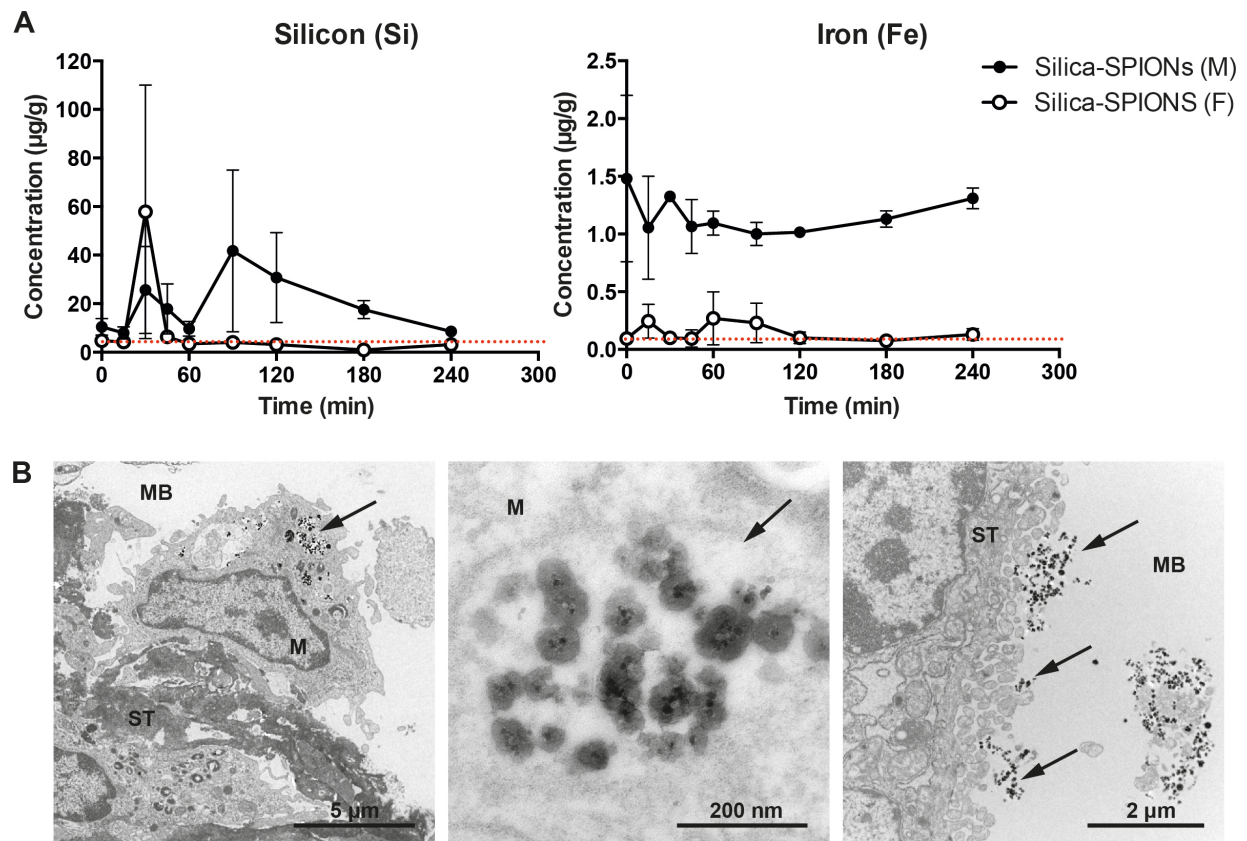


**Figure 9:** (A) Silicon and iron concentration in the fetal (F) and maternal (M) circulation during 4 hours of perfusion with silica-SPIONs was determined by ICP-MS. Data is expressed as mean concentration  $\pm$  SD ( $n=2$ ). (B) TEM micrographs of placental tissue after 6 hours of perfusion with silica-SPIONs. Left and middle panels: Arrows indicate vesicles filled with silica-SPIONs in a macrophage. Middle panel is a magnification of the marked vesicle in the left panel. Right panel: Arrows indicate silica-SPIONs in the maternal blood space near the microvilli of the syncytiotrophoblast.

*MB maternal blood space; ST syncytiotrophoblast; M maternal macrophage*

## Conclusions

Our results demonstrate that there are many practical challenges during investigations about the influence of physicochemical properties of NPs on transport across biological barriers like the human placenta. The characteristics of NPs such as size distribution, fluorescent dye leakage after contact with biological fluids and stability of surface modifications have to be assessed carefully in order to gain reasonable information and understand how NP characteristics such as size, surface charge and chemistry determine not only placental transport but also cellular responses and uptake mechanisms in general. The parameters of NPs physicochemical properties, which have to be analyzed in physiologically relevant conditions, should be always selected according to the question of the study and the biological system. Despite the increasing commercial availability of various NPs with distinct characteristics, the extensive characterization of NP properties requires a similar effort as the investigation of the nanoparticle-cell interactions itself. Finally, this represents a real interdisciplinary challenge.

## References

- AYE, I. L. & KEELAN, J. A. 2013. Placental ABC transporters, cellular toxicity and stress in pregnancy. *Chem Biol Interact*, 203, 456-66.
- CEDERVALL, T., LYNCH, I., LINDMAN, S., BERGGARD, T., THULIN, E., NILSSON, H., DAWSON, K. A. & LINSE, S. 2007. Understanding the nanoparticle-protein corona using methods to quantify exchange rates and affinities of proteins for nanoparticles. *Proc Natl Acad Sci U S A*, 104, 2050-5.
- CRIST, R. M., GROSSMAN, J. H., PATRI, A. K., STERN, S. T., DOBROVOLSKAIA, M. A., ADISESHAIAH, P. P., CLOGSTON, J. D. & MCNEIL, S. E. 2013. Common pitfalls in nanotechnology: lessons learned from NCI's Nanotechnology Characterization Laboratory. *Integr Biol (Camb)*, 5, 66-73.
- DOBROVOLSKAIA, M. A., PATRI, A. K., ZHENG, J., CLOGSTON, J. D., AYUB, N., AGGARWAL, P., NEUN, B. W., HALL, J. B. & MCNEIL, S. E. 2009. Interaction of colloidal gold nanoparticles with human blood: effects on particle size and analysis of plasma protein binding profiles. *Nanomedicine*, 5, 106-17.
- GRAFMULLER, S., MANSER, P., KRUG, H. F., WICK, P. & VON MANDACH, U. 2013. Determination of the transport rate of xenobiotics and nanomaterials across the placenta using the ex vivo human placental perfusion model. *J Vis Exp*.
- HOLE, P., SILLENCE, K., HANNELL, C., MAGUIRE, C. M., ROESSLEIN, M., SUAREZ, G., CAPRACOTTA, S., MAGDOLENOVA, Z., HOREV-AZARIA, L., DYBOWSKA, A., COOKE, L., HAASE, A., CONTAL, S., MANO, S., VENNEMANN, A., SAUVAIN, J. J., STAUNTON, K. C., ANGUISSOLA, S., LUCH, A., DUSINSKA, M., KORENSTEIN, R., GUTLEB, A. C., WIEMANN, M., PRINA-MELLO, A., RIEDIKER, M. & WICK, P. 2013. Interlaboratory comparison of size measurements on nanoparticles using nanoparticle tracking analysis (NTA). *J Nanopart Res*, 15, 2101.
- HWANG, M. N. & EDERER, G. M. 1975. Rapid hippurate hydrolysis method for presumptive identification of group B streptococci. *J Clin Microbiol*, 1, 114-5.
- KREYLING, W. G., HIRN, S. & SCHLEH, C. 2010. Nanoparticles in the lung. *Nat Biotechnol*, 28, 1275-6.
- MAHON, E., HRISTOV, D. R. & DAWSON, K. A. 2012. Stabilising fluorescent silica nanoparticles against dissolution effects for biological studies. *Chem Commun (Camb)*, 48, 7970-2.
- MENEZES, V., MALEK, A. & KEELAN, J. A. 2011. Nanoparticulate drug delivery in pregnancy: placental passage and fetal exposure. *Curr Pharm Biotechnol*, 12, 731-42.
- NEL, A. E., MADLER, L., VELEGOL, D., XIA, T., HOEK, E. M., SOMASUNDARAN, P., KLAESSIG, F., CASTRANOVA, V. & THOMPSON, M. 2009. Understanding biophysicochemical interactions at the nano-bio interface. *Nat Mater*, 8, 543-57.
- OBERDORSTER, G., MAYNARD, A., DONALDSON, K., CASTRANOVA, V., FITZPATRICK, J., AUSMAN, K., CARTER, J., KARN, B., KREYLING, W., LAI, D., OLIN, S., MONTEIRO-RIVIERE, N., WARHEIT, D., YANG, H. & GROUP, I. R. F. R. S. I. N. T. S. W. 2005. Principles for characterizing the potential human health effects from exposure to nanomaterials: elements of a screening strategy. *Part Fibre Toxicol*, 2, 8.
- PIETZONKA, P., ROTHEN-RUTISHAUSER, B., LANGGUTH, P., WUNDERLI-ALLENSPACH, H., WALTER, E. & MERKLE, H. P. 2002. Transfer of lipophilic

- markers from PLGA and polystyrene nanoparticles to caco-2 monolayers mimics particle uptake. *Pharm Res*, 19, 595-601.
- PROUILLAC, C. & LECOEUR, S. 2010. The role of the placenta in fetal exposure to xenobiotics: importance of membrane transporters and human models for transfer studies. *Drug Metab Dispos*, 38, 1623-35.
- REYNOLDS, E. S. 1963. The use of lead citrate at high pH as an electron-opaque stain in electron microscopy. *J Cell Biol*, 17, 208-12.
- RIEHMANN, K., SCHNEIDER, S. W., LUGER, T. A., GODIN, B., FERRARI, M. & FUCHS, H. 2009. Nanomedicine--challenge and perspectives. *Angew Chem Int Ed Engl*, 48, 872-97.
- SALVATI, A., ABERG, C., DOS SANTOS, T., VARELA, J., PINTO, P., LYNCH, I. & DAWSON, K. A. 2011. Experimental and theoretical comparison of intracellular import of polymeric nanoparticles and small molecules: toward models of uptake kinetics. *Nanomedicine*, 7, 818-26.
- TENUTA, T., MONOPOLI, M. P., KIM, J., SALVATI, A., DAWSON, K. A., SANDIN, P. & LYNCH, I. 2011. Elution of labile fluorescent dye from nanoparticles during biological use. *PLoS One*, 6, e25556.
- TENZER, S., DOCTER, D., KUHAREV, J., MUSYANOVYCH, A., FETZ, V., HECHT, R., SCHLENK, F., FISCHER, D., KIOUPTSI, K., REINHARDT, C., LANDFESTER, K., SCHILD, H., MASKOS, M., KNAUER, S. K. & STAUBER, R. H. 2013. Rapid formation of plasma protein corona critically affects nanoparticle pathophysiology. *Nat Nanotechnol*, 8, 772-81.
- WARHEIT, D. B. 2008. How meaningful are the results of nanotoxicity studies in the absence of adequate material characterization? *Toxicol Sci*, 101, 183-5.
- WICK, P., MALEK, A., MANSER, P., MEILI, D., MAEDER-ALTHAUS, X., DIENER, L., DIENER, P. A., ZISCH, A., KRUG, H. F. & VON MANDACH, U. 2010. Barrier capacity of human placenta for nanosized materials. *Environ Health Perspect*, 118, 432-6.
- ZHENG, J., CLOGSTON, J. D., PATRI, A. K., DOBROVOLSKAIA, M. A. & MCNEIL, S. E. 2011. Sterilization of Silver Nanoparticles Using Standard Gamma Irradiation Procedure Affects Particle Integrity and Biocompatibility. *J Nanomed Nanotechnol*, 2011, 001.



## **PART IV**

### **Evaluation of nanoparticle-placenta interactions *in vitro***

Stefanie Grafmueller, Carina Muoth, Tina Buerki-Thurnherr, Peter Wick

#### ***Author contribution***

In this study, I performed the isolation of cytotrophoblasts from the placenta, purity testing by FACS and immunocytochemistry as well as optimization of culture conditions in collaboration with Carina Muoth. I performed the MTS and the DCF assay as well as the interference tests for these assays. I also investigated the uptake of the gold particles in BeWo cells. Together with Carina Muoth I established the ELISA for cytokine and hormone secretion in BeWo cells. In addition, I analyzed and summarized all results. Tina Buerki-Thurnherr and Peter Wick conceived and designed the study.





## Evaluation of nanoparticle-placenta interactions *in vitro*

Stefanie Grafmueller<sup>1,2,3</sup>, Carina Muoth<sup>1</sup>, Tina Buerki-Thurnherr<sup>1</sup>, Peter Wick<sup>1</sup>

<sup>1</sup>Laboratory for Materials-Biology Interactions, Empa, St. Gallen, Switzerland

<sup>2</sup>Perinatal Pharmacology, Department of Obstetrics, University Hospital Zurich, Zurich, Switzerland

<sup>3</sup>Graduate School for Cellular and Biomedical Sciences, University of Berne, Berne, Switzerland

### Introduction

Decades ago the human placenta was thought to be an impenetrable barrier between mother and unborn child. However, the discovery of the thalidomide-induced birth defects and many later studies proved the opposite. Today several harmful xenobiotics like nicotine, heroin or methadone as well as environmental pollutants were described to overcome this barrier (Martin and Holloway, 2014). With the increasing use of engineered nanomaterials (ENM) in many industrial, consumer and medical products, concern about nanoparticle exposure *in utero* is arising. To elucidate the risk of such ENMs to the developing fetus, placental transport studies are required. In addition, a high percentage of women need medication during pregnancy (such as epilepsy drugs) despite of known adverse effects of these drugs for the fetus (Gendron et al., 2009). Nanomedicine is anticipated to provide novel therapeutic strategies to overcome off-target effects to the fetus e.g. by developing nanoparticle drug carriers that are largely retained in the maternal circulation. A better understanding of the specific mechanisms underlying placental transfer of ENMs and its dependence on the physicochemical properties is a prerequisite for the development of ENMs as drug carriers. Since the placenta is the most species-specific organ in mammals, animal models are not appropriate to predict placental transfer in humans (Enders and Blankenship, 1999). To date the *ex vivo* human placental perfusion model is the most reliable and predictive model to study placental transport of ENMs and xenobiotics in general (Grafmuller et al., 2013). However, it has its limit regarding throughput and time of exposure. Due to a success rate of about 20 % for a 6 hour placental

perfusion, only some pre-selected ENMs and questions can be investigated in a reasonable time frame. Duration of exposure to ENMs in the *ex vivo* perfusion model is restricted to few hours because of tissue degradation (Panigel et al., 1967, Schneider et al., 1972, Di Santo et al., 2003). Long-term effects on the placenta as well as specific transport mechanisms have to be studied in an *in vitro* model first. The most often used *in vitro* model for the human placenta is the transwell model with BeWo cells, a human cell line derived from a malignant gestational choriocarcinoma (Ali et al., 2013, Bhabra et al., 2009, Cartwright et al., 2012, Correia Carreira et al., 2013, Faust et al., 2014, Sood et al., 2011). BeWo cells resemble the cytotrophoblast cells, which fuse during placental development and form a syncytium. The resulting syncytiotrophoblast is the main cellular barrier of the human placenta (Enders and Blankenship, 1999). Though, the endothelial cells of the fetal capillaries may also play a role in regulating placental transport of endogenous and exogenous substances (Elad et al., 2014, Firth and Leach, 1996, Levkovitz et al., 2013b). Currently, only few models exist which include both cell types and most transport experiments are conducted under steady state conditions so far (Levkovitz et al., 2013a). Therefore, the aim of our group is to develop an advanced *in vitro* model including several cell types and perfusion flow allowing mechanistic studies and a higher throughput compared to the *ex vivo* perfusion model. Additionally, a three-dimensional placental tissue model with a fibroblast core and a trophoblast shell is under development using the hanging drop technology. At the moment BeWo cells are used in both models, because they are stable, easy to handle and build a confluent cell layers in culture. However, this cell line comprises mainly undifferentiated cytotrophoblasts, which do not spontaneously form a true syncytium without lateral cell membranes as the syncytiotrophoblast *in vivo* (Wice et al., 1990). Thus to exclude paracellular transport, the formation of tight junctions has to be evaluated prior to a transport study which is usually done by measurement of the transepithelial electrical resistance (TEER) and transfer of marker molecules such as fluorescein (Cartwright et al., 2012). To optimize the model, primary cytotrophoblast cells isolated from the human placenta could replace the BeWo cells. We hope this will improve the *in vivo* predictability of the model not only for transport but also for placental toxicity studies. Primary human cytotrophoblasts syncytialize spontaneously and form a polarized syncytium. In this stage the cells are highly differentiated and there is no cell division anymore similar as *in vivo*. In contrast, BeWo cells are largely undifferentiated with an extensive proliferation activity, which is typical for cancer cells. Consequently, the cellular responses to ENMs (e.g. influence on functionality) could be quite different in tumor derived BeWo cells with an altered gene expression and primary cytotrophoblasts (Bilban et al., 2010, Nikitina et al., 2013). The aim of

this still ongoing study is to elucidate if BeWo cells and primary trophoblasts show a different behavior after exposure to ENMs based on the assumption that primary cytotrophoblasts are more physiological relevant and predictive as model for placental studies. In order to reach this goal, acute toxicity induced by ENMs, uptake as well as the impact of ENMs on the endocrine, metabolic and transport function of both cell types have to be compared. To evaluate a broad variety of cellular responses, different toxic and non-toxic ENMs such as multi-walled carbon nanotubes (MWCNTs), gold and polystyrene (PS) particles are used in this study. For the MWCNTs and amine-modified PS beads cytotoxic effects on other cell types have already been described (Elliott et al., 2014, Thurnherr et al., 2011).

## Materials and Methods

**Nanomaterials.** Amine-modified (NH<sub>2</sub>) 58 nm PS beads were purchased from Bangs Laboratories Inc. and were characterized by Elliott and Rösslein et al. (Elliott et al., 2014). Gold nanoparticles (NPs) modified with positive, neutral and negative ligands were kindly supplied and characterized by Dr. Bing Yan from Shandong University, Jinan, China (Table 1). MWCNTs were obtained from Bayer Technologies Services and were extensively characterized by Thurnherr et al. (Thurnherr et al., 2009). Prior to each experiment MWCNTs were dispersed in 160 ppm Pluronic F127 (Sigma-Aldrich) by sonication for 10 min in an ultrasonic bath at a concentration of 500 µg/mL.

**Table 1: Summary of gold nanoparticles characteristics**

|  | Positive    | Neutral      | Negative     |
|--|-------------|--------------|--------------|
|  |             |              |              |
| Diameter (nm) in TEM <sup>a</sup>                    | 5.76 ± 0.99 | 5.79 ± 0.43  | 4.55 ± 0.18  |
| Diameter from DLS in DD water <sup>a</sup>           | 70.68 ± 7.8 | 106.1 ± 1.37 | 147.7 ± 0.87 |
| PDI in DD water                                      | 0.332       | 0.154        | 0.191        |
| Zeta potential in DD water (mV) at pH 7 <sup>a</sup> | 38.6 ± 0.75 | -33.2 ± 2.12 | -39.8 ± 1.7  |

Abbreviations: TEM transmission electron microscopy; DD double distilled; PDI polydispersity index

<sup>a</sup>Mean ± SD

**Cell culture.** BeWo cells (b30 clone) were obtained from Prof. Dr. Ursula Graf-Hausner (Zurich University of Applied Sciences, Waedenswil, Switzerland) with permission of Dr. Alan L. Schwartz (Washington University School of Medicine, MO, USA) and cultured in Ham's F-12K medium (Gibco, Life Technologies) supplemented with 1 % penicillin-streptomycin-neomycin (Sigma-Aldrich) and 10 % fetal calf serum (FCS; Lonza). Cells were grown in tissue culture flasks at 37 °C and 5 % CO<sub>2</sub> and sub-cultured at 80 % confluency using 0.05 % Trypsin-EDTA (Ethylenediaminetetraacetic acid) (Sigma-Aldrich) for detachment.

**Isolation of primary human cytotrophoblasts.** Human placentas were obtained from uncomplicated term pregnancies after caesarean section at the Department of Obstetrics at the Kantonsspital and the Klinik Stephanshorn in St. Gallen. Written informed consent was obtained prior to delivery. The project was approved by the local ethics committee and performed in accordance with the principles of the Declaration of Helsinki. Isolation of primary cytotrophoblasts was performed as described elsewhere (Petroff et al., 2006). After placing the placental tissue in a sterile plate (maternal side at the top) on ice, the superficial basal plate tissue on the maternal side was carefully removed. Above the chorionic plate lies the villous tissue from which 50 g were collected and rinsed with phosphate-buffered saline (PBS; Sigma-Aldrich) until the remaining blood was washed out. Three consecutive steps of tissue digestion in digestion solution containing 25 mM HEPES (4-(2-Hydroxyethyl) piperazine-1-ethanesulfonic acid; Sigma-Aldrich), 0.25 % Trypsin (Invitrogen, Life Technologies) and about 300 U/mL DNase (Sigma-Aldrich) in 1x HBSS (Hank's balanced salt solution consisting of 0.54 mM KCl, 0.44 mM KH<sub>2</sub>PO<sub>4</sub>, 0.14 M NaCl, 0.34 mM Na<sub>2</sub>HPO<sub>4</sub> and 5.55 mM D-glucose dissolved in DD water) followed. Each step was carried out for 20 min at 37 °C. After each step the supernatant was collected and new digestion solution added. The supernatant was filtered through a cell dissociation sieve (60 mesh screen with a pore size of about 230 µm; Sigma-Aldrich) and layered over FCS. After centrifugation at 1000 g for 15 min at room temperature (Figure 1A), the cell pellet was resuspended in cytotrophoblast culture medium, which was high glucose DMEM (Dulbecco's Modified Eagle's Medium; Sigma-Aldrich) supplemented with 10 % FCS and 1 % penicillin-streptomycin-neomycin (Sigma-Aldrich). To remove residual tissue fragments, the suspension was filtered through a 100 µm nylon cell strainer. Afterwards the suspension was centrifuged at 1000 g for 10 min, resuspended in CMF Hank's (Ca/Mg-free 1x HBSS) and layered carefully over two Percoll gradients (Sigma-Aldrich) ranging from 70 % to 5 % (each layer 5 % lower than the last). Gradients were centrifuged at 1200 g for 20 min at room temperature in a swinging bucket rotor without brake. In a 50 mL tube the cytotrophoblasts could be found between the 15 and

30 mL mark corresponding to a density between 1.048 and 1.060 g/cm<sup>3</sup>, while red blood cells were in the pellet, cell debris above and lymphocytes underneath the cytotrophoblasts (Figure 1B). Cytotrophoblast cells were collected, diluted in cytotrophoblast culture medium and centrifuged at 1000 g for 5 min. To increase the purity, immunomagnetic purification was performed. To label the non-cytotrophoblast cells, the suspension was incubated for 10 min at 4 °C with 40 µg/mL mouse anti-human HLA-ABC antibody (Biolegend) in cell separation buffer (CSB) consisting of Ca/Mg-free PBS containing 0.5 % bovine serum albumin (BSA; Sigma-Aldrich) and 2 mM EDTA (Sigma-Aldrich). After washing the cells twice with CSB, MACS<sup>®</sup> goat anti-mouse IgG MicroBeads (Miltenyi Biotec) were added. Following the 15 min incubation period at 4 °C, the cell suspension was washed once with CSB and applied onto a previously prepared MS+ separation column in a MiniMACS magnet system (Miltenyi Biotec). The effluent containing the unlabeled cytotrophoblasts was collected, centrifuged at 400 g for 5 min and resuspended in cytotrophoblast culture medium. Subsequently, residual red blood cells were removed after 5 min incubation at 4 °C in RBC lysis buffer (Sigma-Aldrich). Lysis was stopped with cytotrophoblast culture medium. The yield of isolated primary cytotrophoblast cells was about  $3 \times 10^7$  cells per 50 g tissue. Purity was tested by flow cytometry or immunocytochemistry. Cells not used for the purity assays were diluted in freezing medium containing 10 % dimethylsulfoxide (DMSO) (Sigma-Aldrich) as well as 50 % FCS in PBS and stored in liquid nitrogen until use.

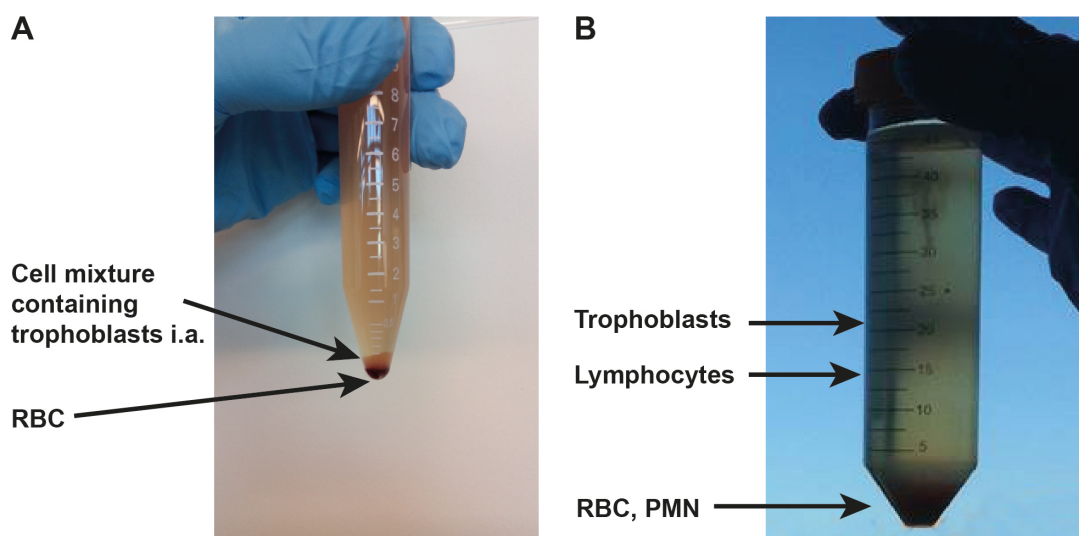


**Figure 1:** Isolation of primary human cytotrophoblasts. (A) Cells after tissue digestion and centrifugation with FCS. Red blood cells (RBC) are found at the bottom of the pellet and the upper white part contains cytotrophoblast cells. (B) Cytotrophoblasts are found around the 20 mL mark after centrifugation in a Percoll gradient. RBCs and polymorphonuclear cells (PMN) accumulated in the pellet at the bottom.

**Flow cytometry.** Approximately  $2 \times 10^6$  cells were used for each sample. After permeabilization with 4 % paraformaldehyde (PFA; Sigma-Aldrich) and 0.2 % Triton X-100 (Sigma-Aldrich) for 10 min at room temperature, cells were blocked with 5 % goat serum (Sigma-Aldrich) for 30 min at room temperature and either stained with mouse IgG1 $\kappa$  (1:1000; Sigma-Aldrich) or mouse anti-human cytokeratin-7 (CK-7, 1:200; Dako) diluted with 0.5 % BSA in PBS. After washing with PBS all samples were labeled with the secondary Alexa 488 goat anti-mouse antibody (1:400; Molecular Probes, Invitrogen). Before FACS (fluorescence-activated cell sorting) analysis using a Partec CyFlow® Space instrument (Sysmex), propidium iodide (1:100; BD Pharmingen) was added in order to allow discrimination between cells and tissue debris.

**Immunocytochemistry.** Primary human cytotrophoblasts before and after immunopurification as well as non-cytotrophoblast cells recovered from the MACS® column were seeded in high glucose DMEM (Sigma-Aldrich) supplemented with 10 % FCS (Lonza), 1 % penicillin-streptomycin-neomycin (Sigma-Aldrich) and 10 ng/mL human epithelial growth factor (EGF, PeproTech) on a glass coverslip in a 24-well plate ( $10^6$  cells/ well). After 2 days of culture, cells were fixed with 4 % PFA and 0.2 % Triton X-100 for 10 min and blocked with

5 % goat serum for 1 hour at room temperature. Primary antibodies mouse anti-human CK-7 (1:200; Dako) and guinea pig anti-human vimentin (1:200; Progen) were diluted in 0.5 % BSA in PBS and applied for 1 hour at room temperature. After three washing steps with PBS incubation with the secondary antibodies goat anti-mouse Alexa 546 (1:400; Molecular Probes, Invitrogen) and goat anti-guinea pig Alexa 488 (1:400; Molecular Probes, Invitrogen) as well as DAPI (1:1000; Sigma-Aldrich) for 1 hour at room temperature followed. Afterwards coverslips were mounted with Mowiol (Sigma-Aldrich) on a glass slide and air-dried. Cells were visualized in a fluorescence microscope (Axioplan 2; Carl Zeiss MicroImaging GmbH).

**Optimization of cell culture conditions for primary human cytotrophoblasts.** Primary cytotrophoblasts were cultured in high glucose DMEM (Sigma-Aldrich) supplemented with 10 % FCS (Lonza), 1 % penicillin-streptomycin-neomycin (Sigma-Aldrich) and 10 ng/mL human epithelial growth factor (EGF, PeproTech). Cells were grown in 24-well ( $10^6$  cells/well) or 96-well ( $10^5$  cells/well) plates coated either with rat collagen type I (BD Bioscience) or human collagen type IV (Sigma-Aldrich) at 37 °C and 5 % CO<sub>2</sub>. Medium was exchanged daily. Cell growth was assessed by DNA quantification (Hoechst assay) and light microscopy.

**DNA quantification (Hoechst assay) in primary human cytotrophoblasts.**  $10^5$  primary cytotrophoblast per well were seeded in a 96-well plate and cultured under different conditions.

After 1, 2, 3 and 4 days cells were washed twice with PBS and incubated with DD (double distilled) water for 10 min. Hoechst 33258 solution (Sigma-Aldrich) was added to the cell lysates and after 1 hour incubation in the dark on a shaker (200 rpm), fluorescence was measured in an FLx800 fluorescence microplate reader (BioTek Instruments) at an excitation wavelength of 350 nm and an emission wavelength of 460 nm. A DNA standard was used to calculate the DNA amount. The fluorochrome contained in the Hoechst 33258 solution binds specifically to DNA and this interaction increases fluorescence emission at 460 nm. Fluorescence intensity is directly proportional to DNA content which in turn is proportional to the cell number.

**MTS viability assay.** The *in vitro* cytotoxicity of the different NMs was tested using the MTS viability assay. Of note, MTS working solution contains the MTS reagent and phenazine ethosulfate (PES), an electron-coupling compound. PES penetrates through the cell membrane and is reduced by mitochondrial enzymes, which are only active in living cells. Reduced PES can leave the cells and converts the MTS to its formazan product, which can be quantified by absorbance measurement at 490 nm. To perform this assay, BeWo cells were seeded in a 96-well plate (8000 cells per well) 24 hours before treatment. 48 hours before treatment primary human cytotrophoblasts were seeded in a 96-well plate coated with rat collagen I ( $4 \times 10^4$  cells per well) to allow a spontaneous syncytialization of the cells, which occurs after 1 - 2 days. Different concentrations of ENMs diluted in high glucose DMEM supplemented with 10 % FCS, 1 % penicillin-streptomycin-neomycin and 10 ng/mL human EGF for primary trophoblasts or in Ham's F-12K medium supplemented with 1 % penicillin-streptomycin-neomycin and 10 % FCS for BeWo cells were applied. As negative control, cells without treatment were used and as positive control 1, 10, 100 and 1000  $\mu\text{M}$   $\text{CdSO}_4$  was applied. After 3 or 24 hours of incubation at 37 °C and 5 %  $\text{CO}_2$ , an MTS assay (CellTiter96® AQueous One Solution Cell Proliferation Assay; Promega) was performed according to the manufacturer's instructions. The MTS working solution was produced using phenol red free DMEM (Gibco, Life Technologies) with 5 % FCS for primary trophoblasts or phenol red free DMEM/F12 Ham (Sigma-Aldrich) supplemented with 5 % FCS for BeWo cells. Optical density (OD) was measured at 490 nm in an EL800 microplate reader (BioTek Instruments). Blank samples containing no cells but treated in the same way with ENMs were run with each assay. Values were corrected using these blanks and results were presented as mean percentage of the untreated control from three independent experiments.

**ENM interference in the MTS assay.** ENM interference with the MTS assay was evaluated in a cell-free set-up. Phenol red free DMEM/F12 Ham cell culture medium alone, medium with MTS working solution or medium with formazan (addition of 1 mM Na<sub>2</sub>SO<sub>3</sub> to MTS working solution resulted in MTS reduction to formazan) was added to the ENM dilutions. Absorbance was measured after 1 hour at 37 °C and 5 % CO<sub>2</sub> in an EL800 microplate reader (BioTek Instruments) at 490 nm.

**Determination of ROS by DCF assay.** The formation of reactive oxygen species (ROS) was detected by the 2',7'-dichlorofluorescein (DCF) assay. 2',7'-dichlorodihydrofluorescein-diacetate (H<sub>2</sub>DCF-DA; Molecular Probes, Invitrogen) enters the cells and is cleaved in H<sub>2</sub>DCF by intracellular esterases. H<sub>2</sub>DCF can be converted in the highly fluorescent DCF by oxidation through ROS. 24 hours before assay performance BeWo cells were seeded in a 96-well plate (2 x 10<sup>4</sup> cells per well). The day after, cells were incubated with 50 µM H<sub>2</sub>DCF-DA in HBSS (1 g/L D-glucose, 185 mg/L CaCl<sub>2</sub>, 400 mg/L KCl, 60 mg/L KH<sub>2</sub>PO<sub>4</sub>, 100 mg/L MgCl<sub>2</sub>, 100 mg/L MgSO<sub>4</sub>, 8 g/L NaCl, 350 mg/L NaHCO<sub>3</sub>, 60 mg/L Na<sub>2</sub>HPO<sub>4</sub>) for 60 min at 37 °C and 5 % CO<sub>2</sub>. After washing twice with HBSS, cells were exposed to the respective ENM dilutions (diluted in HBSS) or to 50 µM 3-Morpholinosydnonimine (Sin-1; Sigma-Aldrich) which is a nitric oxide donor and served as positive control. Fluorescence was measured after 2 hours using an FLx800 fluorescence microplate reader (BioTek Instruments) at an excitation wavelength of 485 nm and an emission wavelength of 528 nm. All results were blank-corrected and normalized to untreated cells. To assess the intrinsic potential of the NMs to induce ROS without cellular contribution, cell-free control wells with 50 µM H<sub>2</sub>DCF were run with every cell-based assay.

**ENM interference in the DCF assay.** ENM interference with the DCF assay was evaluated in a cell-free set-up. DD water or fluorescent DCF (Sigma-Aldrich) at a concentration of 2.5 µM was added to the ENM dilutions. Fluorescence intensities were measured after 2 hours at 37 °C and 5 % CO<sub>2</sub> in an FLx800 fluorescence microplate reader (BioTek Instruments). The measured intrinsic fluorescence intensities of the ENMs showed a slight concentration dependent increase and were therefore subtracted from the fluorescence intensities determined after incubation with DCF as well as normalized to the untreated control. The resulting values illustrate the quenching effect of the ENMs on DCF fluorescence.

**Hormone secretion.** 24 hours before treatment BeWo cells were seeded in a 24-well plate with 10<sup>5</sup> cells per well for 6 hours and 5 x 10<sup>4</sup> cells per well for 24 hours. Cells were stimulated with different concentrations of Phorbol-12-myristat-13-acetat (PMA, Sigma-Aldrich) or forskolin



(Sigma-Aldrich). In addition, appropriate solvent controls were used (DMSO for PMA and ethanol for forskolin). Supernatants were collected after 6 and 24 hours and stored at -80 °C until use. Levels of the placental hormones human chorionic gonadotropin (hCG) and leptin were determined by enzyme-linked immunosorbent assay (ELISA) as described elsewhere (Malek et al., 1997, Malek et al., 2001). Hormone levels induced in the solvent controls were similar to the untreated control and therefore negligible.

**Cytokine assays.** 24 hours before treatment BeWo cells were seeded in a 24-well plate ( $5 \times 10^4$  cells per well). Cells were stimulated with different concentrations of Phorbol-12-myristat-13-acetat (PMA), tumor necrosis factor alpha (TNF $\alpha$ , AdipoGen), lipopolysaccharide (LPS, Sigma-Aldrich) or interleukin-1 beta (IL-1 $\beta$ , eBioscience). In addition, appropriate solvent controls were used (DMSO for PMA and 0.5 % BSA for TNF- $\alpha$  and IL-1 $\beta$ ). Supernatants were collected after 24 hours and stored at -80 °C until use. IL-6, IL-8 and TNF- $\alpha$  levels were determined by ELISA using commercial ELISA Kits (human IL-8 and TNF- $\alpha$  ELISA Ready-SET-Go from eBioscience and human IL-6 DuoSet ELISA from R&D) according to the manufacturer's instructions. Cytokine levels induced in the solvent controls were similar to the untreated control and therefore negligible.

**Statistical analysis.** Data are shown as mean  $\pm$  standard deviation (SD) from three independent experiments. One-way analysis of variance (ANOVA) with Bonferroni test was performed using GraphPad Prism software, version 6 (GraphPad Software). A p value below 0.05 was considered to be statistical significant.

## Results and Discussion

### *Isolation of primary human cytotrophoblasts and optimization of culture conditions*

Primary human cytotrophoblasts were isolated from human term placentas. After tissue digestion, cell separation on a Percoll gradient (Figure 1) and immunopurification, purity of the cells was tested via immunocytochemistry and/or flow cytometric analysis (Figure 2 and 3). Cytokeratin-7 (CK-7) served as a specific marker for cytotrophoblast cells. Placental trophoblast cells have no HLA class I antigen on their surface in order to avoid rejection of the fetal placental tissue by the immune system of the mother. Therefore, immunopurification with magnetic beads against the HLA class I antigen was used to increase the purity of the cytotrophoblast cells. Epifluorescence images after 5 days of culture clearly demonstrated a contamination with elongated mesenchymal cells in the samples without immunopurification (Figure 2A). In contrast, primary cytotrophoblast cells after immunopurification and 3 days of culture fused spontaneously to build several small multinucleated syncytia (Figure 2B). Flow cytometric analysis of the cytotrophoblasts from the same isolation directly after immunopurification also showed a high percentage of CK-7 positive cells (96.13 % CK-7 positive cells; Figure 2D). However, the amount of CK-7 positive cells varied intensely between individual isolations and placentas. Flow cytometry analysis from another isolation did not show a significant difference in CK-7 positive cells before and after immunopurification (68.89 % versus 72.51 % CK-7 positive cells; Figure 3). Indeed, more isolations from different placentae are required to verify if the immunopurification is improving the purity of the cytotrophoblasts. Moreover, purity may be further increased during cell culture if the conditions favor specifically the growth of primary human cytotrophoblasts (e.g. contaminating non-adherent immune cells will be lost). For all further assays primary human cytotrophoblasts solely from isolations with at least 90 % purity were used. To optimize the culture conditions and support syncytialization of primary cytotrophoblasts, different plate coatings with rat or human collagen were applied. Besides visual control by light microscopy, the DNA amount, as indicator for the cell number, was quantified. DNA quantity is the only measurable variable, which remains stable after fusion of the cells (total number of nuclei in the cell culture plate stays the same, while the volume of the cytoplasm and protein production can be altered). After one day of culture there was no difference between these conditions, whereas after 2 days the cell number in the samples with collagen coating (rat and human) was increased compared to the samples without coating (Figure 4). There was no significant difference between rat and human collagen coating. Moreover, cells survival and growth was

impaired on collagen coated plates without addition of EGF (Figure 4) indicating that EGF is also a major determinant of cell proliferation and/or survival, which also has been described in the literature (Maruo et al., 1987, Humphrey et al., 2008, Morrish et al., 1997). After 3 days there was no further increase in cell number and after 4 days even a slight decline due to their limited viability in culture (Figure 4). Of note, a massive proliferation of the isolated primary human cytotrophoblasts after syncytialization (occurs after 24 – 48 hours of culture) was not expected because trophoblast fusion and terminal differentiation leads to a cell cycle arrest (Depoix et al., 2013). Based on our findings primary cytotrophoblast cells could be optimally cultured on rat collagen coated plates in presence of EGF. However, further studies with cells from several independent isolates have to confirm this finding.

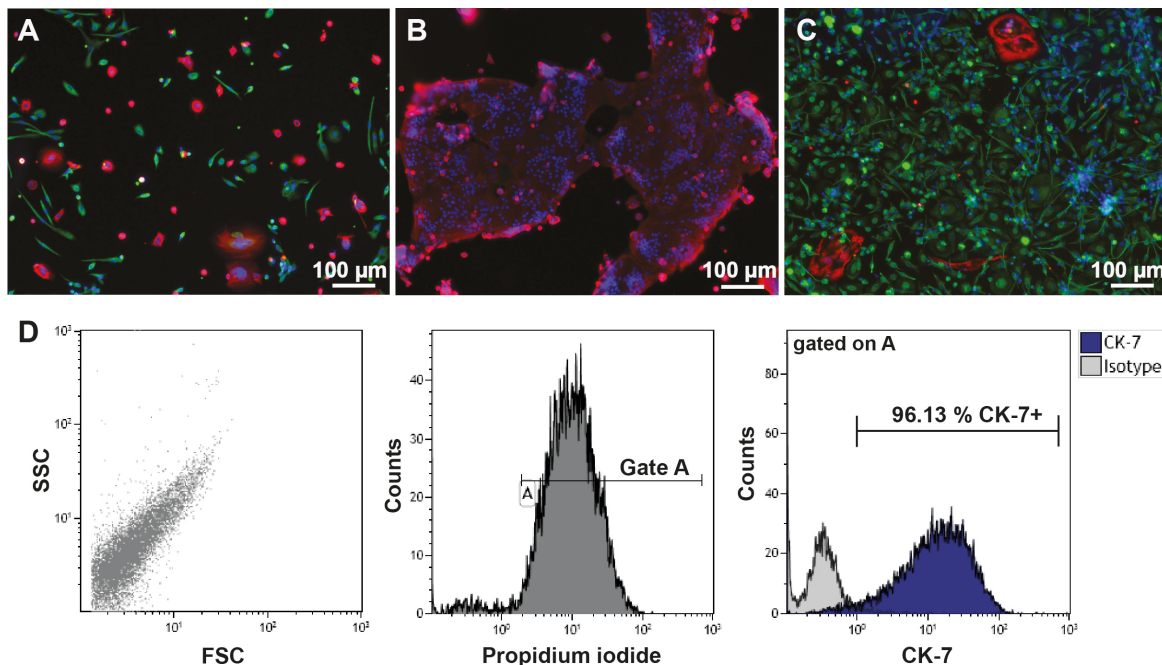


**Figure 2:** Assessment of the purity of the isolated primary human cytotrophoblasts by two different methods. (A – C) Epifluorescence images of isolated primary cytotrophoblasts before (A) and after (B) immunopurification as well as HLA class I positive cells from the column (C) after 3 - 5 days of culture. Cells were stained for the cytoskeletal proteins cytokeratin-7 (CK-7; red) as a marker for trophoblasts and vimentin (green) as a marker for mesenchymal cells. Nuclei were stained with DAPI (blue). (D) Flow cytometric analysis of the isolated primary cytotrophoblasts after immunopurification. Left panel: Cells in the forward (FSC) and side (SSC) scatter. Middle panel: Propidium iodide stained all cell populations and gate A was set to exclude all residual debris from the tissue digestion. Right panel: Isotype control and cytokeratin-7 (CK-7) stained cells in gate A.

### 3. Results - PART IV

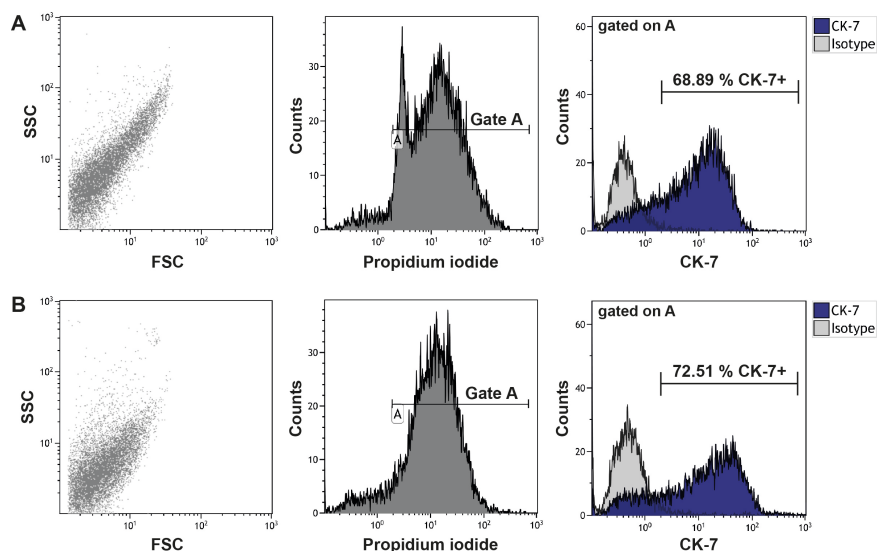


**Figure 3:** Flow cytometric analysis of the purity of isolated primary cytotrophoblasts before (A) and after (B) immunopurification. Left panel: Cells in the forward (FSC) and side (SSC) scatter. Middle panel: Propidium iodide stained all cell populations and gate A was set to exclude all residual debris from the tissue digestion. Right panel: Isotype control and cytokeratin-7 (CK-7) stained cells in gate A.

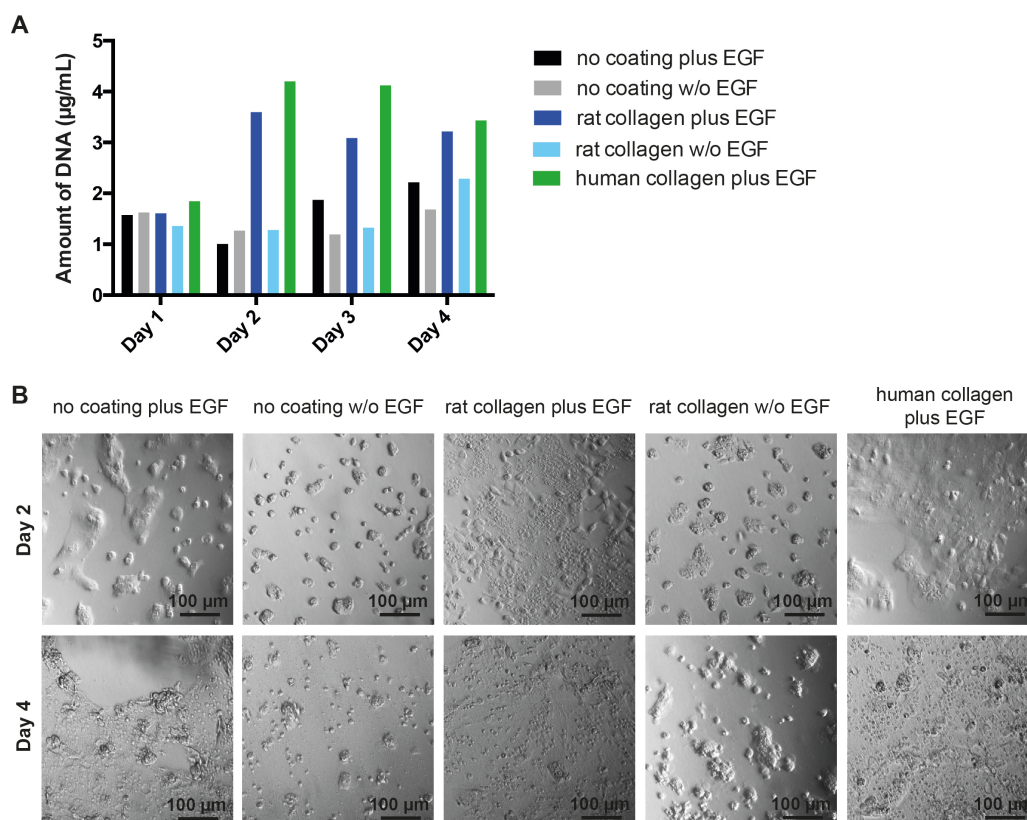


**Figure 4:** (A) Quantification of the DNA amount from isolated primary human cytotrophoblast cells after 1,2,3 or 4 days of culture with or without (w/o) daily addition of 10 ng/mL EGF. Plates were either coated with rat or human collagen or used without coating. On day 0 primary cytotrophoblasts were thawed and  $10^5$  cells/well were seeded (96-well plate). Medium was exchanged every day in all conditions. To assess the DNA amount fluorescent Hoechst 33258 was used after lysis of the cells. Displayed results are from one experiment. (B) Light microscopic images of isolated primary human cytotrophoblasts after 2 and 4 days of culture under the indicated culture conditions.

***Acute toxicity of ENMs on BeWo and primary human cytotrophoblast cells***

If BeWo cells and primary human cytotrophoblasts possess a different sensitivity regarding cytotoxicity to ENMs was investigated in the MTS assay. All three differently modified gold particles did not induce cytotoxicity in BeWo cells even after 24 hours incubation (Figure 5). However, for the amine-modified PS beads and MWCNTs a significant time- and dose-dependent reduction in the number of viable cells was observed (Figure 5). ENMs may bind to the cell culture plate and generate an absorbance signal by themselves, directly reduce the MTS reagent or interfere with the formazan product. Therefore, the potential interference with the assay was examined in a cell-free control experiment. For the positive and neutral gold particles a concentration-dependent intrinsic absorbance, but no interference with the formazan product and no reactivity with the MTS reagent was observed. This is displayed in the left panel of Figure 6, where the slopes of all three curves are similar. Consequently, the OD values from the cell free controls, which were performed simultaneously with the cell-based assay, can be subtracted as blank to totally correct for this intrinsic absorbance of the positive and neutral gold particles at higher concentrations. The negative gold particles (200  $\mu\text{g/mL}$ ) led to a slight increase in formazan absorbance and the amine-modified PS beads ( $\geq 100 \mu\text{g/mL}$ ) as well as the MWCNTs ( $\geq 25 \mu\text{g/mL}$ ) caused a significant decline in formazan absorbance at higher concentrations (Figure 6). Altered absorbance values for formazan would either disguise a cytotoxic effect in the case of elevated values or display a false positive result if ENMs itself induce a decrease of absorbance values. Subsequently, a reliable cytotoxicity evaluation by the MTS assay is only possible for concentrations where no interference occurred. Hence, the negative gold particles could be considered non-cytotoxic up to a concentration of 100  $\mu\text{g/mL}$  after 24 hours of exposure (Figure 5). Amine-modified PS beads demonstrated a significant decrease in enzyme activity already at a concentration of 50  $\mu\text{g/mL}$  after 3 hours and 25  $\mu\text{g/mL}$  after 24 hours, which are both below the threshold where interference arises (Figure 5 and 6). After 24 hours of exposure, MWCNTs illustrated also a trend for decreased cell viability at lower concentrations of 6.25 and 12.5  $\mu\text{g/mL}$  indicating a clear cytotoxic effect of MWCNTs on BeWo cells (Figure 5). Cadmium sulfate ( $\text{CdSO}_4$ ) induces cell death and was used as positive control in the MTS assay with BeWo cells and primary human cytotrophoblasts. After 3 hours primary human cytotrophoblasts demonstrated already a minor decline in cellular activity at 100  $\mu\text{M}$   $\text{CdSO}_4$ , while BeWo cells showed no toxic effect at the same concentration (Figure 5 and 7). These results indicate that primary cytotrophoblasts are slightly more sensitive to  $\text{CdSO}_4$  compared to BeWo cells. However, due to the limited availability of

primary cytotrophoblasts these findings have to be elucidated in further experiments using  $\text{CdSO}_4$  as well as ENMs, which already showed a reduction in BeWo cell viability.

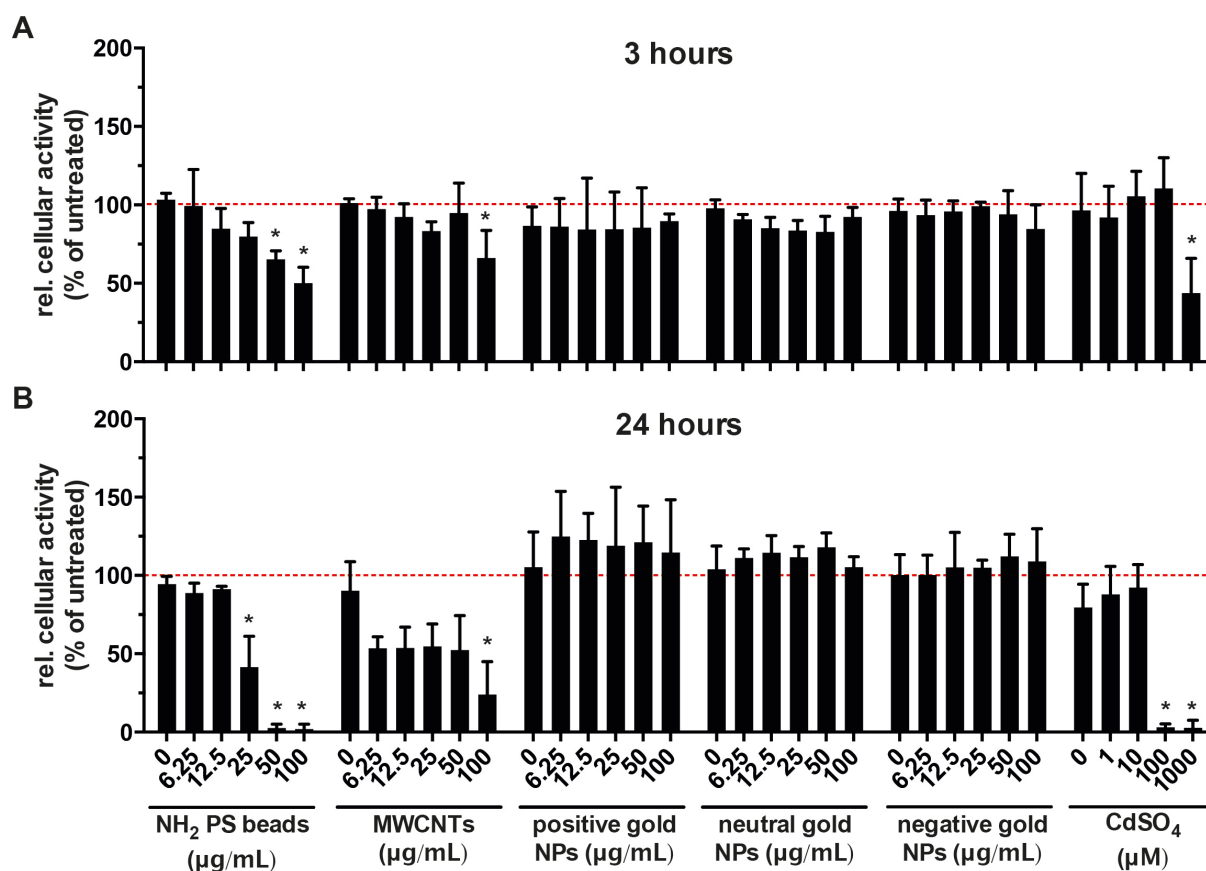


**Figure 5:** Cell viability of BeWo cells was assessed by MTS assay 3 (A) and 24 hours (B) after treatment with the indicated ENM concentrations.  $\text{CdSO}_4$  is a known cell death inducer and served as positive control. Optical density was measured at 490 nm and values were blank-corrected as well as normalized to the untreated samples. The red dashed line indicates the level of the untreated samples at 100 %. Data is expressed as mean  $\pm$  SD of three independent experiments. (\*)  $p < 0.05$  compared to the respective solvent control (0  $\mu\text{g/mL}$ )

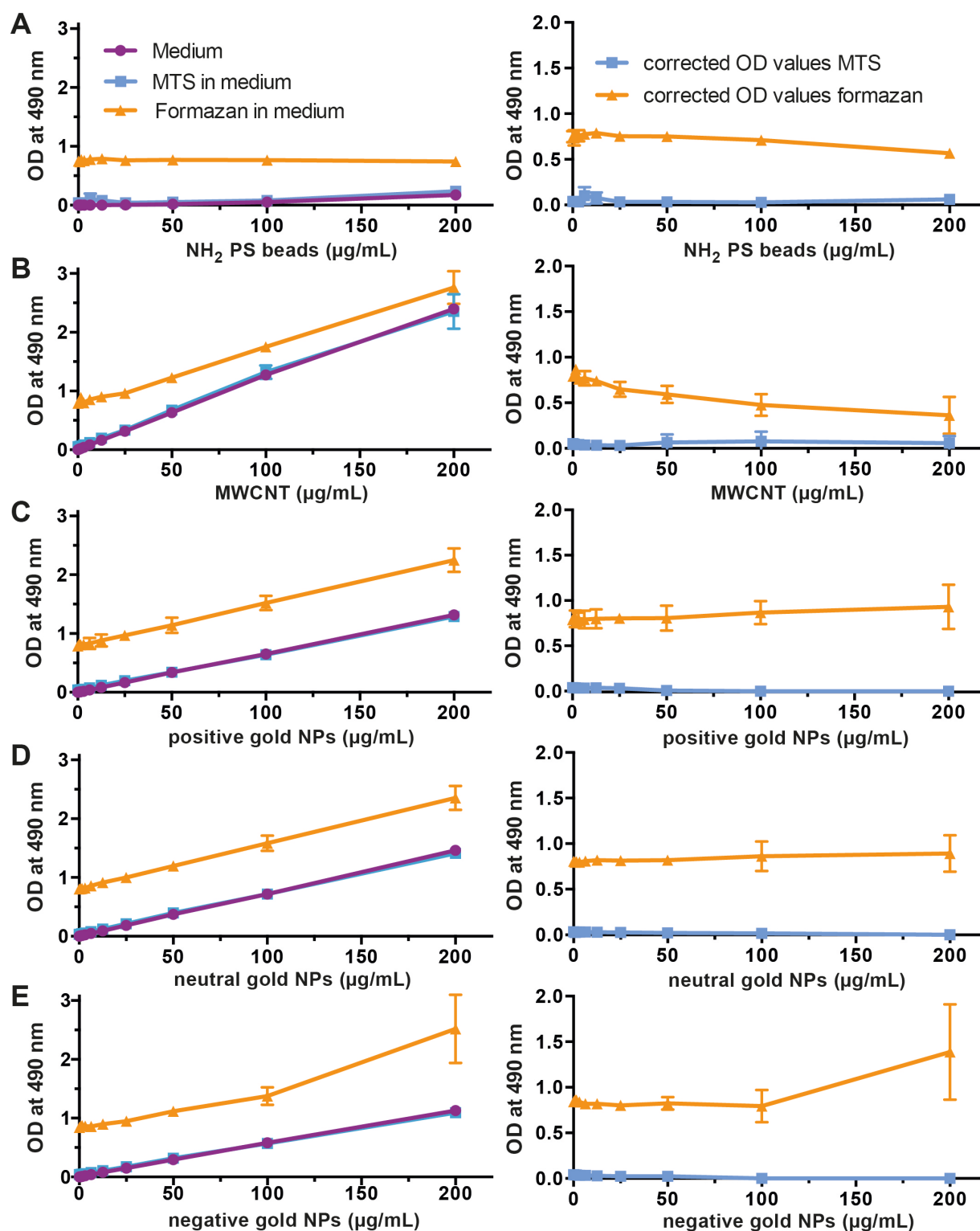


**Figure 6:** Potential interference of ENMs with the MTS assay was assessed by performing a cell-free control experiment. Different concentrations of amine-modified PS beads (A), MWCNTs (B) as well as positive (C), neutral (D) and negative (E) gold nanoparticles (NPs) were added to medium alone, MTS working solution or formazan. The left panel shows the unprocessed OD values of all three conditions. In the right panel OD values were corrected using the OD values resulting from incubation with medium alone as blank. Data represents mean  $\pm$  SD from two technical replicates of one experiment.



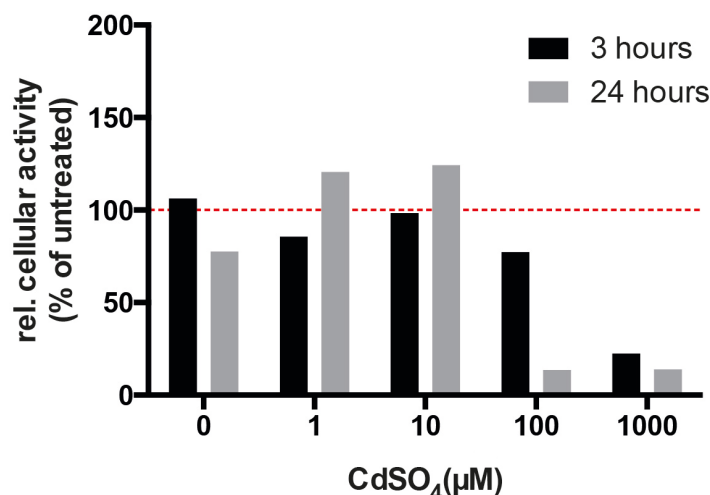


**Figure 7:** Cell viability of primary human cytotrophoblast cells was assessed by MTS assay 3 and 24 hours after treatment with CdSO<sub>4</sub>. Optical density was measured at 490 nm and values are blank-corrected as well as normalized to the untreated samples. The red dashed line indicates the level of the untreated samples at 100 %. Displayed results represent one preliminary experiment.

The formation of ROS could be one possible cause for reduced cell viability after ENM exposure (Schins and Knaapen, 2007, Nel et al., 2006). If elevated ROS levels exceed the protective anti-oxidant defense mechanisms of a cell, oxidative stress will emerge. Consequently, lipids, proteins and DNA will be damaged which leads to genotoxicity, inflammation or cell death (Schins and Knaapen, 2007). ROS formation in BeWo cells was investigated by using the DCF assay. After 2 hours of exposure, significant amounts of ROS were only detected for MWCNTs (Figure 8A). However, cell-free control experiments showed also a dose-dependent intrinsic reactivity of MWCNTs to induce ROS formation (Figure 8B). This indicates that the ROS formation seen in BeWo cells is not solely due to cellular activity, but may also be a consequence of direct interactions between the MWCNTs and the H<sub>2</sub>DCF. Interestingly, at higher MWCNT concentrations (> 50 µg/mL) the ROS level in BeWo cells declined (Figure 8A). Interference testing revealed that increasing concentrations of MWCNTs and gold particles extensively quenched the fluorescence signal from the DCF (Figure 8C), which has been also described for other ENMs (Kroll et al., 2009, Bachmatiuk et al., 2013). Of note, the amine-modified PS beads quenched the DCF fluorescence signal in a dose-dependent manner up to a concentration of 25 µg/mL, but the signal rose again with a further increase in PS concentration (50 – 200 µg/mL). PS beads might interact with DCF in a way that leads to an altered absorbance spectrum, which has to be evaluated in further studies. The ROS production in primary human cytotrophoblast cells could not be assessed yet, but additional experiments will follow in order to show if there is a difference in ROS formation between both cell types.



ENMs can also lead to inflammatory responses of cells (Nel et al., 2006). Therefore, the secretion of the (pro-) inflammatory cytokines IL-8, IL-6 and TNF- $\alpha$  by BeWo cells was examined. Several studies show that BeWo cells as well as placental cells are able to produce these cytokines upon stimulation *in vitro* and *ex vivo* (Bennett et al., 1996, Fujisawa et al., 2000, Shimoya et al., 1999, Tsukihara et al., 2004, Wagner et al., 2000). We observed no IL-8 production by BeWo cells after stimulation with TNF- $\alpha$ , PMA, LPS and IL-1 $\beta$ , but secretion of IL-6 upon stimulation with TNF- $\alpha$ , PMA and IL-1 $\beta$  (Figure 9B). Stable and significant TNF- $\alpha$  production was induced solely by IL-1 $\beta$  stimulation (Figure 9A). Further experiments are in progress to elucidate if BeWo cells and primary human cytotrophoblasts have a distinct capability and sensitivity to produce these cytokines upon stimulation with the known stimulants (TNF- $\alpha$ , PMA, LPS, IL-1 $\beta$ ) or in response to ENMs.

Genotoxicity is usually also investigated if ENM-cell interactions are evaluated. This might be also considered in our model, but the feasibility of genotoxicity assays for primary cytotrophoblasts with limited *in vitro* viability has to be assessed carefully. For example it is not possible to detach primary human cytotrophoblasts from cell culture plates without destroying the syncytia, which is necessary for many assays such as the comet assay.

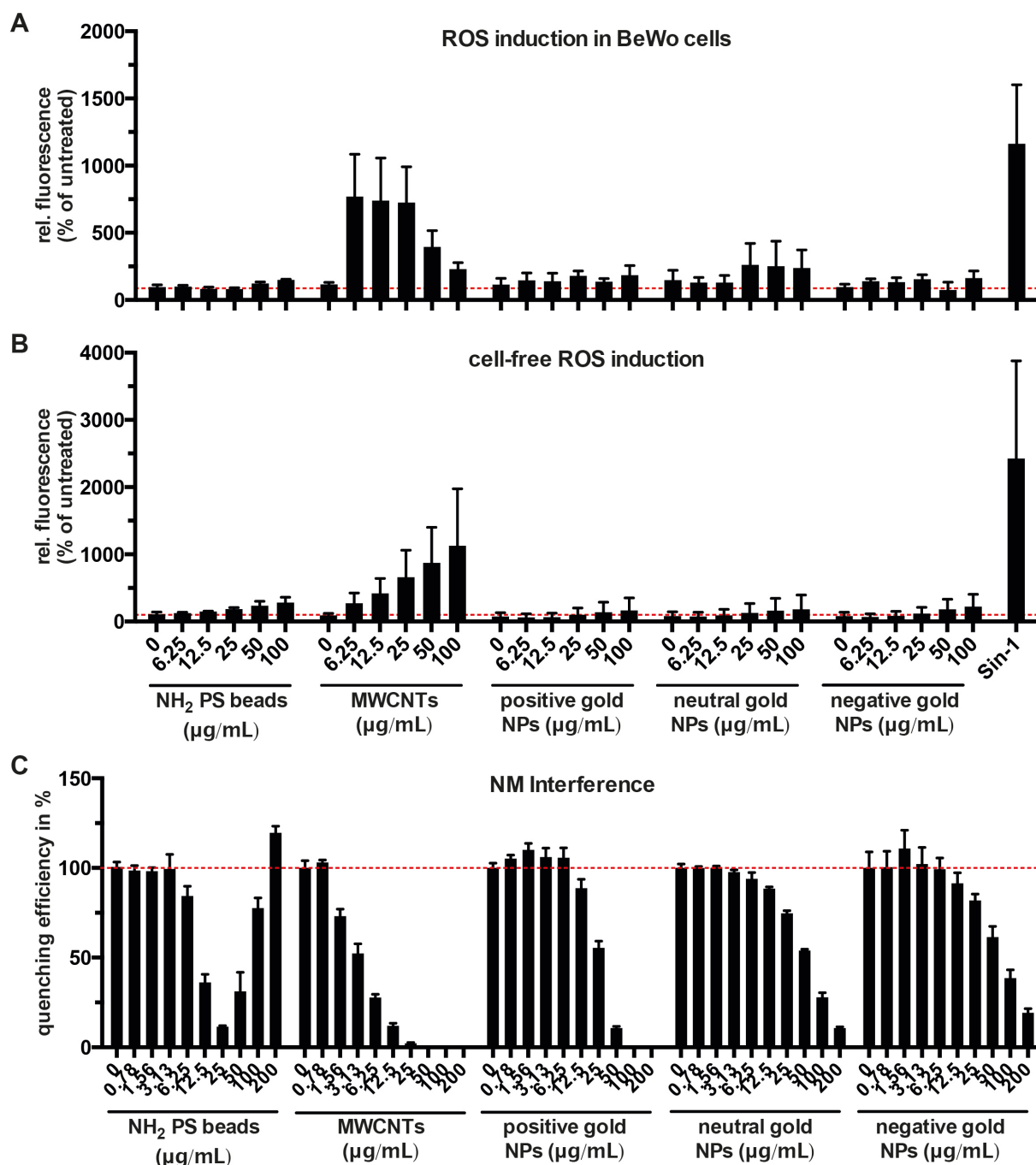


**Figure 8:** Formation of ROS in BeWo cells (A) and intrinsic reactivity of the ENMs under cell-free conditions (B) was determined after 2 hours incubation with the indicated ENM concentrations by using the DCF assay. Sin-1 (50  $\mu\text{M}$ ) served as positive control. 0  $\mu\text{g/mL}$  corresponds to the respective solvent control (DD water or Pluronic F127). Data is expressed as mean  $\pm$  SD of two independent experiments. (C) Quenching effects of the ENMs was determined by incubating DCF with the indicated concentrations of ENMs for 2 hours. Fluorescence values of all three set-ups are blank-corrected and normalized to the untreated control. The red dashed line indicates the level of the untreated samples at 100 %. Data represents mean  $\pm$  SD from three technical replicates of one experiment.

### ***Impact of ENMs on BeWo cells' functionality (subacute toxicity)***

The acute toxicity reactions described in the previous part are similar in many cell types. But to validate an advanced *in vitro* model for the placenta, also cell type-specific readouts are required. Therefore, assays to investigate the expression and activity of efflux transport proteins such as breast cancer resistance protein (BCRP) and p-glycoprotein (P-gp) as well as of placental enzymes like the cytochrome P450 family will be developed in order to reveal differences between BeWo cells and primary human cytotrophoblasts regarding these placenta-specific functions after exposure to ENMs. In a first step, we already established an ELISA to analyze the secretion of the placental hormones leptin and hCG in BeWo cells. To stimulate hormone secretion, forskolin and PMA were applied. Forskolin alone or in combination with PMA are usually used to induce syncytialization and differentiation of BeWo cells, which also leads to a higher hCG production (Omata et al., 2013). While a significant production of hCG was achieved after stimulation for 24 hours with forskolin, Leptin levels remained low and showed a high variance between the experiments (Figure 9C, D).

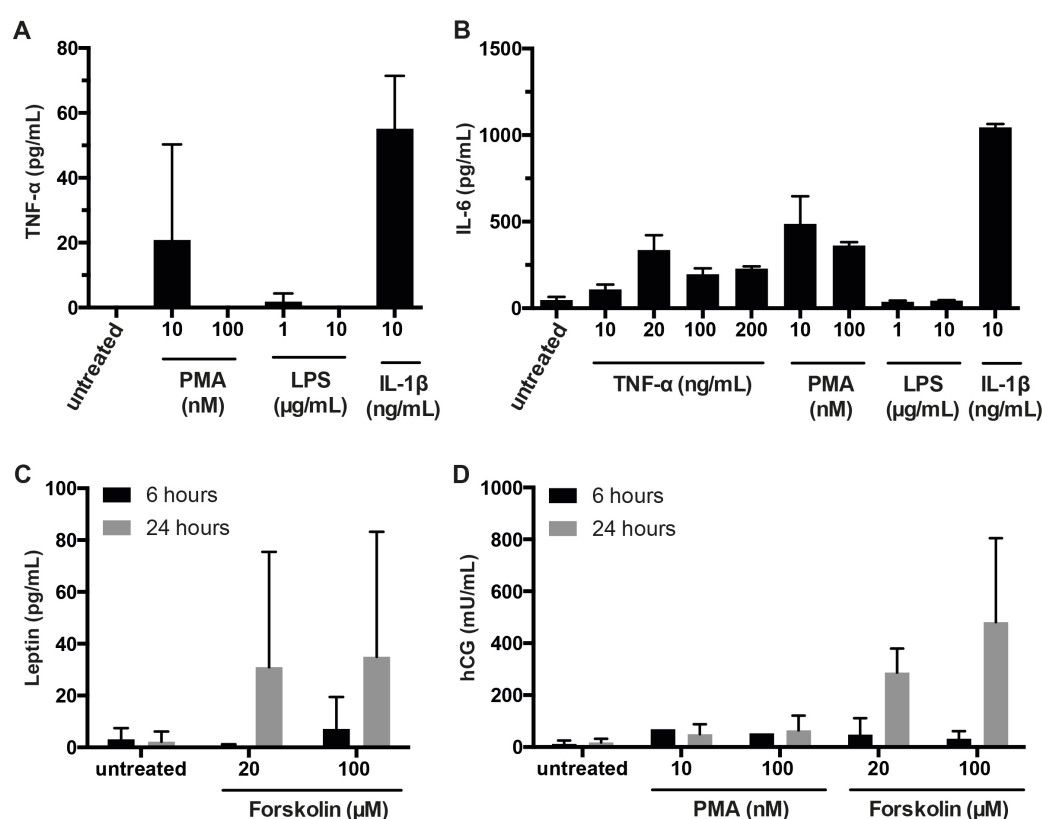


**Figure 9:** (A + B) BeWo cells were incubated with different concentrations of PMA, LPS, IL-1 $\beta$  and TNF- $\alpha$  for 24 hours and induction of inflammatory cytokines TNF- $\alpha$  (A) and IL-6 (B) was measured by ELISA. Data is expressed as mean  $\pm$  SD of two independent experiments. (C + D) BeWo cells were treated with the indicated concentrations of PMA and forskolin to stimulate Leptin (C) and hCG (D) production which was determined after 6 or 24 hours by ELISA. Data represents mean  $\pm$  SD of three independent experiments.

#### *Uptake of ENMs in BeWo cells*

Besides the influence of ENMs on cellular functions, the uptake of ENMs to BeWo and primary human cytotrophoblast cells will be investigated in order to determine if there is a significant difference in intracellular uptake of ENMs between these cells. A first preliminary experiment was performed by exposing BeWo cells to positive, neutral and negative gold particles (100  $\mu\text{g/mL}$ ). After 24 hours of exposure, cells were analyzed by light microscopy. Interestingly, large amounts of the positive gold particles seemed to be taken up by the BeWo cells, whereas the neutral and negative gold particles were rarely co-located with the cells (Figure 10). This finding indicates that the surface charge of these gold particles may determine their uptake in BeWo cells. Studies with other ENMs and at other barriers also showed a surface charge dependent uptake of several ENMs (Choi et al., 2010, Schleh et al., 2012, Tian et al., 2009). Of course, this is only a preliminary as well as qualitative evaluation and further quantitative studies are required. Furthermore, investigations using fluorescent ENMs and analysis by confocal laser scanning microscopy (CLSM) are essential to proof if the ENMs are indeed located inside the cells or just adsorbed to the membrane.

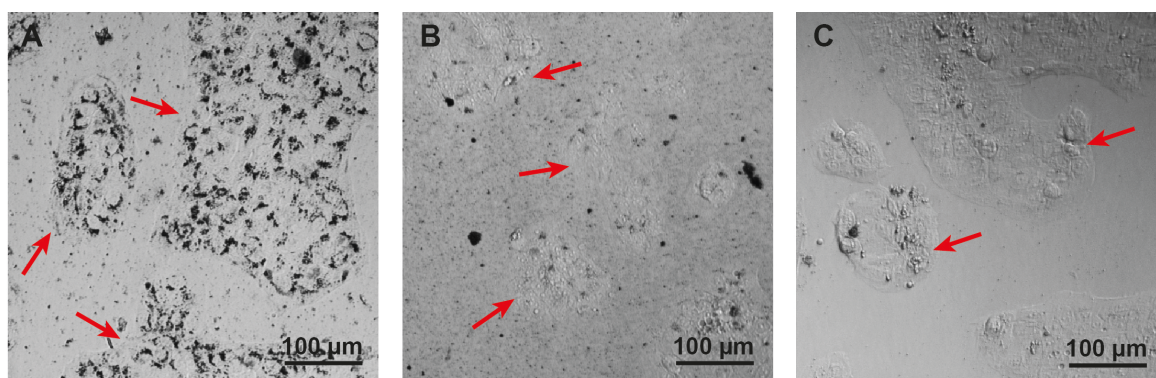


**Figure 10:** Light microscopic images of BeWo cells after 24 hours treatment with 100  $\mu\text{g/mL}$  positive (A), neutral (B) or negative (C) gold particles. Red arrows indicate BeWo cells.

## Conclusions

Overall, the isolation of primary human cytotrophoblast cells requires more time and is more expensive compared to BeWo cell cultures, which are easy to handle. The low yield of such primary cell isolations as well as their limited viability in culture further constrain their applicability for high throughput screenings of ENM-cell interactions. One possible solution would be to use BeWo cells for a first screening of a broad variety of ENMs. Then, based on the respective findings interesting ENMs are selected and their cellular responses further assessed in primary human cytotrophoblasts. However, subacute toxicity of ENM meaning effects on cell functionality might be better reflected in the physiologically more relevant primary cells compared to the tumor-derived BeWo cells. Therefore, another solution would be to implement primary human cytotrophoblasts in advanced *in vitro* models, which do not need a huge number of cells. For example three-dimensional microtissues generated by hanging drop technology, consist of fibroblasts, which are surrounded by one layer of a few hundred trophoblast cells. For the assessment of ENM transport, microfluidic chips would be also interesting and are anticipated for small volumes and cell numbers. Nevertheless, primary human cells require more sophisticated culture conditions and are difficult to standardize compared to established cell lines (Gstraunthaler and Hartung, 2002, Coecke et al., 2005). Whether this concerns also primary cytotrophoblasts remains to be determined in further studies.

## References

- ALI, H., KALASHNIKOVA, I., WHITE, M. A., SHERMAN, M. & RYTTING, E. 2013. Preparation, characterization, and transport of dexamethasone-loaded polymeric nanoparticles across a human placental in vitro model. *Int J Pharm*, 454, 149-57.
- BACHMATIUK, A., MENDES, R. G., HIRSCH, C., JAHNE, C., LOHE, M. R., GROTHE, J., KASKEL, S., FU, L., KLINGELER, R., ECKERT, J., WICK, P. & RUMMELI, M. H. 2013. Few-layer graphene shells and nonmagnetic encapsulates: a versatile and nontoxic carbon nanomaterial. *ACS Nano*, 7, 10552-62.
- BENNETT, W. A., LAGOO-DEENADAYALAN, S., BRACKIN, M. N., HALE, E. & COWAN, B. D. 1996. Cytokine expression by models of human trophoblast as assessed by a semiquantitative reverse transcription-polymerase chain reaction technique. *Am J Reprod Immunol*, 36, 285-94.
- BHABRA, G., SOOD, A., FISHER, B., CARTWRIGHT, L., SAUNDERS, M., EVANS, W. H., SURPRENANT, A., LOPEZ-CASTEJON, G., MANN, S., DAVIS, S. A., HAILS, L. A., INGHAM, E., VERKADE, P., LANE, J., HEESOM, K., NEWSON, R. & CASE, C. P. 2009. Nanoparticles can cause DNA damage across a cellular barrier. *Nat Nanotechnol*, 4, 876-83.
- BILBAN, M., TAUBER, S., HASLINGER, P., POLLHEIMER, J., SALEH, L., PEHAMBERGER, H., WAGNER, O. & KNOFLER, M. 2010. Trophoblast invasion: assessment of cellular models using gene expression signatures. *Placenta*, 31, 989-96.
- CARTWRIGHT, L., POULSEN, M. S., NIELSEN, H. M., POJANA, G., KNUDSEN, L. E., SAUNDERS, M. & RYTTING, E. 2012. In vitro placental model optimization for nanoparticle transport studies. *Int J Nanomedicine*, 7, 497-510.
- CHOI, H. S., ASHITATE, Y., LEE, J. H., KIM, S. H., MATSUI, A., INSIN, N., BAWENDI, M. G., SEMMLER-BEHNKE, M., FRANGIONI, J. V. & TSUDA, A. 2010. Rapid translocation of nanoparticles from the lung airspaces to the body. *Nat Biotechnol*, 28, 1300-3.
- COECKE, S., BALLS, M., BOWE, G., DAVIS, J., GSTRAUNTHALER, G., HARTUNG, T., HAY, R., MERTEN, O. W., PRICE, A., SCHECHTMAN, L., STACEY, G., STOKES, W. & SECOND, E. T. F. O. G. C. C. P. 2005. Guidance on good cell culture practice. a report of the second ECVAM task force on good cell culture practice. *Altern Lab Anim*, 33, 261-87.
- CORREIA CARREIRA, S., WALKER, L., PAUL, K. & SAUNDERS, M. 2013. The toxicity, transport and uptake of nanoparticles in the in vitro BeWo b30 placental cell barrier model used within NanoTEST. *Nanotoxicology*.
- DEPOIX, C., BARRET, L. A., HUBINONT, C. & DEBIEVE, F. 2013. Viability of primary term cytotrophoblast cell culture in normoxia and hypoxia. *Mol Hum Reprod*, 19, 29-34.
- DI SANTO, S., MALEK, A., SAGER, R., ANDRES, A. C. & SCHNEIDER, H. 2003. Trophoblast viability in perfused term placental tissue and explant cultures limited to 7-24 hours. *Placenta*, 24, 882-94.
- ELAD, D., LEVKOVITZ, R., JAFFA, A. J., DESOYE, G. & HOD, M. 2014. Have we neglected the role of fetal endothelium in transplacental transport? *Traffic*, 15, 122-6.
- ELLIOTT, J., RÖSSLEIN, M., WOONG SONG, N., TOMAN, B., KINSNER-OVASKAINEN, A., MANIRATANACHOTE, R., SALIT, M., PETERSEN, E., SEQUEIRA, F., LEE, J., JIN KIM, S., ROSSI, F., HIRSCH, C., KRUG, H.,

- SUCHAOIN, W. & WICK, P. 2014. Toward Achieving Harmonization in a Nanocytotoxicity Assay Measurement through an Interlaboratory Comparison Study. (ready for submission).
- ENDERS, A. C. & BLANKENSHIP, T. N. 1999. Comparative placental structure. *Adv Drug Deliv Rev*, 38, 3-15.
- FAUST, J. J., ZHANG, W., CHEN, Y. & CAPCO, D. G. 2014. Alpha-Fe(2)O(3) elicits diameter-dependent effects during exposure to an in vitro model of the human placenta. *Cell Biol Toxicol*, 30, 31-53.
- FIRTH, J. A. & LEACH, L. 1996. Not trophoblast alone: a review of the contribution of the fetal microvasculature to transplacental exchange. *Placenta*, 17, 89-96.
- FUJISAWA, K., NASU, K., ARIMA, K., SUGANO, T., NARAHARA, H. & MIYAKAWA, I. 2000. Production of interleukin (IL)-6 and IL-8 by a choriocarcinoma cell line, BeWo. *Placenta*, 21, 354-60.
- GENDRON, M. P., MARTIN, B., ORAICHI, D. & BERARD, A. 2009. Health care providers' requests to Teratogen Information Services on medication use during pregnancy and lactation. *Eur J Clin Pharmacol*, 65, 523-31.
- GRAFMULLER, S., MANSER, P., KRUG, H. F., WICK, P. & VON MANDACH, U. 2013. Determination of the transport rate of xenobiotics and nanomaterials across the placenta using the ex vivo human placental perfusion model. *J Vis Exp*.
- GSTRAUNTHALER, G. & HARTUNG, T. 2002. Good cell culture practice: good laboratory practice in the cell culture laboratory for the standardization and quality assurance of in vitro studies. In: LEHR, C. (ed.) *Cell culture models of biological barriers In-vitro test systems for drug absorption and delivery*. London, New York: Taylor & Francis.
- HUMPHREY, R. G., SONNENBERG-HIRCHE, C., SMITH, S. D., HU, C., BARTON, A., SADOVSKY, Y. & NELSON, D. M. 2008. Epidermal growth factor abrogates hypoxia-induced apoptosis in cultured human trophoblasts through phosphorylation of BAD Serine 112. *Endocrinology*, 149, 2131-7.
- KROLL, A., PILLUKAT, M. H., HAHN, D. & SCHNEKENBURGER, J. 2009. Current in vitro methods in nanoparticle risk assessment: limitations and challenges. *Eur J Pharm Biopharm*, 72, 370-7.
- LEVKOVITZ, R., ZARETSKY, U., GORDON, Z., JAFFA, A. J. & ELAD, D. 2013a. In vitro simulation of placental transport: part I. Biological model of the placental barrier. *Placenta*, 34, 699-707.
- LEVKOVITZ, R., ZARETSKY, U., JAFFA, A. J., HOD, M. & ELAD, D. 2013b. In vitro simulation of placental transport: part II. Glucose transfer across the placental barrier model. *Placenta*, 34, 708-15.
- MALEK, A., SAGER, R., LANG, A. B. & SCHNEIDER, H. 1997. Protein transport across the in vitro perfused human placenta. *Am J Reprod Immunol*, 38, 263-71.
- MALEK, A., WILLI, A., MULLER, J., SAGER, R., HANGGI, W. & BERSINGER, N. 2001. Capacity for hormone production of cultured trophoblast cells obtained from placentae at term and in early pregnancy. *J Assist Reprod Genet*, 18, 299-304.
- MARTIN, A. & HOLLOWAY, K. 2014. 'Something there is that doesn't love a wall': Histories of the placental barrier. *Stud Hist Philos Biol Biomed Sci*, 47 Pt B, 300-10.
- MARUO, T., MATSUO, H., OISHI, T., HAYASHI, M., NISHINO, R. & MOCHIZUKI, M. 1987. Induction of differentiated trophoblast function by epidermal growth factor: relation of immunohistochemically detected cellular epidermal growth factor receptor levels. *J Clin Endocrinol Metab*, 64, 744-50.

- MORRISH, D. W., DAKOUR, J., LI, H., XIAO, J., MILLER, R., SHERBURNE, R., BERDAN, R. C. & GUILBERT, L. J. 1997. In vitro cultured human term cytotrophoblast: a model for normal primary epithelial cells demonstrating a spontaneous differentiation programme that requires EGF for extensive development of syncytium. *Placenta*, 18, 577-85.
- NEL, A., XIA, T., MADLER, L. & LI, N. 2006. Toxic potential of materials at the nanolevel. *Science*, 311, 622-7.
- NIKITINA, L., DOHR, G. & JUCH, H. 2013. Studying nanoparticle interaction with human placenta: Festina lente! *Nanotoxicology*.
- OMATA, W., ACKERMAN, W. E. T., VANDRE, D. D. & ROBINSON, J. M. 2013. Trophoblast cell fusion and differentiation are mediated by both the protein kinase C and a pathways. *PLoS One*, 8, e81003.
- PANIGEL, M., PASCAUD, M. & BRUN, J. L. 1967. [Radioangiographic study of circulation in the villi and intervillous space of isolated human placental cotyledon kept viable by perfusion]. *J Physiol (Paris)*, 59, 277.
- PETROFF, M. G., PHILLIPS, T. A., KA, H., PACE, J. L. & HUNT, J. S. 2006. Isolation and culture of term human trophoblast cells. *Methods Mol Med*, 121, 203-17.
- SCHINS, R. P. & KNAAPEN, A. M. 2007. Genotoxicity of poorly soluble particles. *Inhal Toxicol*, 19 Suppl 1, 189-98.
- SCHLEH, C., SEMMLER-BEHNKE, M., LIPKA, J., WENK, A., HIRN, S., SCHAFFLER, M., SCHMID, G., SIMON, U. & KREYLING, W. G. 2012. Size and surface charge of gold nanoparticles determine absorption across intestinal barriers and accumulation in secondary target organs after oral administration. *Nanotoxicology*, 6, 36-46.
- SCHNEIDER, H., PANIGEL, M. & DANCIS, J. 1972. Transfer across the perfused human placenta of antipyrine, sodium and leucine. *Am J Obstet Gynecol*, 114, 822-8.
- SHIMOYA, K., MORIYAMA, A., MATSUZAKI, N., OGATA, I., KOYAMA, M., AZUMA, C., SAJI, F. & MURATA, Y. 1999. Human placental cells show enhanced production of interleukin (IL)-8 in response to lipopolysaccharide (LPS), IL-1 and tumour necrosis factor (TNF)-alpha, but not to IL-6. *Mol Hum Reprod*, 5, 885.
- SOOD, A., SALIH, S., ROH, D., LACHARME-LORA, L., PARRY, M., HARDIMAN, B., KEEHAN, R., GRUMMER, R., WINTERHAGER, E., GOKHALE, P. J., ANDREWS, P. W., ABBOTT, C., FORBES, K., WESTWOOD, M., APLIN, J. D., INGHAM, E., PAPAGEORGIOU, I., BERRY, M., LIU, J., DICK, A. D., GARLAND, R. J., WILLIAMS, N., SINGH, R., SIMON, A. K., LEWIS, M., HAM, J., ROGER, L., BAIRD, D. M., CROMPTON, L. A., CALDWELL, M. A., SWALWELL, H., BIRCHMACHIN, M., LOPEZ-CASTEJON, G., RANDALL, A., LIN, H., SULEIMAN, M. S., EVANS, W. H., NEWSON, R. & CASE, C. P. 2011. Signalling of DNA damage and cytokines across cell barriers exposed to nanoparticles depends on barrier thickness. *Nat Nanotechnol*, 6, 824-33.
- THURNHERR, T., BRANDENBERGER, C., FISCHER, K., DIENER, L., MANSER, P., MAEDER-ALTHAUS, X., KAISER, J. P., KRUG, H. F., ROTHEN-RUTISHAUSER, B. & WICK, P. 2011. A comparison of acute and long-term effects of industrial multiwalled carbon nanotubes on human lung and immune cells in vitro. *Toxicol Lett*, 200, 176-86.
- THURNHERR, T., SU, D. S., DIENER, L., WEINBERG, G., MANSER, P., PFÄNDER, N., ARRIGO, R., SCHUSTER, M. E., WICK, P. & KRUG, H. F. 2009. Comprehensive evaluation of in vitro toxicity of three large-scale produced carbon nanotubes on human Jurkat T cells and a comparison to crocidolite asbestos. *Nanotoxicology*, 3, 319-338.



- TIAN, F., RAZANSKY, D., ESTRADA, G. G., SEMMLER-BEHNKE, M., BEYERLE, A., KREYLING, W., NTZIACHRISTOS, V. & STOEGER, T. 2009. Surface modification and size dependence in particle translocation during early embryonic development. *Inhal Toxicol*, 21 Suppl 1, 92-6.
- TSUKIHARA, S., HARADA, T., DEURA, I., MITSUNARI, M., YOSHIDA, S., IWABE, T. & TERAOKAWA, N. 2004. Interleukin-1beta-induced expression of IL-6 and production of human chorionic gonadotropin in human trophoblast cells via nuclear factor-kappaB activation. *Am J Reprod Immunol*, 52, 218-23.
- WAGNER, R. K., HINSON, R. M., APODACA, C. C., HOELDTKE, N., BUCHANAN, T., HUME, R. F., JR. & CALHOUN, B. C. 2000. Effects of lipopolysaccharide on interleukin-6 production in perfused human placental cotyledons. *J Matern Fetal Med*, 9, 351-5.
- WICE, B., MENTON, D., GEUZE, H. & SCHWARTZ, A. L. 1990. Modulators of cyclic AMP metabolism induce syncytiotrophoblast formation in vitro. *Exp Cell Res*, 186, 306-16.



## 4. FINAL DISCUSSION AND OUTLOOK

### 4.1 Final Discussion

Evaluation of ENM translocation across biological barriers is essential for ENM risk assessment. Thus, it is not surprising that this is an intensive field of research. My PhD thesis was focused on the human placenta as an important internal biological barrier using fluorescently labeled polystyrene beads as model particles. The results of this work illustrate that ENM transport studies in a physiological relevant model such as the *ex vivo* placental perfusion can provide significant information about the relationship of ENM properties and placental transfer as well as transport mechanisms (see chapter 3, part II). Placental transfer of polystyrene particles occurred not via passive diffusion, but rather via energy-dependent mechanisms. This main result of my work is in concert with the findings from studies at other biological barriers. For the air-blood and the blood-brain barrier, active transport mechanisms such as endocytosis are also proposed as potential transport pathways for ENMs (Brandenberger et al., 2010, Kreuter, 2014, Kreyling et al., 2014, Muhlfield et al., 2008, Thorley et al., 2014). Additionally, placental translocation of polystyrene beads was found to be also dependent on their surface modification, whereas the transfer of plain particles was significantly higher than for carboxylate-modified beads (see chapter 3, part II). These findings indicate a potential impact of the protein corona, which is formed around ENMs immediately after contact with biological fluids and can significantly alter ENMs biokinetics (Pietroiusti et al., 2013, Lundqvist et al., 2008, Ehrenberg et al., 2009). It has to be considered that protein expression in the tissue and protein composition of the blood vary between the fetus and the mother suggesting that kinetics and cellular responses to ENMs might be completely different during prenatal development compared to the cellular reactions in adult tissue (Juch et al., 2013, Malek et al., 2001, Linnemann et al., 2000). Of course, further studies using ENMs with different chemistry and surface modifications are needed to corroborate this hypothesis and to build the basis for the development of nanomedical applications of the third generation, which will be specifically designed with an enhanced ability to cross biological barriers.

There is general consent that the physicochemical properties of ENMs mainly determine cellular uptake, biodistribution and toxicity (Nel et al., 2009, Pietroiusti et al., 2013). Though, many studies show controversial results and it is still debated, which ENM characteristic leads

to which cellular response (Johnston et al., 2013, Warheit, 2008). Major problems regarding this issue are insufficient description of the material characterization, preparation procedures of ENM dispersions and selection of physiological relevant concentrations, mode of administration as well as appropriate models (Krug, 2014).

My thesis demonstrates some of these challenges such as identification of a relevant model and pitfalls during ENM evaluation (see chapter 3, part I, III, IV). Although, many ENM are commercially available and are delivered with some information about their properties, an extensive particle characterization in the context of the used biological test system (relevant media) is inevitable and comprises analysis of the size distribution, surface modifications, particle agglomeration, particle stability, potential dye elution as well as degree of contamination with residual manufacturing components or endotoxins (Crist et al., 2013). Furthermore, the testing strategy is just as important as ENM characterization to draw valid conclusions from nanotoxicological studies. To obtain comparable and reliable results validated and standardized methods with a high traceability of the results, an implemented quality control system and an appropriate consideration of measurement uncertainties are required (Hirsch et al., 2011). Additionally, intrinsic controls, reference standards, at least two independent measurement techniques per end point, comparable dose metrics and careful evaluation of ENM interference with the assay should be implemented (Hirsch et al., 2011). Especially the assessment of dosimetry is essential for nanotoxicological *in vitro* studies. Often the colloid stability of ENMs is not given any more after contact with cell culture media. This leads to actual cellular doses, which can be different from the initially applied ENM concentrations and may cause misinterpretations of the data about ENM uptake and toxicity (Teeguarden et al., 2007, DeLoid et al., 2014). Finally, increasing the understanding of nano-bio interactions requires a systematic and multidisciplinary approach. Overall, the field of toxicology research in general is moving from phenomenological towards more mechanistic assessment including high throughput and high content screening of substances for potential toxicity and quantitative analysis of the structure-activity relationships (QSAR). The QSAR regression models in combination with computational biology can be used to develop predictive toxicology approaches in order to reduce traditional animal testing and a safer design of chemicals. Moreover, new projects emerge and aim to map toxicological pathways of chemicals instead of simple cytotoxicity testing. Similar concepts have to be implemented in the risk assessment of ENMs (Nel, 2013). The elucidation of toxicological pathways using genomics and proteomics approaches may be as important as to clarify the cellular transport

mechanisms used by ENMs. For such a strategy the selection of a relevant biological model is crucial.

Besides the animal models, which are not suitable for human assessment due to the interspecies differences in placental structure, there are two models used frequently to study placental transfer of ENMs: the BeWo transwell system and the *ex vivo* human placental perfusion model (Cartwright et al., 2012, Sonnegard Poulsen et al., 2013, Wick et al., 2010). Placental transfer of ENMs *in vitro* across a BeWo cell layer is significantly lower and the equilibration time longer compared to the *ex vivo* human perfusion model (Poulsen et al., 2009, Sonnegard Poulsen et al., 2013). This is mainly due to the absence of both, flow as well as an appropriate hydrostatic pressure on the fetal side. However, the BeWo cell model is easier to handle due to the simple experimental set-up and also longer exposure times (up to several days) are feasible, whereas the *ex vivo* perfusion is technically far more challenging and the duration of perfusion is limited to a few hours because of the starting tissue degradation (Di Santo et al., 2003, Mathiesen and Knudsen, 2013, Poulsen et al., 2009). In addition, many factors such as maternal health, placental disruptions caused during delivery and the ischemic phase after delivery contribute to the low success rate (about 20 %) of *ex vivo* placental perfusions, which constrains throughput of the model (Grafmüller et al., 2013, Mathiesen and Knudsen, 2013). Furthermore, oxidative stress and cell death during the ischemic phase can influence the experimental outcome concerning transfer as well as other cellular responses to ENMs (Mathiesen and Knudsen, 2013). But since the placenta has been described as specifically tolerant to hypoxia and capable to quickly recover during reperfusion in the laboratory, ischemia is not a major problem (Schneider, 2009). BeWo cells are tumor-derived cells and are as such genetically homogenous, while human placentae from various individuals have genetic, dietary as well as maternal health related differences. The latter could lead to a higher variability of the results, but it also reflects the normal variability within the population and therefore increases the *in vivo* relevance of the data obtained by using the *ex vivo* perfusion model. Another disadvantage of the BeWo transwell model is that it lacks the complexity of a whole organ. It is known that many cell types especially macrophages in placental as well as in decidual tissue (the part of the uterus contributing to placenta formation at the site of implantation) play an important role in maintaining maternal immune tolerance against the fetus (Cupurdija et al., 2004). Since ENMs have shown to impair immune cell functions, to induce production of pro-inflammatory cytokines and to change the activation status of macrophages, it has to be evaluated if such reactions may also have an influence on the

sensitive immunological balance in the human placenta (Oberdorster et al., 2005, Scherbart et al., 2011, Juch et al., 2013). Though for such studies a model including all involved cell types would be necessary.

Furthermore, both models do not account for the changes of placental structure and function during gestation. The transfer of immunoglobulins across the human placenta is substantially dependent on gestational age (Palmeira et al., 2012). Hence, differences in placental toxicodynamics and –kinetics of ENMs between term and early gestation might be also possible (Juch et al., 2013, Nikitina et al., 2013). The first trimester is the most critical period during pregnancy regarding vulnerability of the fetus. Most organs are developed in this time and harmful substances with a high placental permeability can induce severe malformations or impair placental development leading to placenta related diseases such as gestational diabetes, preeclampsia or intrauterine growth restriction (Benirschke, 2012). To protect the fetus from exogenous influences during early gestation, the placental barrier is thicker compared to late gestation, because of an additional layer of cytotrophoblast cells covering the syncytiotrophoblast on the fetal side of the placental villous. Although the increased barrier thickness exacerbates placental transfer of ENMs, the toxicity may be even augmented. Sood et al. observed an inverse correlation between barrier thickness and toxicity using a co-culture model with multiple layers of BeWo cells on the apical side of a transwell insert and fibroblasts in the basal chamber. After application of cobalt chromium nanoparticles to the apical chamber more DNA damage in the fibroblasts at the basal chamber was detected with increasing numbers of BeWo layers and without translocation of the nanoparticles indicating an indirect effect mediated by cytokine signalling (Sood et al., 2011). Besides the fact that the transfer of most substances and pathogens is restricted or even prevented during the first trimester, translocation of some natural nanoparticles with a size of 50 – 70 nm such as the rubella virus is enhanced and declines with increasing gestational age (Webster, 1998, Galvan-Ramirez Mde et al., 2014). Thus, a similar phenomenon for ENMs cannot be excluded. Another possibility to study the functions of the early placenta is the use of first trimester placental tissue explants obtained from elective pregnancy terminations. Although placental explants offer a higher degree of tissue complexity compared to transwell models with cell lines, they still lack blood flow and real translocation studies are not possible. Nevertheless, first trimester placental explants are useful for first investigations of ENM uptake, the contribution of distinct transport mechanisms and the cellular responses to ENMs (Juch et al., 2013, Miller et al., 2005). Moreover, little is known about the contribution of the fetal membranes to fetal transfer particularly during early pregnancy. It was demonstrated that

dendrimers in the nanoscale are transported across fetal membranes but only in very low amounts. These findings indicate that the impact of this mode of transfer is rather small, nevertheless it should be considered for the development of nanomedical applications, which are administered intravaginally (Menjoge et al., 2010).

To conclude, it is clear that all models have their limitations and that the selection of the model has to be based on the questions which should be answered. Overall, the BeWo transwell model is suitable to perform a first initial screening of ENM toxicity and to assess the contribution of specific transport mechanisms to ENM transfer, whereas the *ex vivo* human perfusion model is more appropriate to predict the *in vivo* transfer of ENMs.

### 4.2 Outlook

The statistician George E. P. Box wrote, "essentially, all models are wrong, but some are useful". In order to make the placental models more useful for nanotoxicological studies, there are efforts to improve those and develop new advanced human *in vitro* models which allow high throughput screenings but also maintain a certain level of the original organ complexity (Figure 1). The last part of my thesis already dealt with the isolation and characterization of primary human cytotrophoblast cells with the intention to replace the BeWo cells against a physiologically more relevant cell type. However, first preliminary experiments demonstrated that the yield of such primary cell isolations as well as their viability in culture are limited (see chapter 3, part IV) (Depoix et al., 2013). Nevertheless, these cells can be used in models, where only few cells are needed. For example is the microfluidics technology anticipated to manipulate complex fluids at the submillimeter scale and has already led to the development of lab-on-a-chip and organ-on-a-chip approaches (Richter et al., 2011, Sackmann et al., 2014) (Figure 1). The major advantage of such a placenta-on-a-chip model are the low amounts of the test ENMs and the placental barrier cells required for this method, the controllable flow, which could be optimally adjusted to the *in vivo* situation, and the possibility of high throughput screenings. In addition, it is feasible to include more than one cell type into the model and further enhance the *in vivo* relevance. Microfluidics models would be suitable to investigate ENM transfer and to identify distinct transport as well as toxicological pathways by using specific inhibitors. A second model, in which BeWo cells can be replaced by primary human cytotrophoblasts, are the scaffold-free self-organized organoids or microtissues (Astashkina and Grainger, 2014, Kelm and Fussenegger, 2004). Three-dimensional microtissues with a core of fibroblasts and a trophoblast shell can mimic the structure of the placental villi at term or with multiple layers of cytotrophoblasts also at early gestation (Figure 1). ENM uptake into the tissue and their respective mechanisms as well as cellular responses to ENMs can be evaluated in this model. Of note, the practicability of using primary human cytotrophoblasts in these two models has to be analyzed first. Primary cytotrophoblasts do not build a confluent layer as the BeWo cells but instead form large aggregates with large intercellular spaces if cultured on semipermeable membranes (Liu et al., 1997, Yui et al., 1994). Though, this growth pattern may be completely different in a three-dimensional environment as in the microtissues. Another approach especially for the elucidation of placental transport is the integration of perfusion flow and endothelial cells in the BeWo transwell model (Figure 1). Both of these aspects would tremendously increase the physiological relevance of this model, but still preserves the



possibility for medium to high throughput screenings and a certain degree of reproducibility. After an accurate standardization and validation of the model against the *ex vivo* perfusion or epidemiological data, this co-culture transwell perfusion set-up could provide a powerful model to investigate placental transfer of ENMs and to elucidate the mechanisms and cell types contributing to this translocation process.

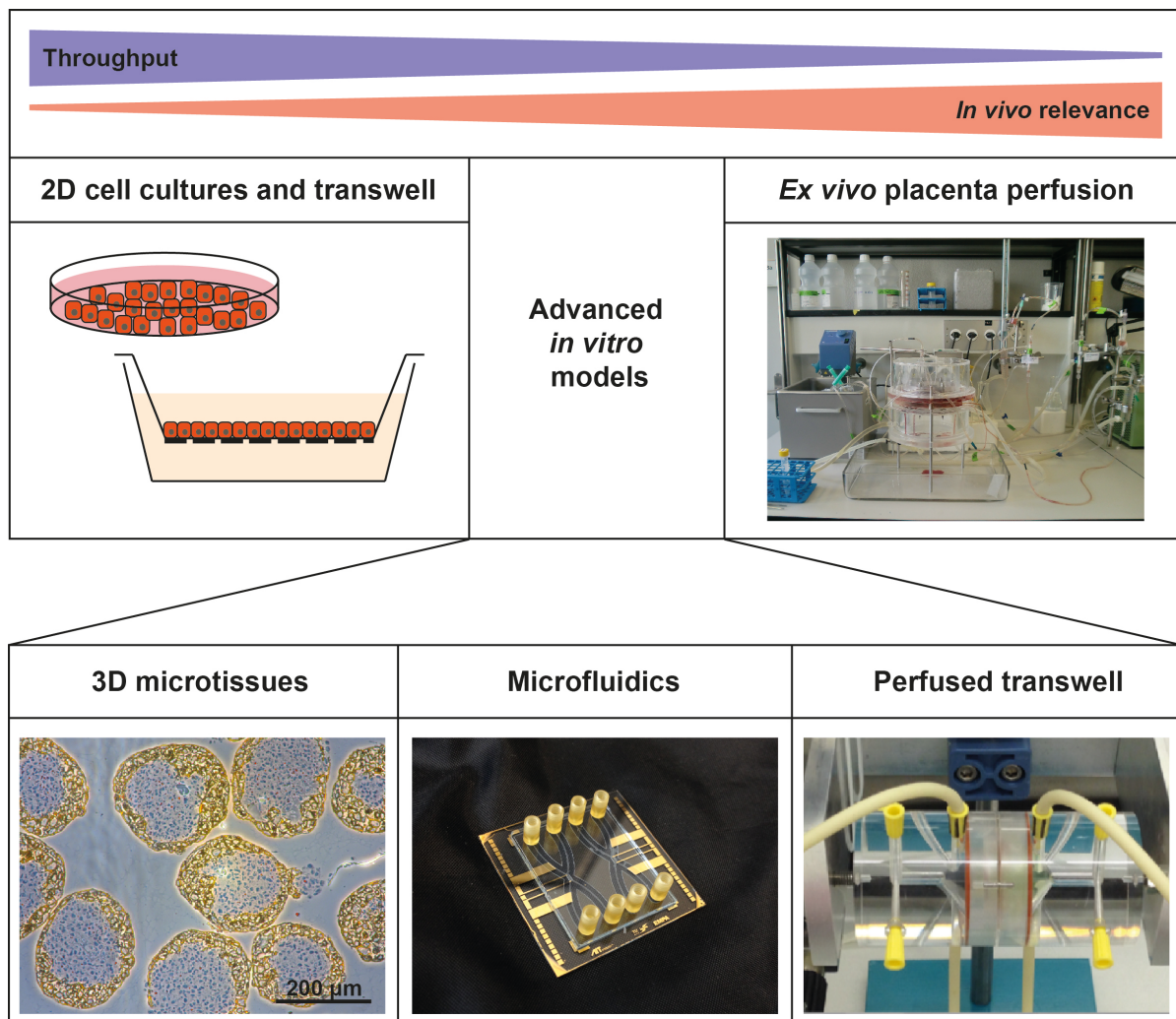


**Figure 1:** In the upper part the most frequently used placental models, the two-dimensional (2D) BeWo cell culture or BeWo transwell system and the *ex vivo* human placental perfusion model, are displayed. In between are some advanced *in vitro* models, which are currently under development: the three-dimensional (3D) microtissues with a fibroblast core and a shell of trophoblast cells e.g. BeWo cells, which are stained with cytokeratin-7 (yellow), the microfluidic placenta chip (Ertl, 2013) and the perfused transwell with BeWo as well as endothelial cells, which both contribute to the placental barrier in this model.

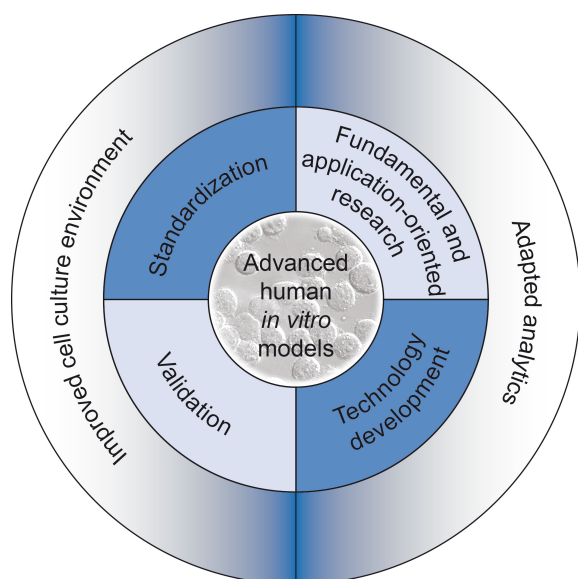


**Figure 2:** Scheme summarizing the actions to be taken to further improve the relevance of advanced human *in vitro* models. Reprinted with permission from (Wick et al., 2014).

Generally, toxicology as well as nanotoxicology is developing towards an evidence-based research discipline, which requires new advanced human *in vitro* models. These models have to be standardized and carefully validated in an improved cell culture environment. Adapted analytics, application-oriented research and implementation of new technologies will lead to models, which support toxicologists in the generation of comparable, reliable and meaningful results (Wick et al., 2014) (Figure 2). These advanced human *in vitro* models will not only change the field of nanotoxicology, but will also lead to a better understanding of the placenta itself. Placental dysfunctions have been linked to several diseases e.g. cardiovascular diseases in the later life of the child (Barker and Thornburg, 2013, Hennington and Alexander, 2013, Saade, 2009). Recently, the National Institutes of Health in the United States issued the ‘Human Placenta Project’ with the aim to increase the knowledge about placental structure, development and functions. Monitoring of critical placental functions could help to identify high risk pregnancies earlier and detailed data about the mechanisms underlying placental abnormalities such as preeclampsia could lead to new therapeutic strategies. Preventive and therapeutic interventions will have a major impact on pregnancy outcome as well as children’s health (Guttmacher et al., 2014).

### 4.3 References

- ASTASHKINA, A. & GRAINGER, D. W. 2014. Critical analysis of 3-D organoid in vitro cell culture models for high-throughput drug candidate toxicity assessments. *Adv Drug Deliv Rev*, 69-70, 1-18.
- BARKER, D. J. & THORNBURG, K. L. 2013. Placental programming of chronic diseases, cancer and lifespan: a review. *Placenta*, 34, 841-5.
- BENIRSCHKE, K. 2012. *Pathology of the human placenta*, New York, Springer.
- BRANDENBERGER, C., MUHLFELD, C., ALI, Z., LENZ, A. G., SCHMID, O., PARAK, W. J., GEHR, P. & ROTHEN-RUTISHAUSER, B. 2010. Quantitative evaluation of cellular uptake and trafficking of plain and polyethylene glycol-coated gold nanoparticles. *Small*, 6, 1669-78.
- CARTWRIGHT, L., POULSEN, M. S., NIELSEN, H. M., POJANA, G., KNUDSEN, L. E., SAUNDERS, M. & RYTTEING, E. 2012. In vitro placental model optimization for nanoparticle transport studies. *Int J Nanomedicine*, 7, 497-510.
- CRIST, R. M., GROSSMAN, J. H., PATRI, A. K., STERN, S. T., DOBROVOLSKAIA, M. A., ADISESHAIAH, P. P., CLOGSTON, J. D. & MCNEIL, S. E. 2013. Common pitfalls in nanotechnology: lessons learned from NCI's Nanotechnology Characterization Laboratory. *Integr Biol (Camb)*, 5, 66-73.
- CUPURDIJA, K., AZZOLA, D., HAINZ, U., GRATCHEV, A., HEITGER, A., TAKIKAWA, O., GOERDT, S., WINTERSTEIGER, R., DOHR, G. & SEDLMAYR, P. 2004. Macrophages of human first trimester decidua express markers associated to alternative activation. *Am J Reprod Immunol*, 51, 117-22.
- DELOID, G., COHEN, J. M., DARRAH, T., DERK, R., ROJANASAKUL, L., PYRGIOTAKIS, G., WOHLLEBEN, W. & DEMOKRITOU, P. 2014. Estimating the effective density of engineered nanomaterials for in vitro dosimetry. *Nat Commun*, 5, 3514.
- DEPOIX, C., BARRET, L. A., HUBINONT, C. & DEBIEVE, F. 2013. Viability of primary term cytotrophoblast cell culture in normoxia and hypoxia. *Mol Hum Reprod*, 19, 29-34.
- DI SANTO, S., MALEK, A., SAGER, R., ANDRES, A. C. & SCHNEIDER, H. 2003. Trophoblast viability in perfused term placental tissue and explant cultures limited to 7-24 hours. *Placenta*, 24, 882-94.
- EHRENBERG, M. S., FRIEDMAN, A. E., FINKELSTEIN, J. N., OBERDORSTER, G. & MCGRATH, J. L. 2009. The influence of protein adsorption on nanoparticle association with cultured endothelial cells. *Biomaterials*, 30, 603-10.
- ERTL, P. 2013. [www.cellchipgroup.com](http://www.cellchipgroup.com) [Online]. Web page.
- GALVAN-RAMIREZ MDE, L., GUTIERREZ-MALDONADO, A. F., VERDUZCO-GRIJALVA, F. & JIMENEZ, J. M. 2014. The role of hormones on Toxoplasma gondii infection: a systematic review. *Front Microbiol*, 5, 503.
- GRAFMULLER, S., MANSER, P., KRUG, H. F., WICK, P. & VON MANDACH, U. 2013. Determination of the transport rate of xenobiotics and nanomaterials across the placenta using the ex vivo human placental perfusion model. *J Vis Exp*.
- GUTTMACHER, A. E., MADDOX, Y. T. & SPONG, C. Y. 2014. The Human Placenta Project: placental structure, development, and function in real time. *Placenta*, 35, 303-4.
- HENNINGTON, B. S. & ALEXANDER, B. T. 2013. Linking intrauterine growth restriction and blood pressure: insight into the human origins of cardiovascular disease. *Circulation*, 128, 2179-80.

- HIRSCH, C., ROESSLEIN, M., KRUG, H. F. & WICK, P. 2011. Nanomaterial cell interactions: are current in vitro tests reliable? *Nanomedicine (Lond)*, 6, 837-47.
- JOHNSTON, H., POJANA, G., ZUIN, S., JACOBSEN, N. R., MOLLER, P., LOFT, S., SEMMLER-BEHNKE, M., MCGUINNESS, C., BALHARRY, D., MARCOMINI, A., WALLIN, H., KREYLING, W., DONALDSON, K., TRAN, L. & STONE, V. 2013. Engineered nanomaterial risk. Lessons learnt from completed nanotoxicology studies: potential solutions to current and future challenges. *Crit Rev Toxicol*, 43, 1-20.
- JUCH, H., NIKITINA, L., DEBBAGE, P., DOHR, G. & GAUSTER, M. 2013. Nanomaterial interference with early human placenta: Sophisticated matter meets sophisticated tissues. *Reprod Toxicol*, 41, 73-9.
- KELM, J. M. & FUSSENEGGER, M. 2004. Microscale tissue engineering using gravity-enforced cell assembly. *Trends Biotechnol*, 22, 195-202.
- KREUTER, J. 2014. Drug delivery to the central nervous system by polymeric nanoparticles: what do we know? *Adv Drug Deliv Rev*, 71, 2-14.
- KREYLING, W. G., HIRN, S., MOLLER, W., SCHLEH, C., WENK, A., CELIK, G., LIPKA, J., SCHAFFLER, M., HABERL, N., JOHNSTON, B. D., SPERLING, R., SCHMID, G., SIMON, U., PARAK, W. J. & SEMMLER-BEHNKE, M. 2014. Air-blood barrier translocation of tracheally instilled gold nanoparticles inversely depends on particle size. *ACS Nano*, 8, 222-33.
- KRUG, H. F. 2014. Nanosafety research-are we on the right track? *Angew Chem Int Ed Engl*, 53, 12304-19.
- LINNEMANN, K., MALEK, A., SAGER, R., BLUM, W. F., SCHNEIDER, H. & FUSCH, C. 2000. Leptin production and release in the dually in vitro perfused human placenta. *J Clin Endocrinol Metab*, 85, 4298-301.
- LIU, F., SOARES, M. J. & AUDUS, K. L. 1997. Permeability properties of monolayers of the human trophoblast cell line BeWo. *Am J Physiol*, 273, C1596-604.
- LUNDQVIST, M., STIGLER, J., ELIA, G., LYNCH, I., CEDERVALL, T. & DAWSON, K. A. 2008. Nanoparticle size and surface properties determine the protein corona with possible implications for biological impacts. *Proc Natl Acad Sci U S A*, 105, 14265-70.
- MALEK, A., WILLI, A., MULLER, J., SAGER, R., HANGGI, W. & BERSINGER, N. 2001. Capacity for hormone production of cultured trophoblast cells obtained from placentae at term and in early pregnancy. *J Assist Reprod Genet*, 18, 299-304.
- MATHIESEN, L. & KNUDSEN, L. E. 2013. Placental Transport of Environmental Toxicants In: NICHOLSON, R. (ed.) *The Placenta: Development, Function and Diseases*. New York: Nova Science Publishers, Inc.
- MENJOGE, A. R., NAVATH, R. S., ASAD, A., KANNAN, S., KIM, C. J., ROMERO, R. & KANNAN, R. M. 2010. Transport and biodistribution of dendrimers across human fetal membranes: implications for intravaginal administration of dendrimer-drug conjugates. *Biomaterials*, 31, 5007-21.
- MILLER, R. K., GENBACEV, O., TURNER, M. A., APLIN, J. D., CANIGGIA, I. & HUPPERTZ, B. 2005. Human placental explants in culture: approaches and assessments. *Placenta*, 26, 439-48.
- MUHLFELD, C., GEHR, P. & ROTHEN-RUTISHAUSER, B. 2008. Translocation and cellular entering mechanisms of nanoparticles in the respiratory tract. *Swiss Med Wkly*, 138, 387-91.
- NEL, A. E. 2013. Implementation of alternative test strategies for the safety assessment of engineered nanomaterials. *J Intern Med*, 274, 561-77.
- NEL, A. E., MADLER, L., VELEGOL, D., XIA, T., HOEK, E. M., SOMASUNDARAN, P., KLAESSIG, F., CASTRANOVA, V. & THOMPSON, M. 2009. Understanding biophysicochemical interactions at the nano-bio interface. *Nat Mater*, 8, 543-57.

- NIKITINA, L., DOHR, G. & JUCH, H. 2013. Studying nanoparticle interaction with human placenta: Festina lente! *Nanotoxicology*.
- OBERDORSTER, G., MAYNARD, A., DONALDSON, K., CASTRANOVA, V., FITZPATRICK, J., AUSMAN, K., CARTER, J., KARN, B., KREYLING, W., LAI, D., OLIN, S., MONTEIRO-RIVIERE, N., WARHEIT, D., YANG, H. & GROUP, I. R. F. R. S. I. N. T. S. W. 2005. Principles for characterizing the potential human health effects from exposure to nanomaterials: elements of a screening strategy. *Part Fibre Toxicol*, 2, 8.
- PALMEIRA, P., QUINELLO, C., SILVEIRA-LESSA, A. L., ZAGO, C. A. & CARNEIRO-SAMPAIO, M. 2012. IgG placental transfer in healthy and pathological pregnancies. *Clin Dev Immunol*, 2012, 985646.
- PIETROIUSTI, A., CAMPAGNOLO, L. & FADEEL, B. 2013. Interactions of engineered nanoparticles with organs protected by internal biological barriers. *Small*, 9, 1557-72.
- POULSEN, M. S., RYTTING, E., MOSE, T. & KNUDSEN, L. E. 2009. Modeling placental transport: correlation of in vitro BeWo cell permeability and ex vivo human placental perfusion. *Toxicol In Vitro*, 23, 1380-6.
- RICHTER, L., CHARWAT, V., JUNGREUTHMAYER, C., BELLUTTI, F., BRUECKL, H. & ERTL, P. 2011. Monitoring cellular stress responses to nanoparticles using a lab-on-a-chip. *Lab Chip*, 11, 2551-60.
- SAADE, G. R. 2009. Pregnancy as a window to future health. *Obstet Gynecol*, 114, 958-60.
- SACKMANN, E. K., FULTON, A. L. & BEEBE, D. J. 2014. The present and future role of microfluidics in biomedical research. *Nature*, 507, 181-9.
- SCHERBART, A. M., LANGER, J., BUSHMELEV, A., VAN BERLO, D., HABERZETTL, P., VAN SCHOOTEN, F. J., SCHMIDT, A. M., ROSE, C. R., SCHINS, R. P. & ALBRECHT, C. 2011. Contrasting macrophage activation by fine and ultrafine titanium dioxide particles is associated with different uptake mechanisms. *Part Fibre Toxicol*, 8, 31.
- SCHNEIDER, H. 2009. Tolerance of human placental tissue to severe hypoxia and its relevance for dual ex vivo perfusion. *Placenta*, 30 Suppl A, S71-6.
- SONNEGAARD POULSEN, M., MOSE, T., LETH MAROUN, L., MATHIESEN, L., EHLERT KNUDSEN, L. & RYTTING, E. 2013. Kinetics of silica nanoparticles in the human placenta. *Nanotoxicology*.
- SOOD, A., SALIH, S., ROH, D., LACHARME-LORA, L., PARRY, M., HARDIMAN, B., KEEHAN, R., GRUMMER, R., WINTERHAGER, E., GOKHALE, P. J., ANDREWS, P. W., ABBOTT, C., FORBES, K., WESTWOOD, M., APLIN, J. D., INGHAM, E., PAPAGEORGIOU, I., BERRY, M., LIU, J., DICK, A. D., GARLAND, R. J., WILLIAMS, N., SINGH, R., SIMON, A. K., LEWIS, M., HAM, J., ROGER, L., BAIRD, D. M., CROMPTON, L. A., CALDWELL, M. A., SWALWELL, H., BIRCHMACHIN, M., LOPEZ-CASTEJON, G., RANDALL, A., LIN, H., SULEIMAN, M. S., EVANS, W. H., NEWSON, R. & CASE, C. P. 2011. Signalling of DNA damage and cytokines across cell barriers exposed to nanoparticles depends on barrier thickness. *Nat Nanotechnol*, 6, 824-33.
- TEEGUARDEN, J. G., HINDERLITER, P. M., ORR, G., THRALL, B. D. & POUNDS, J. G. 2007. Particokinetics in vitro: dosimetry considerations for in vitro nanoparticle toxicity assessments. *Toxicol Sci*, 95, 300-12.
- THORLEY, A. J., RUENRAROENGSAK, P., POTTER, T. E. & TETLEY, T. D. 2014. Critical Determinants of Uptake and Translocation of Nanoparticles by the Human Pulmonary Alveolar Epithelium. *ACS Nano*.
- WARHEIT, D. B. 2008. How meaningful are the results of nanotoxicity studies in the absence of adequate material characterization? *Toxicol Sci*, 101, 183-5.

- WEBSTER, W. S. 1998. Teratogen update: congenital rubella. *Teratology*, 58, 13-23.
- WICK, P., GRAFMUELLER, S., PETRI-FINK, A. & ROTHEN-RUTISHAUSER, B. 2014. Advanced human in vitro models to assess metal oxide nanoparticle-cell interactions. *MRS Bulletin*, 39, 984-989.
- WICK, P., MALEK, A., MANSER, P., MEILI, D., MAEDER-ALTHAUS, X., DIENER, L., DIENER, P. A., ZISCH, A., KRUG, H. F. & VON MANDACH, U. 2010. Barrier capacity of human placenta for nanosized materials. *Environ Health Perspect*, 118, 432-6.
- YUI, J., GARCIA-LLORET, M., BROWN, A. J., BERDAN, R. C., MORRISH, D. W., WEGMANN, T. G. & GUILBERT, L. J. 1994. Functional, long-term cultures of human term trophoblasts purified by column-elimination of CD9 expressing cells. *Placenta*, 15, 231-46.

## 5. ACKNOWLEDGEMENTS

I would like to thank my supervisor Prof. Dr. Harald Krug from Empa St. Gallen for the continuous support, encouragement and confidence in me and in my work. His door was always open and our discussions were inspiring, led to new ideas and kept me motivated despite the many challenges, which emerged during my PhD.

I also want to thank my supervisor Dr. Peter Wick from Empa St. Gallen for the support, the constructive inputs and giving me the chance to work on this interesting project. He was always dedicated to help especially during phases, where I faced one problem after the other.

I want to thank my supervisor Prof. Dr. Ursula von Mandach from the University Hospital Zurich for her unlimited support. Her commitment to fight for better regulations concerning the safety of medications during pregnancy encouraged me to conduct this research with great enthusiasm. Moreover, I had the chance to learn a lot about obstetrics and pharmacology during participation at the numerous congresses and workshops of the SAPP, which she organized.

Special thanks go to my co-advisor Prof. Dr. Barbara Rothen-Rutishauser and my mentor PD Dr. Christophe von Garnier. They supported me during my education and gave substantial inputs to my work.

I deeply like to thank Dr. Tina Bürki-Thurnherr for her help and the critical reading of my thesis particularly during the last months. She supported me substantially in the interpretation of my results and making a good story out of it.

I also want to thank the external co-referee Prof. Dr. med. Patrick Hunziker from the University Hospital Basel for agreeing to review the written part of my thesis.

Thanks go also to Adrian Wichser at Empa in Dübendorf and Dr. Lionel Maurizi as well as Prof. Dr. Heinrich Hofmann at EPFL for the good collaboration. Furthermore, I want to thank Dr. Pierre-André Diener and Prof. Dr. Wolfram Jochum from the Kantonsspital St. Gallen for the excellent collaboration and the histopathological evaluation of the placental tissue samples.

I also want to thank Dr. Martin Ehrbar and all present and former members of the research lab of the Department of Obstetrics at the University Hospital Zurich for the great working environment during the first 3 years of my PhD. I specially owe Esther for her support in organizational issues in the lab and obtaining the placentas from the clinic, which was not

always easy. I want to thank Corina and Yvonne for their help with all the administrative things and for organizing the ladies nights, which I enjoyed a lot. Many thanks go to Alex and Karin for their friendship and the great time in the lab. Alex also showed me the placenta perfusion technique and helped during the starting phase of my project, many thanks for that.

I also want to acknowledge PD Dr. Franz Weber and Dr. Chafik Ghayor at the University Hospital Zurich for letting me use the microplate reader in their lab.

Thanks also to the physicians and midwives in the team of Prof. Dr. Roland Zimmermann, who recruited the pregnant women for my studies. I would like to thank also all women, who donated their placenta for my research project.

I would like to thank all people from the Materials-Biology Interactions lab at Empa in St. Gallen (also all former lab members) for the warm welcome, for being good colleagues, which were always willing to help me and for the familiar working environment. Although I only spent the last 8 months full time at Empa, I already feel at home and as I would be here since several years. Special thanks go to Liliane for her support and the supply with numerous TEM micrographs of the placenta and the polystyrene beads, to Cordula for the productive discussions and the critical reading of my thesis, to Matthias for his help with the Nanosight and computer problems, and to Pius for his help with the perfusion experiments and the various improvements of the perfusion model. I also want to thank Annabé for her help in structuring my thesis and for the critical reading. I am grateful to Carina for teaching me many *in vitro* methods, for the good teamwork and for encouraging and cheering me up when I thought I will never finish with this thesis.

I would like to thank my sister Marlene for listening to all my problems and for never getting tired to explain me the chemical background of the analytical methods I had to use. Thanks also for joining my trips around the world and helping me recover from work and regain my motivation.

Finally, I want to thank my family and friends, especially my parents and Bernd for sharing all heights and depths during my PhD, their support, patience and love.

I dedicate this work to my grandfather, who died few months before I could finalize this thesis and who was always notably interested in my studies.